Sede Amministrativa: Università degli Studi di Padova

Dipartimento di Scienze Chimiche

SCUOLA DI DOTTORATO DI RICERCA IN SCIENZE MOLECOLARI

INDIRIZZO: SCIENZE CHIMICHE

CICLO XXVIII

CHEMICAL ELABORATION OF SYNTHETIC AND NATURAL BIOACTIVE COMPOUNDS TO IMPROVE BIOAVAILABILITY AND ACTIVITY

Direttore della Scuola: Ch.mo Prof. Antonino Polimeno

Coordinatore d'indirizzo: Ch.mo Prof. Antonino Polimeno

Supervisore: Ch.mo Prof. Cristina Paradisi

Dottorando: Matteo Romio

Dedico questo lavoro a tutte le persone oneste che ancora sognano
di poter migliorare il mondo con la loro ricerca.

A tutti gli amici e colleghi che mi hanno accompagnato in questi anni
con coraggio, determinazione, collaborazione ed ispirandomi ogni giorno ad essere migliore.

Ai miei genitori,
che vicini ed umili tifano per me ogni giorno.

Ai miei fratelli,
che sempre mi hanno ispirato e sempre lo faranno.

A te zio,
che sei l'unico grande assente di questa mia ultima conquista
il tuo sorriso è ancora qui con me.

Per chi viaggia in direzione ostinata e contraria
col suo marchio speciale di speciale disperazione
e tra il vomito dei respinti muove gli ultimi passi
per consegnare alla morte
una goccia di splendore
di umanità
di verità.

For those traveling in an obstinate and contrary direction
with their special brand of special desperation
and in the vomit of the rejected move the last steps
to bring to Death
a drop of glory
of humanity
of truth.

Fabrizio de Andrè

Smisurata Preghiera – Anime salve, 1996

TABLE OF CONTENTS

ABBREVIATIONS AND ACRONYMS

5-HOP: 5-hydroxypsoralen

5-MOP:5 -methoxypsoralen

5-OBDMPPIPs: 5-(butoxy-4-dimethyl-phenylphosphonium iodide) psoralen

5-OBTPIPs: 5-(butoxy-4-triphenyphosphonium iodide) psoralen

ACN: acetonitrile

AFM: atomic force microscopy

ATP: adenosine triphosphate

CLL: Chronic Lymphocytic Leukemia

CMC: critical micellar concentration

DCI: carbonyldiimidazole

DCM: dichloromethane

DIPEA: di-isopropyl ethyl amine

DLS: dynamic lught scattering

DMAP: 4-dimethylamino piridine

DMF: dimethylformamide

DMSO: dimethyl sulfoxide

EPR: Enhanced Permeability and Retention EsaGME or 6GME: hexa-ethylenglycol monomethyl ether

ESI-MS: Electro Spray Ionization – Mass Spectroscopy

EtOAc: ethyl Acetate

EtOH: ethanol

FSGC: flash silica gel chromatography

IMM: Inner Mitochondrial Membrane

MDR: multidrug resistance

MeOH: methanol

MTS: (3-(4,5-dimethylthiazol-2-yl)-5-(3-carboxymethoxyphenyl)-2-(4-sulfophenyl)-2H-tetrazolium)

MTT: 3-(4,5-dimethylthiazol-2-yl)-2,5-diphenyltetrazolium bromide

NMR: Nuclear Magnetic Resonance

OEG: oligo-ethylenglycol monomethyl ether

OMM: Outer Mitochondrial Membrane

PBS: Phosphate Buffer Solution

PEG: polyethyleneglycol

PM: Plasma membrane

PMOXA: polymethyloxazoline

PNP: 4-nitrophenol

PNPC: bis(4-nitrophenyl) carbonate

PTS: pterostilbene

Pyr: pyridine

RES: reticuloendothelial systems

ROS: Reactive Oxygen Species

RSV: resveratrolo

TEA: triethylamine

TEM: transmission electron microscopy

TFA: trifluoroacetic acid

THF: tetrahydrofuran

TLC: Thin Layer Chromatography

TMS-Cl: trimethylsilyl chloride

TPP or PPh_3^+: triphenylphosphonium cation

TetraGME or 4GME: tetra-ethylenglycol monomethyl ether

TriGME or 3GME: tri-ethylenglycol monomethyl ether

Ts: tosyl group

TsCl: 4-toluenesulfonyl chloride (Tosyl Chloride)

UPLC: Ultra Performance Liquid Chromatography

UV: Ultraviolet

ABSTRACT

The project aimed to synthesize new prodrugs of bioactive molecules and new self-assembling fully biocompatible macromolecular structures as vehicles for drug delivery. Initially, I worked on the chemical modification of the phenolic group of pterostilbene – a natural bioactive polyphenol used as model in this study – in order to improve its bioavailability after oral administration. I synthesized and tested new pterostilbene derivatives using five different types of protecting groups to functionalize the hydroxyl group and convert the natural phenol, specifically, into a methylthiomethyl ether (MTM), a phosphonic ester, an alkylcarbonyloxymethyl (ACOM) ether, an alkyloxycarbonyloxymethyl (AOCOM) ether and an N-alkyl-N-alkyloxycarbonylaminomethyl (NANAOCAM) ether. The derivatives display very different chemical stability profiles. In preliminary screenings, the AOCOM and ACOM derivatives gave the best results in terms of chemical and biological stability. These compounds were thus tested in pharmacokinetic experiments *in vivo*. The blood concentration vs. time profiles of pterostilbene and its sulfate obtained with the ACOM prodrug were very similar to those determined after administrating pterostilbene as such. Those afforded by the AOCOM derivative showed instead a considerable shift to longer times after administration, indicating that it indeed behaves as a prodrug.

During the second year, I developed two new classes of selective tumor killing agents based on the natural phenol 5-hydroxypsoralen and on the anti-leprosy drug clofazimine. The aim of this part of my project was the design, synthesis and test of novel selective inhibitors of the mitochondrial potassium channel Kv 1.3. This channel is expressed in the inner mitochondrial membrane of many types of cancer cells and its inhibition plays an important role in the induction of apoptosis. In a series of *in vitro* and in vivo tests three of my psoralen derivatives (patented) proved to be remarkably effective. As for the clofazimine derivatives, only a few *in vitro* assays have been performed so far and further in depth tests are currently under way.

More recently during the time I spent at ETH in Zürich, I worked on the design and synthesis of biocompatible polymeric micelles for drug delivery. In particular, I developed and characterized a series of novel resveratrol –OEG-co-adipate and polymethyloxazolines -co-pterostilbene based copolymers that self-assemble in water to form core-shell nanocarriers. In order to test their ability as nanocarriers I loaded them with clofazimine and studied their behavior under various experimental conditions. In the case of

polyoxazolines-co-pterostilbene constructs, these preliminary tests gave encouraging results which prove the value of this approach to obtain a highly modular copolymer platform to be used for the safe delivery of its drug load into solid tumors by exploiting the Enhanced Permeability and Retention (EPR) effect.

RIASSUNTO

Lo scopo del progetto è la sintesi di nuove molecole di interesse biomedico e di nuovi co-polimeri auto-assemblanti completamente biocompatibili per il drug delivery di farmaci. Inizialmente, mi sono dedicato allo studio ed all'applicazione di diversi gruppi protettori delle funzionalità fenoliche di composti naturali bioattivi, utilizzando come modello lo pterostilbene. Ho effettuato uno screening di possibili gruppi protettori bioreversibili seguendo un approccio prodrug al fine di migliorare la biodisponibilità dello pterostilbene a seguito della somministrazione orale. Ho sintetizzato cinque diverse tipologie di prodrugs in cui il composto fenolico è funzionalizzato ad estere fosfonico, metil tiometil etere (MTM), alchilcarbonilossimetil (ACOM) etere, alchilossicarbonilossimetil (AOCOM) etere ed N-alchil-N-alchilossicarbonilaminometil (NANAOCAM) etere. Questi derivati mostrano profili idrolitici, sia in mezzi acquosi a vari pH che in sangue di ratto, molto diversi e modulabili in funzione del gruppo utilizzato come promoiety. In questi saggi i derivati protetti con il gruppo AOCOM ed ACOM hanno dato i risultati migliori e sono stati quindi utilizzati in studi farmacocinetici *in vivo.* I grafici della concentrazione in sangue dello pterostilbene e del suo solfato – il principale metabolita - contro il tempo nel caso del derivato ACOM sono risultati molto simili a quelli ottenuti mediante somministrazione dello pterostilbene stesso. Nel caso del precursore AOCOM si osserva invece un netto spostamento a tempi più lunghi, il che indica che il composto si comporta in effetti come prodrug.

Durante il secondo anno di dottorato, ho sintetizzato due nuove classi di antitumorali selettivi derivati rispettivamente del 5-idrossipsoralene (composto naturale) e della clofazimina (farmaco anti-lebbra). Questi nuovi agenti chemioterapici (brevettati) agiscono inibendo il canale del potassio Kv 1.3 che risulta essere largamente espresso nella membrana interna mitocondriale di molti tipi di cellule tumorali. L'inibizione di tale canale porta alla morte cellulare per apoptosi. Dopo una serie di test *in vitro*, *ex vivo* ed *in vivo*, sono stati selezionati tre composti psoralenici che risultano particolarmente promettenti. I test dei derivati della clofazimina sono tuttora in corso.

Nel corso dell'ultimo anno di dottorato e soprattutto durante il periodo di collaborazione all'estero presso il Politecnico Federale di Zurigo (ETH) mi sono occupato della sintesi di nuove strutture macromolecolari auto-assemblanti per il drug delivery di farmaci antitumorali. In particolare, ho sviluppato e testato una serie di co-polimeri polimetilossazolina-co-pterostilbene e resveratrolo-OEG-co-adipato in grado di auto-

assemblare in acqua dando nanostrutture polimeriche stabili e capaci di rilasciare nel tempo i principi attivi con cui vengono prodotte e caricate. La scelta di incorporare in questi nanocarrier clofazimina è dovuta alla sua nota attività di inibizione delle pompe per la resistenza multifarmaco (MDR pumps) ed al suo nuovo potenziale impiego come agente antitumorale. I risultati conseguiti con i copolimeri di polimetilossazolina e pterostilbene mostrano la validità dell'approccio adottato in questo progetto per creare strutture co-polimeriche altamente modulabili in grado di veicolare farmaci antitumorali in tumori solidi sfruttando l'effetto EPR (Enhanced Permeability and Retention).

CHAPTER 1

GENERAL INTRODUCTION

The advent of modern medicine led to a significant improvement in the conditions and life expectancy of mankind. While humanity has always made use of natural remedies for the treatment of diseases, with the advent of the modern age, many things have changed or at least evolved. Since the mid-nineteenth century, scientists have discovered and studied tens of thousands of new chemicals with pharmacological activities. The great progress of molecular biology has led to a deeper understanding of the mechanisms that underlie many diseases such as cancer and genetic or autoimmune ailments. We also understand how deeply our diet and lifestyle influence our health.

At the same time, in the last 30 years the advent of computational chemistry allowed the creation of huge libraries of potentially bioactive molecules through predictive algorithms of increasing accuracy and reliability. Finally, improved synthetic techniques, biotechnology and more efficient, sensitive and specific characterization equipment has allowed chemists to synthesize, even on an industrial scale, almost any desired molecular structure.

Currently, research in medicinal chemistry is mainly moving in two directions: the first is oriented towards the discovery of new drugs, with increased specificity, activity and with fewer side effects; the second seeks to improve and/or enhance existing drugs that often have some problems related to their physical-chemical properties[1,2]. The project of this PhD thesis is undoubtedly ambitious. I tried to apply different types of prodrug approaches to improve the physicochemical properties and activity of synthetic and natural molecules of potential biomedical interest. The prodrug concept has been used to improve undesirable properties of drugs since the late 19th century, although it was only at the end of the 1950s that the actual term prodrug was introduced for the first time. Prodrugs are inactive, bioreversible derivatives of active molecules that must undergo an enzymatic and/or chemical transformation *in vivo* to release the active parent drug, which can then perform its desired pharmacological effect in the body. In most cases, prodrugs are simple chemical derivatives that are only one or two chemical or enzymatic steps away from the active parent drug[3], in other cases they are part of more complex structures (i.e. polymers).

The three chapters in which the thesis is divided describes and discusses results obtained in the three projects in which my research developed. Specifically, Chapter 2 deals with the *molecular* prodrug approach applied to a natural phenolic compound, pterostilbene (Figure 1), to improve its oral bioavailability. Chemical elaboration was then applied to another natural active compound, psoralen (Figure 1), and to a synthetic drug, clofazimine (Figure 1), to develop derivatives (Chapter 3) to increase their solubility and to deliver them selectively to mitochondria.

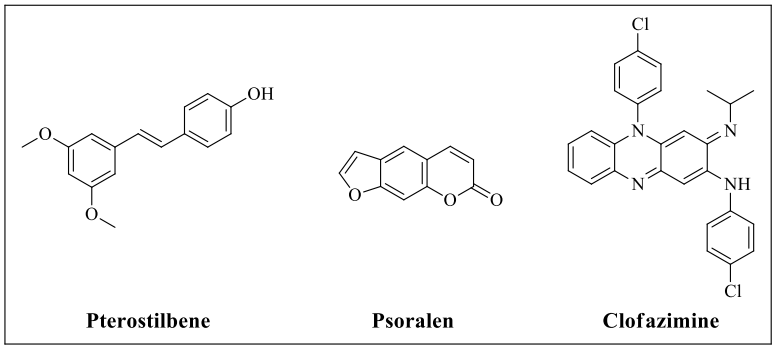

Figure 1

Finally, a *macromolecular* prodrug approach was developed (Chapter 4) with the purpose to create polymeric core-shell nanostructure for anticancer drug delivery. More details concerning these two different approaches are discussed in depth in the single chapters and briefly in the following paragraphs.

1.1. MOLECULAR PRODRUG APPROACH

The *molecular* prodrug approach is based on the synthesis of reversible derivatives with the purpose of improving the parental compounds properties altering reversibly the nature and thus the reactivity of sensitive functional groups. For example, in the case of pterostilbene, the synthetic modifications were done on the 4'-hydroxy moiety, in order to obtain a significant increase of absorption in the gut and consequently a tangible increase of the active compound concentration in blood and target tissues. To obtain this result, one should be able to modify the chemical-physical properties of the parent compound by converting it into a prodrug with suitable solubility, lipophilicity and polarity. In the case of the synthesis of new selective anticancer agents – psoralen and clofazimine derivatives – the applied approach was specifically focused to improve the accumulation capacity of these substances within the target organelles: mitochondria. For this purpose, I have decided to employ, as promoiety, short polyethylene glycol (PEG) chains or the highly specific lipophilic triphenylphosphonium cation, which is able to accumulate within mitochondria due to the potential gradient between the mitochondrial matrix and the cytoplasm. The individual synthetic strategies adopted are discussed in detail in the individual chapters.

1.2. MACROMOLECULAR PRODRUG APPROACH

The *macromolecular* prodrug approach consists in the use of drug delivery systems such as polymeric nanocarriers. This second solution may involve a direct modification of the molecular structure of the drug, or at least its physical incorporation within the structures generated by an amphiphilic co-polymer capable of self-assembling to form core-shell polymeric micelles. Among the different nanostructures, they are particularly versatile because they are characterized by an inner section (core), which can be loaded with hydrophobic drugs, and a highly hydrophilic shell that separates it from the outside (shell). The purpose of these structures is to protect the anticancer drug during its delivery to the tumor where they will be degraded releasing the drug inside the tumoral tissue. To reach the solid tumor environment, without an active targeting shell surface, these nanoparticles should be smaller than 200 nm in order to exploit the EPR (Enhanced Permeability and Retention) effect[4] as briefly discussed in Chapter 4. The systems that I have studied are constituted by new amphiphilic polymers in which the hydrophobic section is decorated with a natural polyphenol (resveratrol or pterostilbene). Once dispersed in water, these

compounds naturally tend to aggregate to give well-defined and stable polymeric micellar structures that may be loaded with highly lipophilic drugs giving an additional stabilization by exploiting hydrophobic interactions.

1.3. RATIONALE AND ORGANIZATION OF THE THESIS

As already commented in the previous sections, my thesis work is structured in three different projects, each discussed in a dedicated chapter. The common thread linking these projects is the rational design and development of new prodrugs with the aim of improving the final bioactivity of natural and synthetic compounds of potential biomedical interest.

Chapter 2 deals with the screening of different phenolic protecting group with the goal of improving pterostilbene bioavailability. This stilbenoid of the resveratrol's family is currently widely studied due to its interesting anticancer, chemopreventive and antiobesity properties[5–7]. Within this project, I have synthesized and tested several prodrugs for oral administration with the aim of increasing the final level of pterostilbene in the blood as a result of intestinal absorption. All the new synthesized derivatives have been preliminarily tested *in vitro* to study their stability under gastric- and gut-like pH conditions. Subsequently, their stability in rat blood was investigated to verify their reactivity in enzyme catalyzed hydrolysis. Only the derivatives that satisfied all our stability criteria under the different conditions mentioned above, were also tested *in vivo* in pharmacokinetic experiments in rats. These studies are necessary to determine the final concentrations in blood of the prodrug itself, of pterostilbene and of all possible metabolites after oral administrations. All these studies were performed in collaboration with the research group of Dr. Mario Zoratti of C.N.R. – Institute of Neuroscience – Padova.

In **Chapter 3,** I report the design and synthesis of two new classes of highly selective anticancer drugs. Our pharmacological target was the mitochondrial Kv 1.3 channel that seems to be expressed in many types of different cancer cell lines. The first group of synthesized compounds includes derivatives of 5-hydroxypsoralen, a natural bioactive phenolic compound. Despite the fact that this compound and a few of its known derivatives, like 5-(4-phenoxybutoxy)psoralen (PAP-1), are already inhibitors of the Kv 1.3 channel, it was decided to improve the activity of these drugs by introducing structural modification to optimize their physical-chemical properties. Specifically, the natural compound has been elaborated to improve both solubility and selectivity in order to target it efficiently to mitochondria. The same approach was also adopted for the design and synthesis of

clofazimine-based anticancer agents. Clofazimine, a synthetic drug used for the treatment of leprosy, is highly insoluble in aqueous media. To overcome this limitation, I have developed new derivatives, with solubilities in water which are up to 300 times higher than that of clofazimine. Both classes of compounds are currently be tested (*in vitro*, *in vivo* and *ex vivo*) for their activity and selectivity against several types of cancer including melanoma and chronic leukemia. All these studies are conducted in collaboration with the research group of Prof. Dr. Ildiko Szabò at the Biology Department of Padova University.

Finally, in **Chapter 4** I describe my efforts to apply the prodrug approach to a macromolecular contest. By using resveratrol and pterostilbene as models, I have synthesized two different kinds of amphiphilic copolymers capable of self-assembling in water forming stable core-shell aggregates. These can hopefully be used for the delivery of anticancer drugs to solid tumors by exploiting EPR (Enhanced Permeability and Retention) effect. During the time I spent at the ETH in Zürich, I have developed a novel class of polymethyloxazoline-pterostilbene copolymers. These constructs, definitely more performing than resveratrol-based ones, stably self-assemble in water remaining in suspension for several weeks without aggregating. Additionally, I observed that they undergo further stabilization when loaded with highly lipophilic drugs such as clofazimine. This drug was chosen both because once released in the cells it is expected to exhibit its known ability to inhibit the MDR pumps that are responsible for resistance to anticancer drugs, and because it was found to stabilize, even at very low concentration, the core of the polymeric micelles, probably thanks to hydrophobic interactions with pterostilbene units. Finally, these nanostructures have been preliminarily tested on macrophages to assess the toxicity and uptake using fluorescence microscopy techniques. The results of these very preliminary experiments are encouraging. One interesting development of this project envisions the replacement of pterostilbene with some highly lipophilic anticancer drugs to form the bioactive hydrophobic part of the copolymer.

1.4. REFERENCES

(1) Férriz, J. M.; Vinsová, J. Curr. Pharm. Des. 2010, 16, 2033–2052.

(2) Oh, D.; Oliyai, R.; Rautio, J.; Savolainen, J.; Järvinen, T.; Kumpulainen, H.; Heimbach, T. Nat. Rev. Drug Discov. 2008, 7.

(3) Raunio, H.; Rautio, J.; Huttunen, K. M. Pharmacol. Rev. 9AD, 63, 750–771.

(4) Yasuhiro, M.; Hiroshi, M. Cancer Res. 1986, 46, 6387–6392.

(5) McCormack, D.; McFadden, D. J. Surg. Res. 2012, 173, 53.

(6) Rimando, A. M.; Kalt, W.; Magee, J. B.; Dewey, J.; Ballington, J. R. J. Agric. Food Chem. 2004, 52, 4713–4719.

(7) Nikhil, K.; Sharan, S.; Singh, A. K.; Chakraborty, A.; Roy, P. Anticancer Activities of Pterostilbene-Isothiocyanate Conjugate in Breast Cancer Cells: Involvement of PPARγ. PLOS ONE, 13AD, 9.

CHAPTER 2

DEVELOPMENT AND SCREENING OF PTEROSTILBENE PRODRUGS

This chapter deals with the screening of various protecting groups for phenolic hydroxyls with the goal of improving the bioavailability of pterostilbene. This stilbenoid natural phenol of the resveratrol's family is currently been studied due to its interesting anticancer, chemopreventive and antiobesity properties. Within this project, I have synthesized and tested several potential prodrugs for oral administration with the aim of increasing the final level of pterostilbene in blood as a result of intestinal absorption. All the new synthesized derivatives have been preliminarily tested in vitro to study their stability under gastric- and gut-like pH conditions. Subsequently, their stability in rat blood was investigated to determine their resistance against enzymatic activities. Only the derivatives that satisfied all our stability criteria under the different experimental conditions mentioned above, were then tested in vivo in rats. These pharmacokinetic studies are necessary to determine the final concentration of prodrug, pterostilbene and metabolites in blood after oral administration.

2.1. INTRODUCTION

Part of my thesis research focused on extending and completing a large and comprehensive project to develop a pharmacology of natural phenolic compounds based on the prodrug approach[1]. Prodrugs intended for oral administration of natural phenolic active compounds are uncommon; therefore, a major task of the project involved finding a chemical bond system to reversibly protect the phenolic hydroxyls of polyphenols during absorption. Figure 2 summarizes the types of linkages envisioned. Several were tested including carboxyl esters[2–4], alkyl ethers, sulfonate esters[4], acetals (emiacetals and ketals)[5], N,N-disubstituted carbamates[6] and N-monosubstituted carbamates[7–9].

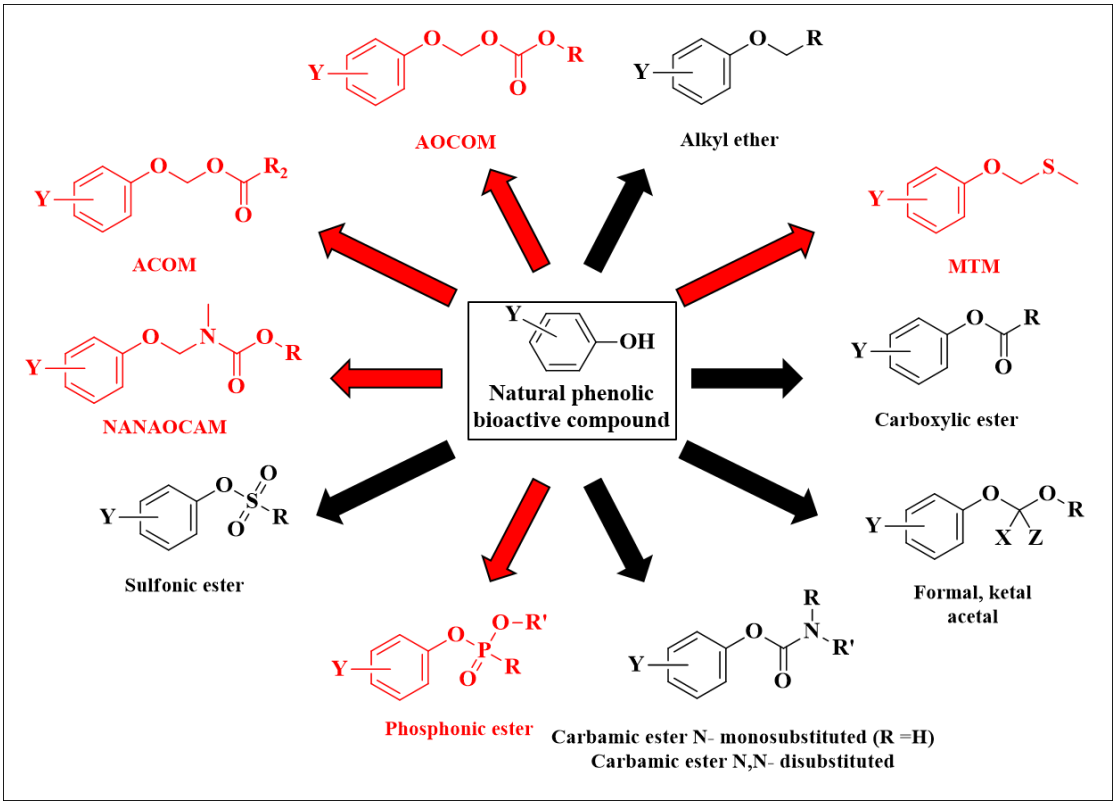

Figure 2. Phenolic protecting groups tested by my research group. In red are represented those which I developed and used during my PhD.

Most turned out to be unsuitable for a prodrug approach due to either excessive (e.g. sulfonic esters, alkyl ethers, N,N-disubstituted carbamate esters, formals) or insufficient stability (e.g. carboxylic esters, acetals, ketals) under physiological conditions to achieve first pass metabolism protection and bioconversion to the desired active phenolic compound with appropriate kinetics.

Good results were instead obtained with the N-monosubstituted carbamate ester linkage[7–9] leading also to a patent[10]. This protecting group is resistant to hydrolysis in the stomach and intestine, but releases the active compound at convenient rates in blood. Despite the

promising results obtained with this type of linkage, optimal hydroxyl protection for prodrugs of natural phenolic active compounds is still to be achieved. To tackle this goal during my thesis I developed and tested new prodrugs of pterostilbene, chosen as model natural phenol, based on the red linkages illustrated in Figure 2.

2.1.1. DEVELOPMENT OF NEW PRODRUGS OF PTEROSTILBENE

Pterostilbene (PTS, **3**, Figure 3) is a stilbenoid phenol (like resveratrol, **2**, Figure 3) that is very widespread in nature and well-studied for its interesting properties.

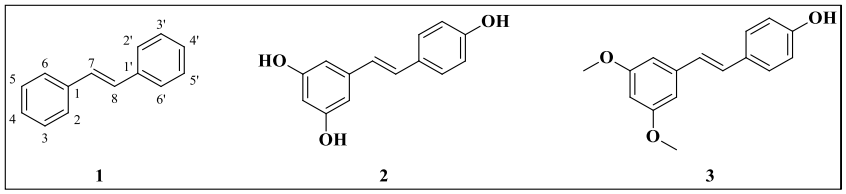

Figure 3. **1** stilbene, **2** resveratrol (RES), **3** pterostilbene (PTS).

From the biological point of view, PTS is a phytoalexin[11]. These compounds are synthesized by a number of plant species (i.e. Vitis and Vaccinum) in order to protect themselves from various molds and pathogenic agents. Pterostilbene is a resveratrol analogue and, in the last decades, it was studied to understand its important beneficial properties for human health. At variance from resveratrol that is characterized by three free hydroxyl groups, pterostilbene bears only one, because the other two (at positions 3 and 5) are methylated. This apparently slight difference has a strong impact on the chemical properties and physiological behavior of PTS. In comparison with RES (logP 3.1), PTS is more lipophilic (logP 4.1), more capable of diffusing easily into cellular compartments and more stable against metabolic modifications. This last characteristic is the most relevant because metabolic modifications often represent the major limitation in polyphenols action after dietary intake. In particular, the pharmacological interest in pterostilbene is related with its anti-inflammatory, antineoplastic and antioxidant activities[12].

In recent years many studies have investigated the biomedical properties of PTS, which can be summarily classified as 5 major activities[12–14]:

I. Antimicrobial activity: pterostilbene seems to be 5 to 10 times more effective than resveratrol in protecting plants against microbial and fungal infections. This property may reasonably also be exploited for animals and humans.

II. Antineoplastic activity: by modulating intracellular signaling and gene expression, pterostilbene is able to antagonize the onset of many types of cancer.

III. Antioxidant activity: PTS has strong antioxidant dose-dependent properties mediated by gene expression effects.

IV. Anti-inflammatory activity: many in vitro studies demonstrated that PTS inhibits prostaglandin E2 synthesis, in particular in colorectal cancer cells. Analogous studies were conducted also concerning its effects on interleukin 1-beta and on Tumor Necrosis Factor alpha (TNF-a). An upregulation of TNF-alpha, an inflammation mediator, is involved in a series of diseases including cancer and cardiovascular problems.

V. Other metabolic activities: recent studies have proved that both PTS and RES have anti-diabetes and lipid-lowering properties. They are also able to moderate the damaging effects of aging on, for example, cognition and memory.

Many different in vitro studies on normal cells demonstrated that PTS administration didn't cause adverse effects or toxicity[12].

2.1.2. PTEROSTILBENE LOW BIOAVAILABILITY AND THE PRODRUG APPROACH

Low intestinal uptake, phase-I and phase-II metabolism are the major obstacles to pterostilbene and resveratrol biological activity. In food, both RES and PTS are present in glycosylated forms. In blood, these derivatives have never been found, because the glycosidic moiety is lost during intestinal uptake. Hydroxyl groups are very reactive substrates for conjugative enzymes of phase-II metabolism that convert polyphenols into more hydrophilic metabolites (sulfonates and glucuronides[15]) that are rapidly eliminated. In view of these problems, I tried to increment the bioavailability of natural phenols – after oral administration – by protecting the critical sites against phase-II metabolic modifications.

The prodrug approach involves the reversible protection of sensitive chemical groups in order to prevent their modification. By definition, a prodrug is an inactive form of a drug, which acts as a precursor of the active principle. In case of oral administration, the modified molecular entity must be able to withstand the low stomach pH to be efficiently absorbed in the gut. Concerning the general concept and mechanism of prodrug action, Figure 4 shows a schematic representation[16].

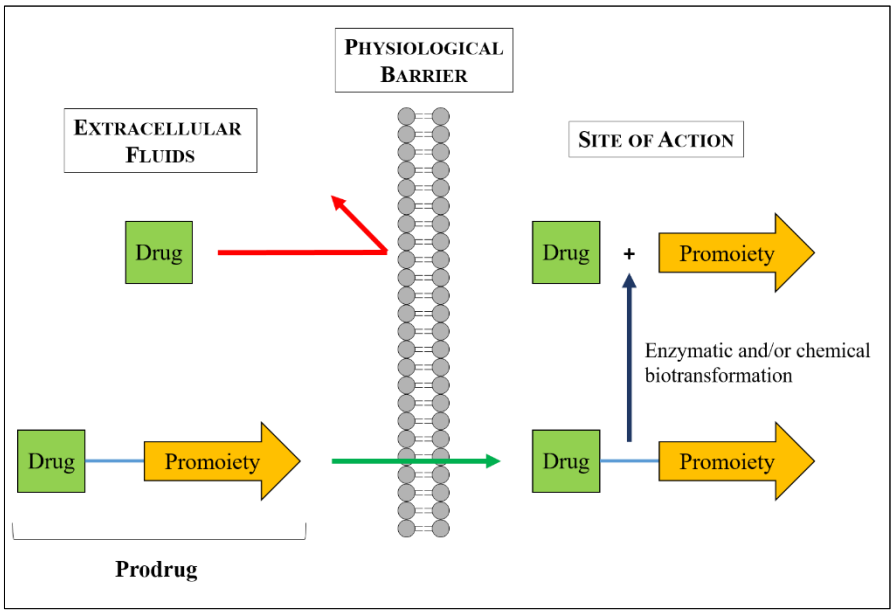

Figure 4. Schematic mechanism of prodrug action.

As shown in Figure 4, a prodrug is formed by two different components: the drug and the promoiety, linked by one of a variety of possible bioreversible groups. During my thesis, I have investigated many different linking groups with different stability profiles in order to find the best one for oral delivery purposes. In almost all cases, I used an oligoethylenglycol (OEG) chain as promoiety with the aim of improving the drug solubility. These moieties are expected to exhibit, to a degree, the favorable properties of longer polyethyleneglycol (PEG) chains, while their relatively small size allows for a more favorable drug loading capacity[5].

2.1.3. PRODRUG TYPES AND STABILITY TESTS

All the chemical modifications I have performed on pterostilbene were done in an oral delivery perspective. This kind of administration route is the most encouraged by doctors and pharmaceutical industries because it is simple, safe and the production costs are lower if compared with injectable preparations. For these reasons all the synthesized compounds were tested in buffer solution at pH 1 and 6.8 (for further details see the Material and Methods section) to simulate the stomach and gut pH values, respectively. Finally, only for the candidates that had shown the most promising hydrolysis profiles, I also performed tests in heparinized rat blood and then directly in rats. The requisites that a compound had to possess to be eligible for *in vivo* pharmacokinetics tests were as follows: slow hydrolysis rate (no more than 25% in the first 8 hours) in both buffer solutions at pH 1 and 6.8 and a half-life of more than 30 minutes in rat blood.

The results are expected to be a reasonably good approximation of the behavior in humans for our purposes, even though the stomach pH is higher in the rat (pH 3) than in humans (pH 1) and also blood enzymatic activities are somewhat different[7].

2.1.4. OVERVIEW OF SYNTHESIZED PTEROSTILBENE PRODRUGS

In Figure 5, I show all the new prodrugs of pterostilbene (PTS) I have synthesized and tested. I worked on PTS, used as a model natural polyphenol, but in principle, the same approach could be extended to other natural phenolic compounds.

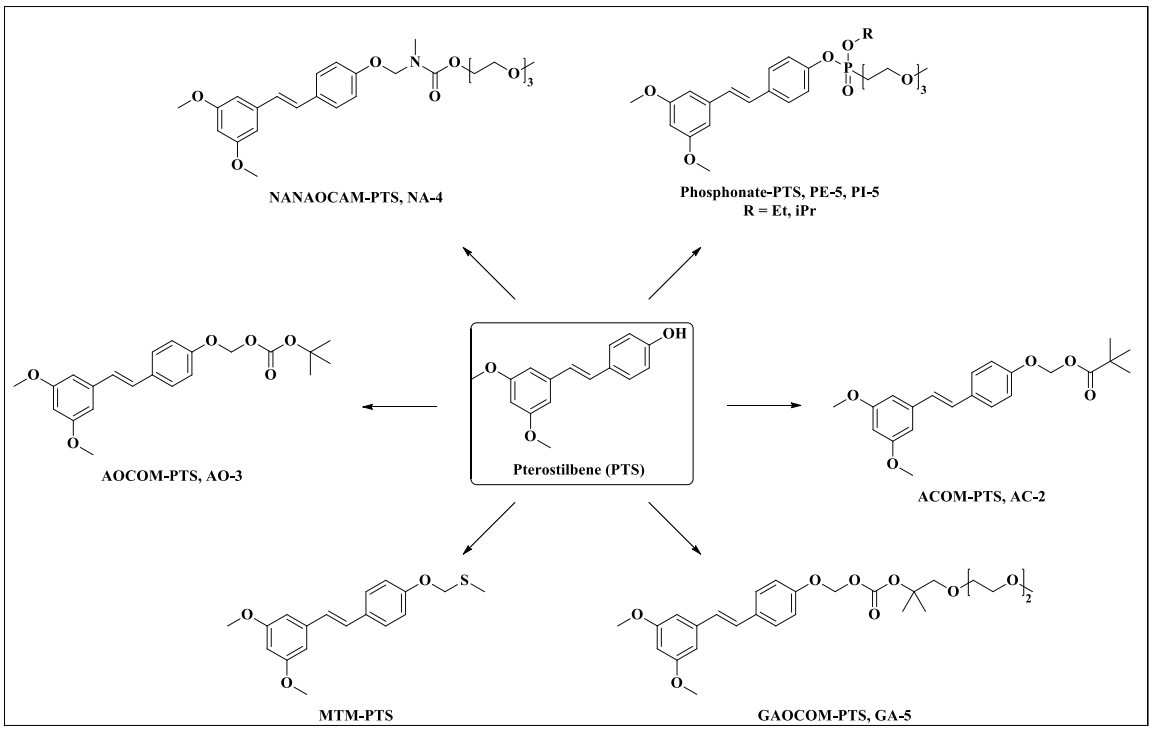

Figure 5. Summary of all the PTS prodrugs I have synthesized.

If similar derivatives were to be synthesized using other phenolic compounds, some aspects would need to be considered. The pK_a value of pterostilbene is around 9, and it is the most important parameter that could affect the stability of the linking group. Moreover, in the presence of other hydroxyl groups, which is the case in polyphenols, possible synergistic effects and charge delocalization phenomena on preferential positions of the conjugated rings system could play a role.

In the next section, I show the optimized synthetic pathways for the preparation of all the prodrugs, I comment on their characterization and I illustrate the results of stability tests.

2.2. RESULTS AND DISCUSSION

Figure 5 summarizes all the PTS derivatives I have synthesized, characterized and tested for this part of the project. In the following paragraphs, I present the complete synthesis and characterization of the PTS prodrug derivatives and the results of their stability tests already mentioned.

2.2.1. N-ALKYL-N-ALKYLOXYCARBONYLAMINOMETHYL (NANAOCAM) PTEROSTILBENE

This bioreversible group was initially designed as a carboxylic acid protecting group[17] (Figure 6). With very few modifications, I sought to apply it for phenolic group protection.

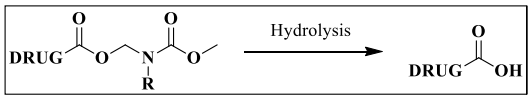

Figure 6

The synthetic strategy developed for the synthesis of NANAOCAM protecting group for pterostilbene is shown in Figure 7. All the reactions were optimized in order to obtain high purity products in good yield. The first three steps were required for the synthesis of the promoiety and only in the last step PTS was conjugated to obtain the final prodrug called NANAOCAM-PTS (**NA-4**). The first reaction is the alcohol activation of TriGME-OH by using carbonyldiimidazole (CDI) in order to create an activated carbamate group which reacts in the second step with methylamine. The obtained primary carbamate was then modified by attaching a chloro-methylene spacer by reaction with paraformaldehyde to obtain the secondary carbamate **NA-3**. Finally, the promoiety **NA-3** was conjugated with pterostilbene giving the final desired product NANAOCAM-PTS in 20% overall yield (4 steps).

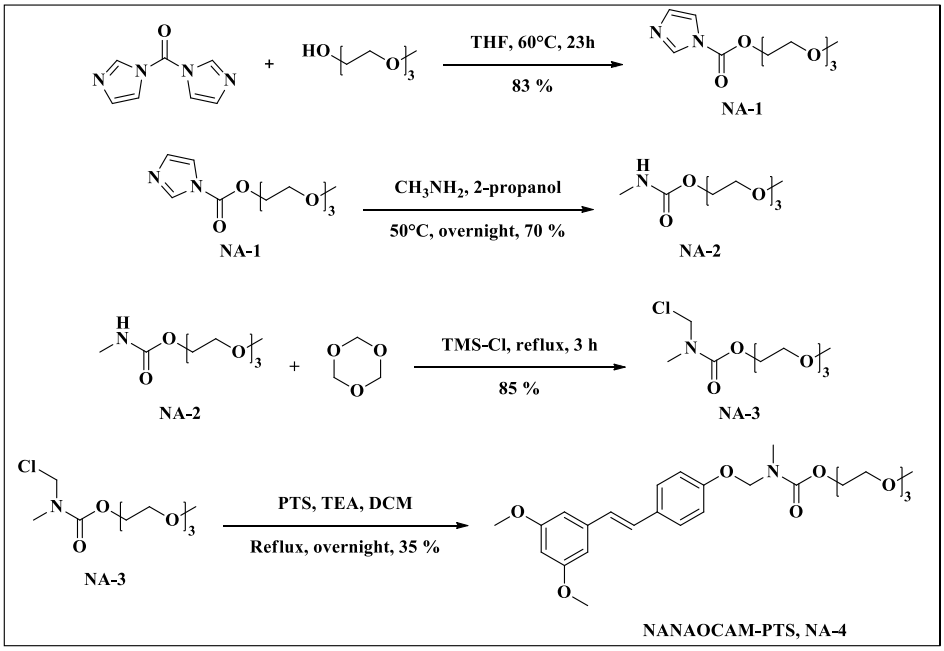

Figure 7. Synthesis of NANAOCAM-PTS.

NANAOCAM-PTS was purified and characterized by ^{1}H-NMR, ^{13}C-NMR and ESI-MS (see Materials and Methods). Concerning the stability tests, this derivative undergoes rapid hydrolysis at pH 1 in 30 minutes; at pH 6.8 the compound turned out to be stable over 8 hours. **NA-4** was then tested in heparinized rat blood and it was recovered unaltered even after 4 hours of incubation. These assays show that NANAOCAM-PTS is too stable to be of practical use as pterostilbene prodrug. Therefore, I didn't proceed with further *in vivo* test.

2.2.2. METHYLTHIOMETHYL (MTM) PTEROSTILBENE

The MTM moiety is a well-known protecting group that is usually applied to alcoholic functions. We were interested in evaluating its stability in comparison with acetal protecting groups that are reported in the literature[12]. The synthetic strategy developed for the synthesis of MTM protecting group for pterostilbene is shown in Figure 8.

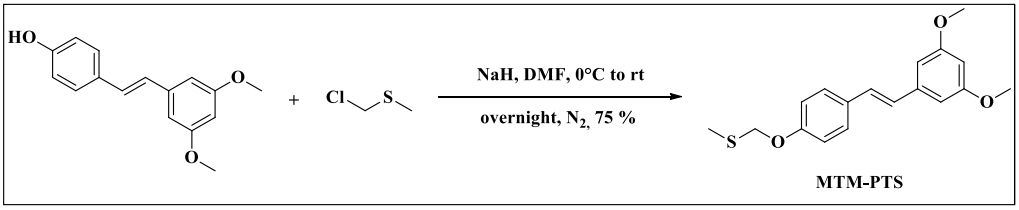

Figure 8. Synthesis of MTM-PTS.

The reaction is an S_N2 reaction between the nucleophile specie (deprotonated PTS) and the electrophilic carbon of methylthiomethyl chloride to form the methylthiomethyl ether of pterostilbene called MTM-PTS in good yield.

MTM-PTS was purified and characterized by ^{1}H-NMR, ^{13}C-NMR and ESI-MS (see Materials and Methods). This derivative exhibits a moderately fast hydrolysis rate at pH 1 with a half-life of 1 hour; at pH 6.8 the compound was stable over 8 hours. MTM-PTS was then tested in heparinized rat blood and it was recovered unaltered even after 4 hours of incubation. In view of this behavior, *in vivo* tests were not performed.

2.2.3. ALKYLCARBONYLOXYMETHYL (ACOM) PTEROSTILBENE

This protecting group can be viewed as a hybrid between an ester and an acetal and was designed for the bioreversible protection of hydroxyl groups. In particular, it is expected to be stable under pH conditions found in the stomach and in the gut, but it should rapidly reconvert to pterostilbene by esterase-mediated hydrolysis[18]. The synthetic strategy developed for the synthesis of the ACOM protecting group for pterostilbene is shown in Figure 9. For the purpose of testing preliminarily this type of protecting group on pterostilbene I chose to use the commercially available chloromethyl pivalate with a tert-butyl group on the carbonyl carbon.

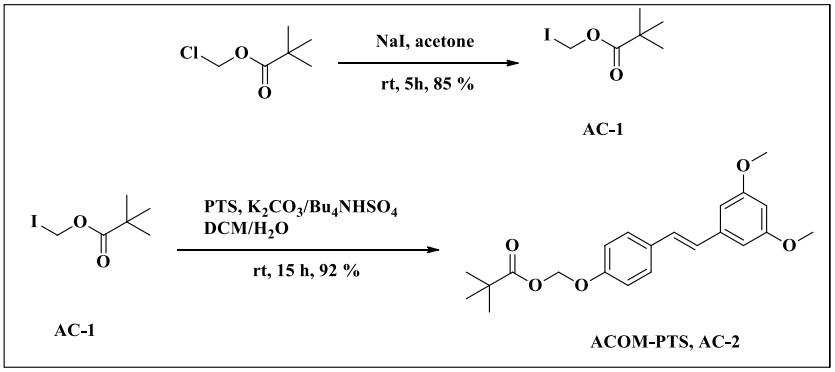

Figure 9. Synthesis of ACOM-PTS.

All the reaction steps were optimized in order to obtain high purity products in good yield. The first step involved a Finkelstein reaction (halogen substitution) performed to increase the elecrophilicity of the acetalic methylene. This derivatization was done to prevent a possible transesterification side reaction that might have occurred during the second step of the synthesis[18]. After some work to optimize the reaction conditions, the promoiety iodomethyl pivalate (**AC-1**) was successfully conjugated with pterostilbene giving the final desired product ACOM-PTS in 78% overall yield (2 steps).

ACOM-PTS was purified and characterized by ^{1}H-NMR, ^{13}C-NMR and ESI-MS (see Materials and Methods). In hydrolysis tests, this derivative turned out to be stable over 8 hours at both pH 1 and 6.8. ACOM-PTS was then tested in heparinized rat blood showing hydrolysis with a half-life of less than 10 minutes. This compound was therefore selected for *in vivo* pharmacokinetic experiments, which are described and discussed later in comparison with the results obtained with AOCOM-PTS.

2.2.4. ALKYLOXYCARBONYLOXYMETHYL (AOCOM) PTEROSTILBENE

This protecting group can be viewed as a hybrid between a carbonate and an acetal and was designed for the bioreversible protection of hydroxyl groups[19]. It is expected to be stable at pH conditions found in the stomach and the gut, but it should fast reconvert to pterostilbene by esterase-mediated hydrolysis.

In this case, I first synthesized a promoiety similar to the one used in the case of the ACOM derivative, with a tert-butyloxy group attached to the carbonyl group. The synthetic strategy developed for the synthesis of the AOCOM protecting group for pterostilbene is shown in Figure 10. All the reactions were optimized in order to obtain high purity products in good yield. The first two steps were required for promoiety synthesis and only in the last step PTS was conjugated to obtain the final prodrug, named AOCOM-PTS (**AO-3**). The first step involves the nucleophilic substitution of tert-butanol on chloromethyl chloroformate to obtain the intermediate **AO-1**. The second step, in analogy to the synthesis of the ACOM prodrug, is a Finkelstein reaction. After optimization of the reaction conditions, the iodo-promoiety was successfully conjugated with pterostilbene giving the final desired product AOCOM-PTS in 35% overall yield (3 steps).

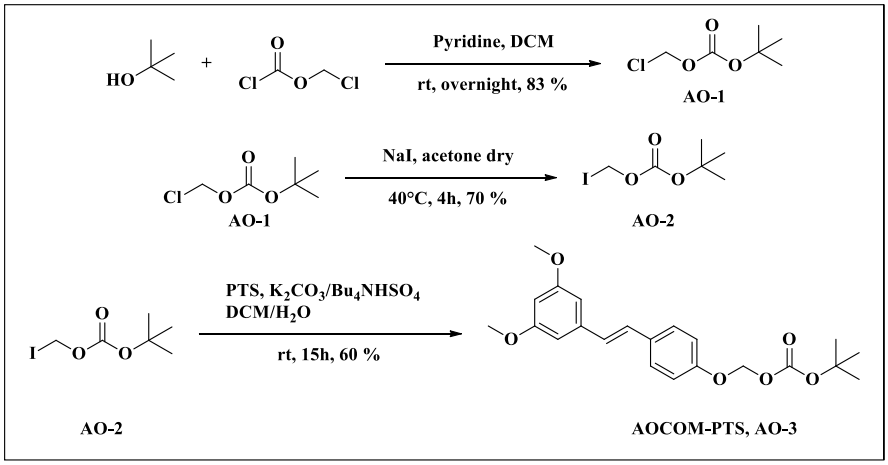

Figure 10. Synthesis of AOCOM-PTS.

AOCOM-PTS was purified and characterized by ^{1}H-NMR, ^{13}C-NMR and ESI-MS (see Materials and Methods). This derivative turned out to be stable over 8 hours at pH 1 and moderately stable at pH 6.8 with a hydrolysis conversion of around 20% over the same period. AOCOM-PTS was then tested in heparinized rat blood showing an interesting hydrolysis profile with a half-life of 35 minutes (Figure 11).

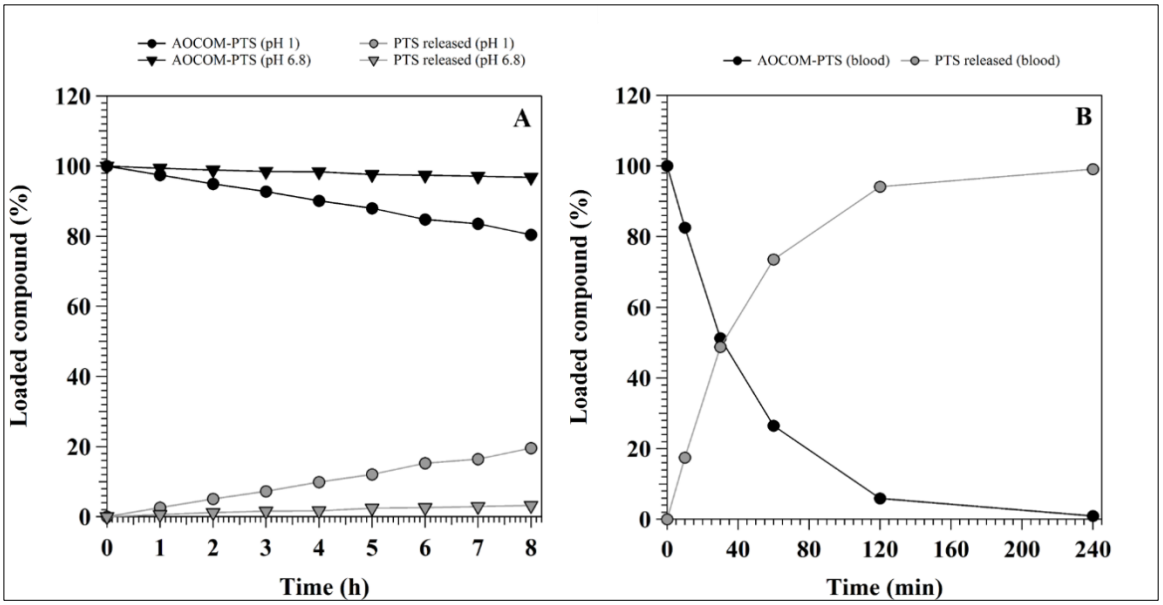

Figure 11. Stability assays for AOCOM-PTS: A) hydrolysis profiles at pH 1 and 6.8; B) hydrolysis rate in heparinized rat blood.

The compound is therefore a good candidate for pharmacokinetic tests in order to investigate the time profile of its absorption and metabolization *in vivo*. To carry out a comparative study, the two derivatives AOCOM-PTS and ACOM-PTS were tested by performing pharmacokinetic studies after oral administration to rats (Figure 12). These experiments were performed by the group of Dr. M. Zoratti at the CNR Institute of Neuroscience in Padova. Each compound was administered as a single intragastric bolus, in an equimolar dose/kg body weight (88 μmol/kg). Blood samples were taken at different time points over a 24 h period, treated and analyzed as described in the Materials and Methods section. Each experiment was replicated at least 4 times.

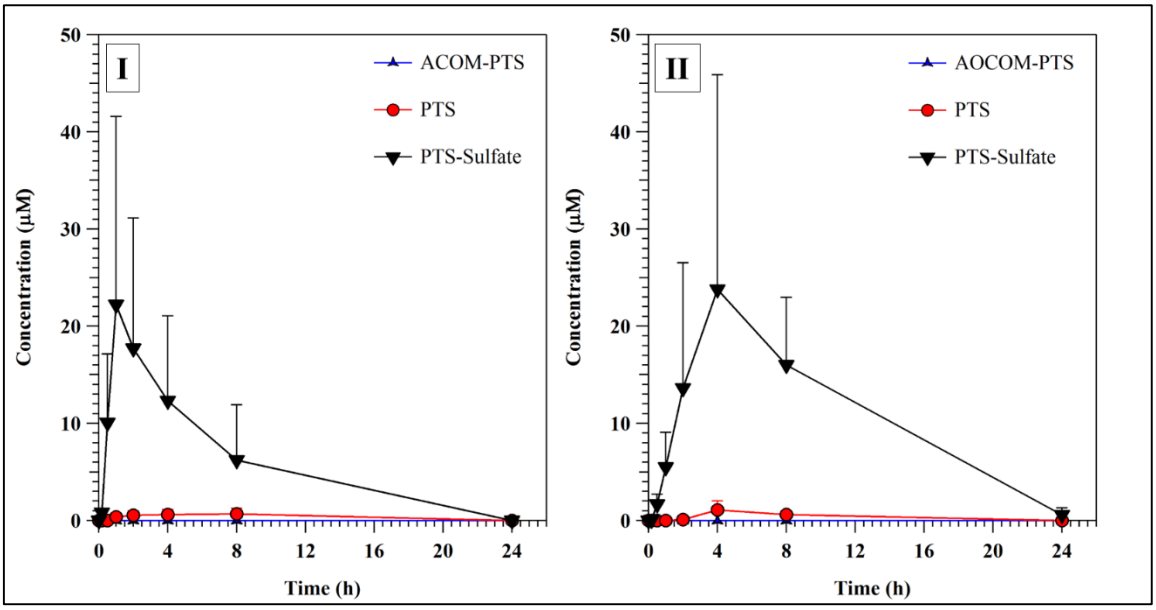

Figure 12. Blood pharmacokinetic profiles after oral administration of: (I) derivative AOCOM-PTS and (II) derivative ACOM-PTS. Results for administration of PTS itself are not shown. Reported are mean values ± SD (N = 4).

Figure 12 shows shows that the most abundant species found in the bloodstream after oral administration of both derivatives is pterostilbene-4'-sulfate (PTS-Sulfate), the main PTS phase-II metabolite in rats[20]. The most interesting difference between ACOM and AOCOM derivatives is the time needed to reach the maximum blood concentration: t_{max} for PTS-Sulfate was 1h and 4h when ACOM-PTS and AOCOM-PTS were administered, respectively. It is also important to note that in both cases the intact derivative was not detected at any time.

Time-concentration profiles obtained after administration of ACOM were very similar to that obtained after administration of pterostilbene itself[20]; this may suggest a rapid hydrolysis of the prodrug at the intestinal level, with subsequent absorption of pterostilbene. $AUC_{0\text{-}24h}$ values obtained from pharmacokinetics of the two examined derivatives were not significantly different from that obtained after administration of PTS itself (Table 1).

Administered compound	**$AUC_{0\text{-}24h}$ [(nmol/mL) x h]**		
	Intact prodrug	**PTS**	**PTS-Sulfate**
AOCOM-PTS	0	9.6 ± 5.3	261.4 ± 108.8
ACOM-PTS	0	9.8 ±7.7	146.8 ± 118.5
PTS	-	10.6 ± 3.8	327.5 ± 98.6

Table 1. AUC estimated values from AOCOM-PTS, ACOM-PTS and PTS pharmacokinetic assays. Reported are mean values ± SD (N = 4).

Even though the preliminary stability results on AOCOM-PTS have shown that it may be a good candidate for *in vivo* assays, it is still too sparingly soluble in water. In order to overcome this limit, I developed a slightly modified derivative with the same steric hindrance around the carbonate moiety, but with a shorter OEG (n = 3) substituent. This approach was adopted in an attempt to improve the solubility in physiological environments without excessively increasing the molecular weight of the prodrug and without compromising its ability to cross biomembranes.

The synthetic strategy developed for the synthesis of this derivative, GAOCOM-PTS, is shown in Figure 13. Synthesis of GAOCOM-PTS. The first step is a Fisher esterification with methanol and a catalytic amount of sulfuric acid that gives compound **GA-2** in high yield. In the second step the ester undergoes a Grignard reaction with Me-MgBr to obtain the sterically hindered tertiary alcohol **GA-3**. The next step involves the nucleophilic substitution of the alcohol **GA-3** on chloromethyl chloroformate to obtain the product **GA-4** that was modified with a Finkelstein reaction as done in the case of the ACOM and AOCOM prodrugs. Finally, the iodo-containing promoiety intermediate was successfully conjugated with pterostilbene giving the final desired product GAOCOM-PTS (**GA-5**) in 26% overall yield (5 steps).

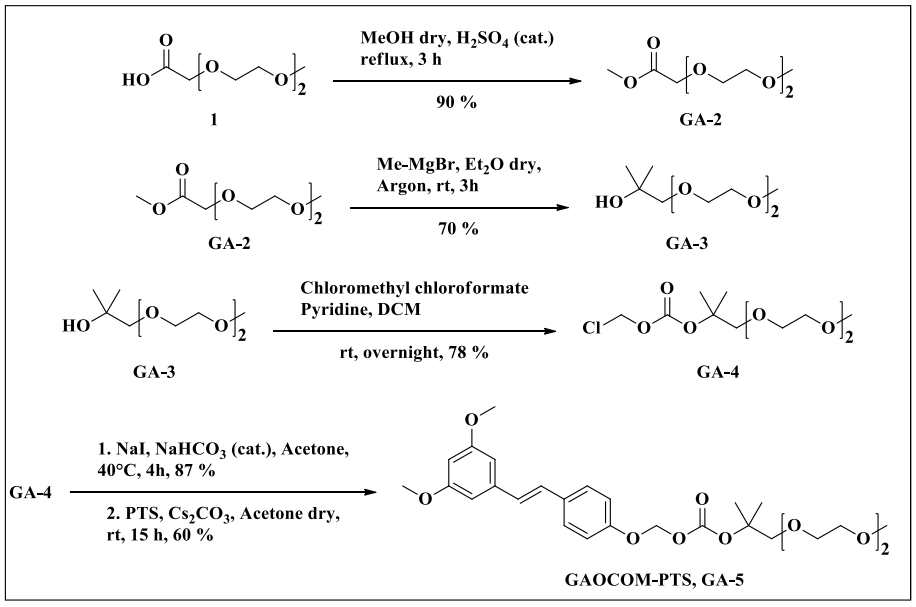

Figure 13. Synthesis of GAOCOM-PTS.

GAOCOM-PTS was purified and characterized by ^{1}H-NMR, ^{13}C-NMR and ESI-MS (see Materials and Methods). In stability tests, this derivative turned out to be stable over 8 hours at pH 1 and 6.8, showing almost the same hydrolysis behavior as AOCOM-PTS. GAOCOM-PTS was then tested in heparinized rat blood showing a rapid hydrolysis with

a half-life of less than 10 minutes. Due to this too fast blood bio-conversion rate, similar to that of ACOM-PTS, pharmacokinetic tests were not performed on this derivative.

2.2.5. PHOSPHONIC ESTER OF PTEROSTILBENE

Phosphonic acid salts and their esters have been frequently used in pharmacology (in particular for iv delivery). Their conjugation with drugs can improve the water solubility of the final prodrug[21]. Moreover, from the chemical point of view, the phosphonic esters are more stable than their carbonic counterparts.

Based upon these considerations, I synthesized two derivatives with different steric hindrance on the phosphonate ester group. These elaborations were introduced in order to improve the stability of these promoieties in the presence of lytic enzymes. The synthetic pathway used is the same for both derivatives and is shown in Figure 14.

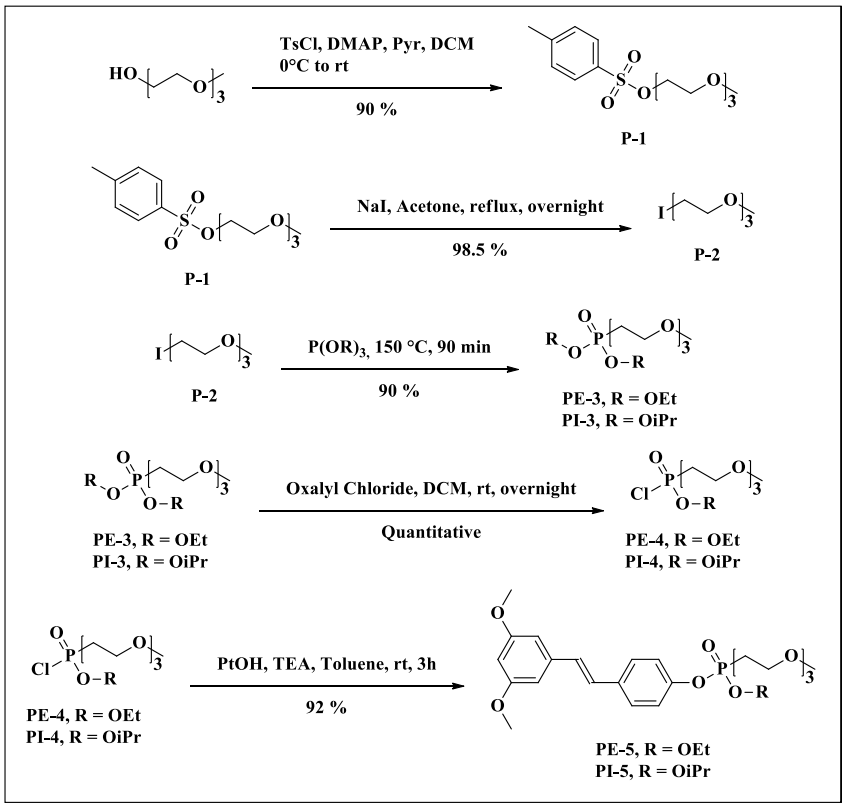

Figure 14. Synthesis of phosphonic pterostilbene esters (PE-5 and PI-5).

PE-5 and PI-5 were purified and characterized by ^{1}H-NMR, ^{13}C-NMR and ESI-MS (see Materials and Methods). These derivatives also proved stable in solutions at pH 1 and 6.8, with no hydrolysis over 8 hours. The results of blood stability assays on both PE-5 and PI-5 were at first unexpected. The percentage of PI-5 or PE-5 hydrolyzed to PTS was about 20% after 10 minutes, and remained unaltered until the end of the experiment (Figure 15,

A). One explanation for this behavior may be the irreversible inhibition by our derivatives of the enzymatic activity hydrolyzing them. In fact, organo-phosphorus compounds are well-known irreversible inhibitors of acetylcholinesterases[22]. I thus decided to investigate further this phenomenon, in order to clarify if PI-5 and PE-5 could irreversibly inhibit these enzymes. Since the two derivatives have a very similar behavior, I chose to perform the study only with PI-5.

I set up two different experiments to demonstrate the effect of enzymatic irreversible inhibition by PI-5. In the first (Figure 15, B), different volumes of blood were added to an initial blood sample spiked with 50 μM PI-5, and the amount of released PTS was monitored by UHPLC. In the second (Figure 15, C), three different blood samples were spiked with three different concentrations of PI-5 (5, 25 and 50 μM), and the amount of released PTS was monitored.

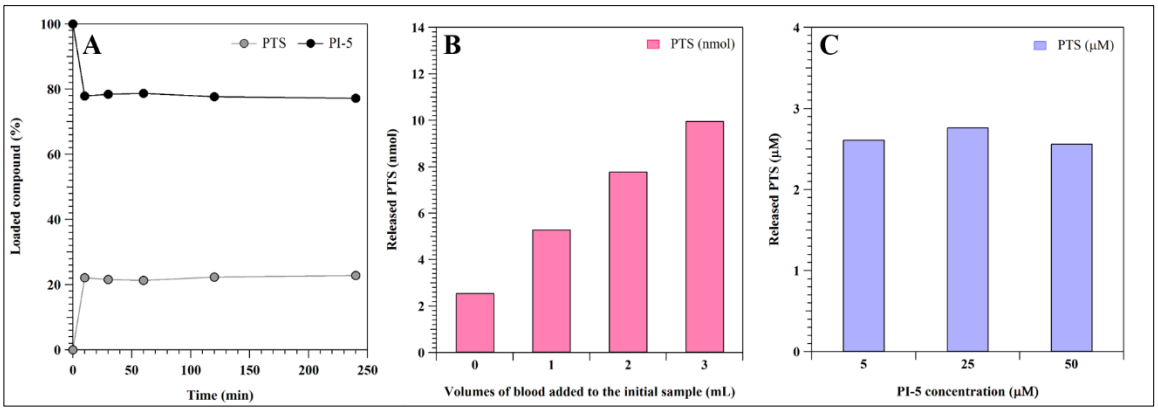

Figure 15. Blood stability profiles of PI-5. (A). Relative percentages of PI-5 and released Pterostilbene in blood; an initial concentration of 5 μM PI-5 was used. (B). Released pterostilbene as a function of increasing volumes of blood added to the initial sample (1 mL; 50 μM PI-5). (C). Released pterostilbene as a function of the initial PI-5 concentration.

The obtained results confirm our hypothesis of an irreversible enzymatic inhibition, with 0.27 ± 0.01 nmol of derivative poisoning the enzymatic component of 1 mL of rat blood. Based on these results it is evident that these PTS prodrugs will not ever be applicable as prodrugs, because of their irreversible poisoning effect on fundamentals enzymes like acetylcholinesterase. Due to this reason, I did not proceed with pharmacokinetic tests.

2.3. Conclusions and Perspectives

In conclusion, the screening of bioreversible protecting groups for developing useful prodrugs of the bioactive natural phenol pterostilbene revealed two promising candidates. ACOM-PTS was synthesized easily using commercially available reagents and showed good stability under stomach- and gut-like pH. Its “Achille’s heel” may however be a fast

enzymatic blood hydrolysis with a half-life of less than 10 minutes. Deprotection may be too rapid to allow ACOM-PTS to be taken up by enterocytes in the gut wall and to be effectively distributed into the organism avoiding phase-II metabolism modifications. On the other hand, a more favorable behavior was observed with AOCOM-PTS. Also in this case, the synthesis was straightforward and the results of hydrolysis experiments in buffer solutions were encouraging. Moreover, half-life in blood was nearly 40 minutes. This derivative showed interesting pharmacokinetic profiles, with a blood concentration vs. time curve shifted to longer times in comparison to PTS. $AUC_{0\text{-}24h}$ for PTS was substantially the same as that obtained administering pterostilbene itself. With the goal of maintaining AOCOM-bond properties while improving water solubility, I synthesized a slightly modified derivative (GAOCOM-PTS) decorated with an OEG chain. The synthesis was challenging and indeed the solubility was improved, but unfortunately stability in blood was unsatisfactory, with a half-life time of less than 10 minutes.

Even though GAOCOM-PTS and ACOM-PTS are not promising for oral delivery purposes, they remain interesting alternatives for other ways of administration (i.e. intravenous or intraperitoneal). In addition, I would like to emphasize that this was a screening study for new possible protecting groups for phenolic functions, with many possible applications in the pharmaceutical field. My work has confirmed the important role of the promoiety; as in the case of AOCOM-PTS and GAOCOM-PTS a modest modification of the structure in that part of the prodrug drastically changed the behavior of the prodrug. This example points to the possibility of modulating drug intestinal adsorption and blood stability by making relatively small chemical variations in the promoiety, without affecting the hydrolysis rate during stomach and gut transit.

2.4. EXPERIMENTAL SECTION

2.4.1. MATERIALS AND METHODS

Pterostilbene was purchased from Wonda Science (Changzhou, Jiang, People's Republic of China, batch n. WF12062501). Resveratrol was purchased from Waseta Int. Trading Co. (Shangai, China). Other starting materials and reagents were purchased from Sigma-Aldrich (Milan, Italy), Fluka (Milan, Italy), Merck-Novabiochem (Milan, Italy), Riedel de Haen (Milan, Italy), J.T. Baker (Milan, Italy), Cambridge Isotope Laboratories Inc. (Rome, Italy), Acros Organics (Milan, Italy), Carlo Erba (Milan, Italy), and Prolabo (Milan, Italy) and were used as received. TLCs were run on silica gel supported on plastic (Macherey-Nagel Polygram®SIL G/UV254, silica thickness 0.2 mm, Duren, Germany) and visualized by UV detection. Flash chromatography was performed on silica gel (Macherey-Nagel 60, 230–400 mesh granulometry (0.063–0.040 mm)) under air pressure. The solvents were analytical or synthetic grade and were used without further purification. ^{1}H-NMR spectra were recorded with a Bruker spectrometer operating at 300 MHz and a Bruker AVII500 spectrometer (Milan, Italy) operating at 500 MHz. Chemical shifts (δ) are given in ppm relative to the signal of the solvent. HPLC-UV analyses were performed with an Agilent 1290 Infinity LC System (Agilent Technologies, Milan, Italy), equipped with binary pump and a diode array detector (190–500 nm). HPLC/ESI-MS analyses and mass spectra were performed with a 1100 Series Agilent Technologies (Milan, Italy) system, equipped with binary pump (G1312A) and MSD SL Trap mass spectrometer (G2445D SL) with ESI source. ESI-MS positive spectra of reaction intermediates and final purified products were obtained from solutions in acetonitrile, eluting with a water:acetonitrile = 1:1 mixture containing 0.1% formic acid. HPLC/ESI-MS analysis was used to confirm the purity (>95%).

Animals. Adult male Wistar rats (approximately 400 g body weight) from the facility of the Department of Biomedical Sciences were used for pharmacokinetic experiments. All experiments involving animals were performed after approval by the University of Padova Ethical Committee for Experimentation on Animals (CEASA) (Permit Number: 80/2011) and by the Italian Ministry of Health, and with the supervision of the Central Veterinary Service of the University of Padova, in compliance with Italian Law DL 116/92, embodying UE Directive 86/609.

HPLC-UV Analysis. Samples (2 µl) were analyzed by HPLC/UV (1290 Infinity LC System, Agilent Technologies) using a reverse phase column (Zorbax RRHD Eclipse Plus C18, 1.8 µm, 50 x 2.1 mm i.d.; Agilent Technologies) and a UV diode array detector (190-500 nm). Solvents A and B were water containing 0.1% trifluoroacetic acid (TFA) and acetonitrile, respectively. The gradient for B was as follows: 10% (0.5 min) then from 10% to 100% in 5 min; the flow rate was 0.6 mL/min. The eluate was preferentially monitored at 286, 300 and 320 nm (corresponding to absorbance maxima of the internal standard, derivatives/metabolites and pterostilbene, respectively). The column compartment was maintained at 35°C.

Hydrolysis Reactions. The chemical stability of all new compounds was tested in aqueous media approximating gastric (0.1 N HCl, NormaFix) and intestinal (0.1 M PBS buffer, pH 6.8) pH values. A 5 µM solution of the compound was prepared from a 5 mM stock solution in DMSO, and incubated at 37°C for 24 hours; samples withdrawn at different times were analyzed by HPLC-UV. Hydrolysis products were identified by comparison of chromatographic retention time with true samples.

Hydrolysis in blood. Rats were anesthetized and blood was withdrawn from the jugular vein, heparinized and transferred into tubes containing EDTA. Blood samples (1 mL) were spiked with compound (5 µM; dilution from a 5 mM stock solution in DMSO), and incubated at 37°C for 4 hours (the maximum period allowed by blood stability). Aliquots were taken after 10 min, 30 min, 1 h, 2 h and 4 h and treated as described below. Cleared blood samples were finally subjected to HPLC-UV analysis.

Blood Sample Treatment and Analysis. Before starting the treatment, 4,4'-dihydroxybiphenyl was added as internal standard to a carefully measured blood volume (25 µM final concentration). Blood was then stabilized with a freshly-prepared 10 mM solution of ascorbic acid (0.1 vol) and acidified with 0.6 M acetic acid (0.1 vol); after mixing, an excess of acetone (4 vol) was added, followed by sonication (2 min) and centrifugation (12,000 g, 7 min, 4°C). The supernatant was finally collected and stored at -20°C. Before analysis, acetone was allowed to evaporate at room temperature using a Univapo 150H (UniEquip) vacuum concentrator centrifuge, and up to 40 µL of ACN were added to precipitate residual proteins. After centrifugation (12,000 g, 5 min, 4°C), cleared samples were directly subjected to HPLC-UV analysis.

Metabolites and hydrolysis products were identified by comparison of chromatographic retention time with true samples. Briefly, the recovery yield of each analyte was calculated as the ratio of the amount recovered to that of recovered internal standard. Knowledge of

these ratios allowed us to determine the amount of analyte in a blood/organ sample by measuring the recovery of the internal standard.

Pharmacokinetics Studies:

Blood. Analyzed derivatives were administered to overnight-fasted male rats as a single intragastric dose (88 µmol/Kg, dissolved in 250 µL DMSO). Blood samples were obtained by the tail bleeding technique: before drug administration, rats were anesthetized with isoflurane and the tip of the tail was cut off; blood samples (80-100 µL each) were then taken from the tail tip at different time points after drug administration. Blood was collected in heparinized tubes, kept in ice and treated as described above (blood sample treatment and analysis) within 10 min.

NANAOCAM Synthesis

2-(2-(2-methoxyethoxy)ethoxy)ethyl 1H-imidazole-1-carboxylate, [NA-1]: 2-(2-(2-methoxyethoxy)ethoxy)ethanol (TriGME, 1.5 g, 9 mmol, 1 equiv) was reacted with 1,1'-carbonyldiimidazole (4.5 g, 27 mmol, 3 equiv) in THF (60 mL) at 60°C for 18 hours. The solvent was evaporated under vacuum, the oily residue was purified by using DCM/acetone (50:50) as eluent to afford **NA-1** (1.95 g, 7.5 mmol, 83 %). ^{1}H-NMR (500 MHz, $CDCl_3$) δ = 8.04 (s, 1H), 7.33 (t, J = 1.4 Hz, 1H), 6.96 – 6.93 (m, 1H), 4.48 – 4.41 (m, 2H), 3.76 – 3.70 (m, 2H), 3.61 – 3.57 (m, 2H), 3.56 – 3.54 (m, 2H), 3.53 – 3.50 (m, 2H), 3.43 – 3.39 (m, 2H), 3.25 (s, 3H) ppm. ^{13}C NMR (126 MHz, $CDCl_3$) δ 148.52, 137.00, 130.42, 117.03, 77.16, 71.73, 70.54, 70.44, 70.43, 68.42, 66.99, 58.83 ppm. ESI-MS (ion trap): m/z: 259 [$M+H^+$].

2-(2-(2-methoxyethoxy)ethoxy)ethyl methylcarbamate, [NA-2]: **NA-1** (1.95 g 7.5 mmol, 1 equiv) was coupled with aqueous methylamine (760 mg, 10 mmol, 1.3 equiv) in 2-propanol (25 mL) at 50°C overnight. The reaction mixture was then concentrated under vacuum. The oily residue was purified by flash chromatography by using DCM/acetone (70:30, R_f = 0.3) as eluent to afford **NA-2** (1.2 g, 5.3 mmol, 70 %). ^{1}H NMR (200 MHz, $CDCl_3$) δ = 4.83 (s, 1H), 4.18 (dd, J = 5.4, 4.0 Hz, 3H), 3.76 – 3.57 (m, 10H), 3.55 – 3.44 (m, 2H), 3.34 (s, 3H), 2.74 (s, 4H) ppm. ^{13}C NMR (50 MHz, $CDCl_3$) δ = 77.16, 71.97, 70.56, 69.67, 63.97, 59.05, 27.58 ppm. ESI-MS (ion trap): m/z: 244 [$M+Na^+$].

2-(2-(2-methoxyethoxy)ethoxy)ethyl (chloromethyl)(methyl)carbamate, [NA-3]: a suspension of **NA-2** (370 mg, 1.7 mmol, 1 equiv), paraformaldehyde (255 mg, 2.8 mmol, 1.7 equiv) and trimethylsilyl chloride (2.4 g, 23.5 mmol, 13 equiv) was refluxed with $CaCl_2$ drying tube on the top of water condenser, for 3 hours. The suspension was diluted with DCM (50 mL) and filtered to remove the unreacted paraformaldehyde. The filtrate solution was concentrated under reduced pressure. The yellow oil **NA-3** (359 mg, 1.4 mmol, 85 %) was used without any further purification. ^{1}H NMR (500 MHz, $CDCl_3$) δ = 5.29 (s, 2H), 4.24 (dd, J = 14.0, 8.2 Hz, 2H), 3.76 – 3.56 (m, 8H), 3.54 – 3.46 (m, 2H), 3.34 (s, 3H), 2.97 (s, 3H) ppm. ^{13}C NMR (126 MHz, $CDCl_3$) δ = 155.62, 77.16, 71.97, 70.65, 69.25, 65.64, 62.57, 62.00, 59.06, 33.98, 33.75 ppm. ESI-MS (ion trap): m/z: 288 [$M+H_2O^+$].

(E)-2-(2-(2-methoxyethoxy)ethoxy)ethyl ((4-(3,5-dimethoxystyryl)phenoxy)methyl) (methyl)carbamate, [NA-4]: triethylamine (125 mg, 1.3 mmol, 1 equiv) and pterostilbene (310 mg, 1.2 mmol, 1 equiv) were dissolved in dry DCM (20 mL) and stirred for 1 hour. After this time, a solution of **NA-3** (360 mg, 1.3 mmol, 1.1 equiv) in DCM (5 mL) was added dropwise. The resulting mixture was stirred for 48 hours at reflux. The reaction mixture was washed with water and brine (40 mL). The organic phase was dried over $MgSO_4$, filtered and dried under vacuum. The resulting material was purified by flash chromatography by using DCM/acetone (85:15, R_f = 0.3) as eluent to afford 4 (135 mg, 0.3 mmol, 25 %). ^{1}H NMR (500 MHz, $CDCl_3$) δ 7.43 (d, J = 8.6 Hz, 1H), 7.06 – 6.86 (m, 2H), 6.64 (d, J = 1.6 Hz, 1H), 6.37 (s, 1H), 5.31 (d, J = 17.9 Hz, 1H), 4.26 (s, 1H), 3.82 (s, 3H), 3.73 – 3.57 (m, 4H), 3.52 (d, J = 4.3 Hz, 1H), 3.35 (d, J = 7.2 Hz, 1H), 3.02 (d, J = 9.7 Hz, 1H) ppm. ^{13}C NMR (126 MHz, $CDCl_3$) δ 161.06, 156.44, 156.26, 139.67, 130.94, 128.69, 127.92, 127.29, 127.10, 116.65, 116.11, 104.46, 99.80, 72.01, 70.70, 70.66, 69.46, 65.16, 59.11, 55.43, 33.85, 33.08 ppm. ESI-MS (ion trap): m/z: 508, [$M+H_2O^+$].

MTM Synthesis

(E)-((4-(3,5-dimethoxystyryl)phenoxy)methyl)(methyl)sulfane (PtO-MTM): pterostilbene (600 mg, 2.3 mmol, 1 equiv) was stirred for 30 minutes at 0°C in DMF (20 mL) with NaH (60 mg, 2.6 mmol, 1.1 equiv). Then, a solution of (chloromethyl)(methyl)sulfane (255 μL, 3.0 mmol, 1.3 equiv) in DMF (5 mL) was added dropwise. After the addition, the ice-water bath was removed and the reaction was stirred under nitrogen overnight. Then, 25 mL of deionized water were added to the mixture and the aqueous phase was extracted twice with 50 mL of EtOAc. The organic phases were

collected and dried over $MgSO_4$. The solution was dried under vacuum and next it was purified by flash chromatography by using petroleum ether/DCM (50:50, R_f = 0.4) as eluent to afford ACOM-MTM (550 mg, 1.75 mmol, 75 %) as pale yellow oil. ^{1}H NMR (500 MHz, $CDCl_3$) δ = 7.43 (d, J = 8.6 Hz, 1H), 7.06 – 6.86 (m, 2H), 6.64 (d, J = 1.6 Hz, 1H), 6.37 (s, 1H), 5.31 (d, J = 17.9 Hz, 1H), 4.26 (s, 1H), 3.82 (s, 3H), 3.73 – 3.57 (m, 4H), 3.52 (d, J = 4.3 Hz, 1H), 3.35 (d, J = 7.2 Hz, 1H), 3.02 (d, J = 9.7 Hz, 1H) ppm. ^{13}C NMR (126 MHz, $CDCl_3$) δ = 161.06, 156.44, 156.26, 139.67, 130.94, 128.69, 127.92, 127.29, 127.10, 116.65, 116.11, 104.46, 99.80, 72.01, 70.70, 70.66, 69.46, 65.16, 59.11, 55.43, 33.85, 33.08 ppm. ESI+-MS (ion trap): m/z: 508, $[M+H_2O^+]$.

ACOM Synthesis

Iodomethyl pivalate, [AC-1]: chloromethyl pivalate (500 mg, 3.3 mmol, 1 equiv) was dissolved in dry acetonitrile (25 mL) and NaI (1000 mg, 6.5 mmol, 2 equiv) was added and the resulting mixture was stirred for 5 hours at 40°C. Then the mixture was concentrated using rotary evaporator and triturated with DCM for 30 minutes. The mixture was filtered and concentrated to give crude **AC-1** (288 mg, 1.2 mmol) as a brown oil and was used without any further purification.

(**E)-(4-(3,5-dimethoxystyryl)phenoxy)methyl pivalate, [AC-2]**: a mixture of pterostilbene (235 mg, 0.9 mmol, 1 equiv) and K_2CO_3 (380 mg, 2.7 mmol, 3 equiv) in 14 mL of water was stirred several minutes before adding tetrabutylammonium hydrogen sulfate (310 mg, 0.9 mmol, 1 equiv) and 7 mL of DCM. After several minutes of stirring, a solution of **AC-1** (290 mg, 1.2 mmol, 1.3 equiv) in 7 mL of DCM was added dropwise to the mixture. The resulting biphasic system was allowed to mix overnight and after this time, the organic phase was separated and the organic phase was extracted twice with DCM (2 x 40 mL). All organic phases were combined, dried over $MgSO_4$. The solution was dried under vacuum and next it was purified by flash chromatography by using petroleum ether/acetone (95:5 to 90:10, R_f = 0.3) as eluent to afford ACOM-OPt (313 mg, 0.8 mmol, 92 %) as pale yellow oil. ^{1}H NMR (300 MHz, $CDCl_3$) δ = 7.44 (d, J = 8.7 Hz, 2H), 7.12 – 6.85 (m, 4H), 6.64 (d, J = 2.2 Hz, 2H), 6.38 (s, 1H), 5.77 (s, 2H), 3.81 (s, 6H), 1.21 (s, 9H) ppm. ^{13}C NMR (75 MHz, CDCl3) δ = 177.46, 161.12, 156.71, 139.58, 132.00, 128.49, 127.92, 127.70, 116.48, 104.59, 99.91, 85.76, 55.45, 39.04, 27.09, 27.01 ppm. ESI+-MS (ion trap): m/z: 371, $[M+H^+]$.

AOCOM Synthesis

Tert-butyl (chloromethyl) carbonate, [AO-1]: to an ice-cold solution of chloromethyl chloroformate (835 mg, 6.5 mmol, 1.2 equiv) in DCM (15 mL) was added pyridine (515 mg, 6.5 mmol, 1.2 equiv) dissolved in DCM (5 mL) dropwise over 10 minutes. The mixture was allowed to warm to room temperature and was stirred overnight. The reaction mixture was then washed with 1M HCl (20 mL) and water (40 mL). The extracted organic phase was dried over $MgSO_4$, filtered and concentrated under vacuum (35°C, 650 mbar) to give **AO-1** as a colorless oil (740 mg, 4.4 mmol, 82% yield). ^{1}H-NMR (500 MHz, $CDCl_3$): δ = 5.68 (s, 2H), 1.52 (s, 9H) ppm; ^{13}C-NMR (126 MHz, $CDCl_3$): δ = 151.44 (C=O), 84.31 (CH_2), 71.77, 27.67 (CH_3) ppm; ESI-MS (ion trap): m/z: 168 [$M+H^+$].

Tert-butyl (chloromethyl) carbonate, **[AO-2]**: **AO-1** was dissolved in dry acetone (25 mL) and NaI (630 mg, 4.2 mmol, 2 equiv) was added. After some minutes, $NaHCO_3$ (18 mg, 0.2 mmol, 0.1 equiv) was added to the solution and the resulting mixture was stirred for 4 hours at 40°C. Then the mixture was concentrated under vacuum and triturated with DCM for 30 minutes. The mixture was filtered and concentrated to give crude **AO-2** (368 mg, 1.4 mmol) as a brown oil and was used without any further purification.

(E)-tert-butyl ((4-(3,5-dimethoxystyryl)phenoxy)methyl) carbonate, [AO-3]: a mixture of pterostilbene (280 mg, 1.1 mmol, 1 equiv) and K_2CO_3 (455 mg, 3.3 mmol, 3 equiv) in 14 mL of water was stirred several minutes before adding tetrabutylammonium hydrogen sulfate (370 mg, 1.1 mmol, 1 equiv) and 7 mL of DCM. After several minutes of stirring, a solution of **AO-2** (370 mg, 1.4 mmol, 1.3 equiv) in 7 mL of DCM was added dropwise to the mixture. The resulting biphasic system was allowed to mix overnight and after this time, the organic phase was separated and the organic phase was extracted twice with DCM (2 x 40 mL). All organic phases were combined, dried over $MgSO_4$. The solution was dried under vacuum and next it was purified by flash chromatography by using petroleum ether/acetone (95:5 to 90:10, R_f = 0.2) as eluent to afford **AO-3** (320 mg, 0.8 mmol, 82 %). ^{1}H-NMR (300 MHz, $CDCl_3$): δ = 7.44 (d, J = 8.6 Hz, 2H), 7.10 – 6.97 (m, 3H), 6.94 (s, 1H), 6.64 (d, J = 1.8 Hz, 2H), 6.38 (s, 1H), 5.72 (s, 2H), 3.81 (s, 6H), 1.50 (s, 9H) ppm. ^{13}C-NMR (75 MHz, $CDCl_3$): δ = 161.11, 156.64, 152.44, 139.55, 132.13, 128.48, 127.91, 127.70, 116.59, 104.56, 99.95, 87.84, 83.34, 77.16, 55.43, 27.75 ppm. ESI+-MS (ion trap): m/z: 387, [$M+H^+$].

GAOCOM Synthesis

Methyl 2-(2-(2-methoxyethoxy)ethoxy)acetate, [GA-2]: to a solution of dry methanol (50 mL, 2 mL/mmol) and 1 (4 mL, 26.0 mmol) was added H_2SO_4 (2.1 mL, 81μL/mmol) and was stirred at reflux for 3 hours. The mixture was allowed to room temperature and concentrated under vacuum. The resulted yellow oil was diluted in Et_2O (100 mL) and washed with $NaHCO_3$ (1 x 50 mL, satured solution) and brine (1 x 50 mL); the aqueous phases were mixed and extracted using DCM (3 x 75 mL). All the organic phases were dried with $MgSO_4$, filtered and concentrated to give a pale yellow oil. Next it was purified by flash chromatography by using DCM/Et_2O (80:20, R_f = 0.7) as eluent to afford **GA-2** (4.40 g, 23 mmol, 88 %). ^{1}H NMR (300 MHz, $CDCl_3$) δ = 4.17 (s, 2H), 3.81 – 3.68 (m, 7H), 3.60 (ddd, J = 9.1, 6.4, 4.0 Hz, 4H), 3.38 (s, 3H) ppm. ^{13}C NMR (75 MHz, $CDCl_3$) δ = 170.76, 71.83, 70.84, 70.58, 70.45, 68.53, 58.89, 51.61 ppm. ESI-MS (ion trap): m/z: 193 [M+H$^+$].

1-(2-(2-methoxyethoxy)ethoxy)-2-methylpropan-2-ol, [GA-3]: to an ice-cold solution of **GA-2** (1.0 g, 5.2 mmol, 1 equiv) in dry Et_2O (20 mL) under Argon atmosphere was added CH_3MgBr (3 M solution in Et_2O, 5.2 mL, 15.7 mmol, 3 equiv) by syringe pump over 30 minutes. After the addition, the ice-water bath was removed and the system was allowed to room temperature for 3 hours. After this time, the reaction was quenched with NH_4Cl (100 mL, satured solution). The organic phase was washed with brine (2 x 80 mL) and then the aqueous phases were mixed and extracted with DCM (3 x 75 mL). All the organic phases were dried with $MgSO_4$, filtered and concentrated to give a colorless oil. Next it was purified by flash chromatography by using DCM/Et_2O + 1% MeOH (50:50, R_f = 0.2) as eluent to afford **GA-3** (698 mg, 3.6 mmol, 70 %). ^{1}H NMR (300 MHz, $CDCl_3$) δ = 3.72 – 3.63 (m, 6H), 3.58 – 3.52 (m, 2H), 3.38 (s, 3H), 3.33 (s, 2H), 2.81 (s, 1H), 1.20 (s, 6H) ppm. ^{13}C NMR (75 MHz, $CDCl_3$) δ = 125.47, 79.74, 71.94, 71.12, 70.53, 70.49, 70.21, 58.98, 58.97, 26.09, 25.99 ppm. ESI-MS (ion trap): m/z: 210 [M+NH_4^+].

Chloromethyl (1-(2-(2-methoxyethoxy)ethoxy)-2-methylpropan-2-yl) carbonate [GA-4]: to an ice-cold solution of **GA-3** (700 mg, 3.6 mmol, 1 equiv) and chloromethyl chloroformate (515 mg, 4.0 mmol, 1.1 equiv) in dry DCM (25 mL), pyridine (287 mg, 4.4 mmol, 1.2 equiv) was added dropwise. After the addiction the reaction was allowed to room temperature for 15 hours. After this time, the mixture was diluted with DCM (100 mL) and

washed with HCl 0.5 M (50 mL) and brine (50 mL). Then the aqueous phases were mixed and extracted with DCM (2 x 50 mL). All the organic phases were dried with $MgSO_4$, filtered and concentrated to give a colorless oil. Next it was purified by flash chromatography by using DCM/Et_2O (50:50, R_f = 0.7) as eluent to afford **GA-4** (805 mg, 2.8 mmol, 78 %). ^{1}H NMR (300 MHz, $CDCl_3$) δ = 5.68 (s, 2H), 3.70 – 3.61 (m, 8H), 3.57 – 3.51 (m, 2H), 3.38 (s, 3H), 1.51 (s, 6H) ppm. ^{13}C NMR (75 MHz, $CDCl_3$) δ = 151.31, 85.00, 75.99, 72.01, 71.78, 71.20, 70.60, 59.03, 23.00, 22.88 ppm. ESI-MS (ion trap): m/z: 302 [M+NH4+], 308 [M+Na^+].

Iodomethyl (1-(2-(2-methoxyethoxy)ethoxy)-2-methylpropan-2-yl) carbonate [GA-4i]: to a stirred solution of **GA-4** (400 mg, 1.4 mmol, 1 equiv) and NaI (315 mg, 2.1 mmol, 1.5 equiv) in dry acetone (20 mL) at 40°C was added $NaHCO_3$ (12 mg, 0.1 mmol, 0.1 equiv). After 4 hours, the solvent was evaporated and the residue was triturated in cold DCM (60 mL) for 1 hour. Then the solution was filtered and evaporated under vacuum to give **GA-4i** as a pale yellow oil (460 mg, 1.2 mmol, 87% crude yield) that was used for the next step without any further purifications.

(E)-(4-(3,5-dimethoxystyryl)phenoxy)methyl (1-(2-(2-methoxyethoxy)ethoxy)-2-methylpropan -2-yl) carbonate [GA-5]: a mixture of pterostilbene (115 mg, 0.4 mmol, 1 equiv) and Cs_2CO_3 (145 mg, 0.4 mmol, 1 equiv) in dry acetone (20 mL) was stirred at 0°C. After 30 minutes, **GA-4i** (250 mg, 0.7 mmol, 1.5 equiv) was added and the mixture was heated at 40°C for 4 hours. Acetone was removed in vacuum. The residue was taken up with DCM (40 mL) and filtered. The filtrate was condensed and the residue was purified by preparative HPLC (Ace 5 AQ column, V10-2677, 150 x 21.2 mm id) using ACN (with 0.05% of TFA) and water (with 0.05 % of TFA) as eluents staring from 10% of ACN to 100% of ACN in 25 minutes to give **GA-5** as colorless oil (135 mg, 0.3 mmol) in 60% yield. ^{1}H NMR (300 MHz, $CDCl_3$) δ = 7.44 (d, J = 8.7 Hz, 2H), 7.04 (d, J = 8.8 Hz, 2H), 6.92 (d, J = 16.3 Hz, 2H), 6.65 (d, J = 2.3 Hz, 2H), 6.38 (t, J = 2.2 Hz, 1H), 5.71 (s, 2H), 3.82 (s, 6H), 3.61 (dd, J = 6.6, 3.3 Hz, 8H), 3.54 – 3.47 (m, 2H), 3.36 (s, 3H), 1.49 (s, 6H) ppm. ^{13}C NMR (75 MHz, $CDCl_3$) δ = 161.09, 156.60, 152.35, 139.53, 132.16, 128.45, 127.90, 127.72, 116.61, 104.55, 99.95, 87.97, 84.17, 76.17, 72.04, 71.24, 70.62, 59.07, 55.82, 55.44, 23.17, 23.05 ppm. ESI+MS (ion trap): m/z: 522, [M+Na^+].

Etyloxy-Phosphate Synthesis

2-(2-(2-methoxyethoxy)ethoxy)ethyl 4-methylbenzenesulfonate [**P-1**]: Pyridine (1.1 mL, 13.5 mmol, 2 eq.) and DMAP (1.65 g, 13.5 mmol, 2 eq.) were added to a solution of 2-(2-(2-methoxyethoxy)ethoxy)ethanol (1.11 g, 6.75 mmol, 1 eq.) in dichloromethane (10 mL), and the mixture was stirred at 0 °C for 15 min. A solution of tosyl chloride (1.95 g, 10.1 mmol, 1.5 eq.) in dichloromethane (10 mL) was then added dropwise and the mixture was stirred at room temperature for 4 hours. The mixture was diluted in dichloromethane (150 mL) and washed with 0.5 N HCl (100 mL). The aqueous layer was washed with dichloromethane (5 × 75 mL) and all the organic fractions were collected, dried over $MgSO_4$ and filtered. The solvent was evaporated under reduced pressure and the residue was purified by flash chromatography by using DCM/EtOAc (80: 20, R_f = 0.3) to obtain **P-1** (1.7 g, 6.1 mmol, 90% yield) as a colorless oil. ^{1}H-NMR (250 MHz, $CDCl_3$) δ = 2.43 (s, 3H, Ar-C*H*$_3$), 3.35 (s, 3H, -O-C*H*$_3$), 3.49-3.66 (m, 10H, 2 × -O-C*H*$_2$-C*H*$_2$-O- + -O-C*H*$_2$-), 4.14 (t, 2H, Ts-C*H*$_2$-, $^3J_{H-H}$ = 5.75 Hz), 7.32 (d, 2H, 2 × Ar-*H*, $^3J_{H-H}$ = 8.25 Hz), 7.77 (d, 2H, 2 × Ar-*H*, $^3J_{H-H}$ = 8.25 Hz) ppm. ^{13}C-NMR (62.9 MHz, $CDCl_3$) δ = 144.7, 132.9, 129.7, 127.9, 71.8, 70.6, 70.5, 70.4, 69.2, 68.6, 58.9, 21.6 ppm. ESI-MS (ion trap): m/z 337 $[M+H_2O+H]^+$.

1-iodo-2-(2-(2-methoxyethoxy)ethoxy)ethane [P-2]: a solution of **P-1** (1 g, 3.10 mmol, 1 eq.), NaI (990 mg, 9.4 mmol, 2 eq.) in dry acetone (8 mL) was stirred under reflux for overnight. The mixture was filtered, washed with acetone and dried under vacuum. The residue was dissolved in 150 mL of DCM and washed twice with 1 M sodium thiosulfate (50 mL) and brine (50 mL). The organic phase was dried over MgSO4 and filtered. The solvent was removed under reduced pressure and the residue was purified by flash chromatography by using DCM/Et_2O (80:20, R_f = 0.4) to obtain **P-2** (835 mg, 3.05 mmol, 98% yield) as a pale yellow oil. ^{1}H NMR (300 MHz, $CDCl_3$) δ = 3.76 (t, *J* = 6.9 Hz, 2H), 3.70 – 3.63 (m, 6H), 3.56 (dd, *J* = 5.8, 3.2 Hz, 2H), 3.38 (s, 3H), 3.30 – 3.22 (m, 2H) ppm**.** ^{13}C NMR (75 MHz, $CDCl_3$) δ = 71.98, 70.65, 70.26, 59.09, 2.94 ppm. ESI-MS (ion trap): m/z 275 $[M+H]^+$.

Diethyl (2-(2-(2-methoxyethoxy)ethoxy)ethyl)phosphonate [PE-3]: the compound **P-2** (365 mg, 1.34 mmol, 1 eq.) was dissolved in $P(OEt)_3$ (1.90 mL, 8.03 mmol, 6 eq.) and

heated up to 150°C and stirred for 1h at this temperature. The excess of $P(OEt)_3$ was removed in high vacuum and the residue was purified by flash chromatography by using $CHCl_3$/Acetone (80:20, R_f = 0.25) to obtain **PE-3** (325 mg, 1.15 mmol, 85% yield) as a pale oil. ^{1}H NMR (300 MHz, $CDCl_3$) δ = 4.18 – 4.02 (m, 4H), 3.73 (dt, *J* = 11.0, 7.6 Hz, 2H), 3.67 – 3.59 (m, 6H), 3.58 – 3.51 (m, 2H), 3.38 (s, 3H), 2.13 (dt, *J* = 18.7, 7.6 Hz, 2H), 1.32 (t, *J* = 7.1 Hz, 6H) ppm. ^{13}C NMR (75 MHz, $CDCl_3$) δ = 73.90, 72.46, 72.05, 70.52, 70.18, 68.70, 68.33, 67.08, 65.15, 63.58, 63.36, 61.56, 59.99, 59.67, 58.12, 56.26, 27.96, 27.83, 26.15, 24.46, 18.95, 17.23, 15.61 ppm. ESI-MS (ion trap): m/z 285 $[M+H]^+$.

Ethyl (2-(2-(2-methoxyethoxy)ethoxy)ethyl)phosphonochloridate [PE-4]: to a solution of **PE-3** (325 mg, 1.1 mmol, 1 eq.) in dry DCM (6 mL) was added dropwise oxalyl chloride (2.9 g, 22.7 mmol, 20 eq.) and the resulting mixture was stirred overnight at room temperature. The solvent was removed under a stream of nitrogen and dried under high vacuum. The remaining residue **PE-4** (290 mg, 1.06 mmol, 93 %) was used for the next step without any further purification. ^{1}H NMR (200 MHz, $CDCl_3$) δ = 4.29 (td, *J* = 16.2, 7.2 Hz, 2H), 3.94 – 3.48 (m, 10H), 3.38 (s, 3H), 2.54 (dt, *J* = 17.9, 7.3 Hz, 2H), 1.40 (t, *J* = 7.1 Hz, 3H) ppm.

(E)-4-(3,5-dimethoxystyryl)phenyl ethyl (2-(2-(2-methoxyethoxy) ethoxy) ethyl) phosphonate [PE-5]: to a solution of **PE-4** (290 mg, 1.06 mmol, 1 eq.) in dry toluene (4 mL) was added a solution of pterostilbene (PTS, 545 mg, 2.1 mmol, 2 eq.) and triethylamine (538 mg, 5.3 mmol, 5 eq.) in dry toluene (4 mL). The resulting mixture was stirred for 3 h at room temperature and then concentrated to dryness. The residue was purified by flash chromatography by using DCM/Acetone (80:20, R_f = 0.25) to obtain **PE-5** (480 mg, 0.97 mmol, 91% yield) as a pale pink oil. ^{1}H NMR (500 MHz, $CDCl_3$) δ = 7.46 (d, *J* = 8.6 Hz, 2H), 7.20 (d, *J* = 8.3 Hz, 2H), 7.03 (d, *J* = 16.3 Hz, 1H), 6.95 (d, *J* = 16.2 Hz, 1H), 6.65 (d, *J* = 2.2 Hz, 2H), 6.39 (t, *J* = 2.2 Hz, 2H), 4.28 – 4.11 (m, 2H), 3.82 (s, 8H), 3.65 – 3.60 (m, 6H), 3.54 (dd, *J* = 5.6, 3.7 Hz, 2H), 3.37 (s, 3H), 2.30 (dt, *J* = 18.8, 7.5 Hz, 2H), 1.31 (t, *J* = 7.1 Hz, 3H) ppm. ^{13}C NMR (126 MHz, $CDCl_3$) δ = 161.25, 150.23, 150.16, 139.43, 134.33, 128.90, 128.29, 128.06, 121.05, 121.01, 104.79, 100.29, 72.17, 70.81, 70.74, 70.53, 65.13, 62.95, 62.89, 59.27, 55.59, 27.90, 26.79, 16.64, 16.59 ppm. ESI^+-MS (ion trap): m/z: 495, $[M+H^+]$; 517, $[M+Na^+]$.

Isopropyloxy-Phosphate Synthesis

Diisopropyl (2-(2-(2-methoxyethoxy)ethoxy)ethyl)phosphonate [PI-3]: the compound **P-2** (400 mg, 1.46 mmol, 1 eq.) was dissolved in $P(OiPr)_3$ (2.16 mL, 8.76 mmol, 6 eq.) and heated up to 150°C and stirred overnight at this temperature. The excess of $P(OiPr)_3$ was removed in high vacuum and the residue was purified by flash chromatography by using $CHCl_3$/Acetone (80:20, R_f = 0.30) to obtain **PI-3** (413 mg, 1.32 mmol, 90% yield) as a pale oil. ^{1}H NMR (500 MHz, $CDCl_3$) δ = 4.75 – 4.64 (m, 2H), 3.71 (dd, *J* = 15.9, 8.7 Hz, 2H), 3.67 – 3.60 (m, 6H), 3.55 (dd, *J* = 5.7, 3.7 Hz, 2H), 3.38 (s, 3H), 2.15 – 2.04 (m, 2H), 1.31 (dd, *J* = 6.2, 1.1 Hz, 12H) ppm. ^{13}C NMR (126 MHz, $CDCl_3$) δ = 70.50 (d, *J* = 5.3 Hz), 70.07 (d, *J* = 5.3 Hz), 24.00 (d, *J* = 6.9 Hz) ppm. ESI-MS (ion trap): m/z 313 [$M+H^+$].

Isopropyl (2-(2-(2-methoxyethoxy)ethoxy)ethyl)phosphonochloridate [PI-4]: to a solution of **PI-3** (413 mg, 1.3 mmol, 1 eq.) in dry DCM (6 mL) was added dropwise oxalyl chloride (3.6 g, 26.4 mmol, 20 eq.) and the resulting mixture was stirred overnight at room temperature. The solvent was removed under a stream of nitrogen and dried under high vacuum. The remaining residue **PI-4** (376 mg, 1.3 mmol, 99 %) was used for the next step without any further purification. ^{1}H NMR (500 MHz, $CDCl_3$) δ = 4.96 (qd, *J* = 12.3, 6.2 Hz, 1H), 3.87 – 3.78 (m, 2H), 3.68 – 3.61 (m, 6H), 3.56 (dd, *J* = 5.6, 3.5 Hz, 2H), 3.38 (s, 3H), 2.52 (dt, *J* = 18.1, 7.3 Hz, 2H), 1.40 (t, *J* = 6.0 Hz, 6H) ppm. ^{13}C NMR (126 MHz, $CDCl_3$) δ = 73.47 (d, *J* = 8.3 Hz), 23.91 (d, *J* = 4.6 Hz), 23.34 (d, *J* = 4.8 Hz) ppm.

(E)-4-(3,5-dimethoxystyryl)phenyl isopropyl (2-(2-(2-methoxyethoxy)ethoxy)ethyl) phosphonate [PI-5]: to a solution of **PI-4** (376 mg, 1.3 mmol, 1 eq.) in dry toluene (4 mL) was added a solution of pterostilbene (670 mg, 2.6 mmol, 2 eq.) and triethylamine (660 mg, 6.5 mmol, 5 eq.) in dry toluene (4 mL). The resulting mixture was stirred for 3 h at room temperature and then evaporated to dryness. The residue was purified by flash chromatography by using DCM/Acetone (80:20, R_f = 0.30) to obtain **PI-5** (415 mg, 0.8 mmol, 63% yield) as a colorless oil. ^{1}H NMR (200 MHz, $CDCl_3$) δ = 7.46 (d, *J* = 8.6 Hz, 2H), 7.21 (d, *J* = 7.7 Hz, 2H), 7.11 – 6.87 (m, 2H), 6.66 (d, *J* = 2.2 Hz, 2H), 6.40 (t, *J* = 2.1 Hz, 1H), 4.82 (dhept, *J* = 18.5, 6.1 Hz, 1H), 3.89 – 3.73 (m, 8H), 3.68 – 3.50 (m, 6H), 3.37 (s, 3H), 2.28 (dt, *J* = 18.8, 7.6 Hz, 2H), 1.30 (dd, *J* = 19.3, 6.2 Hz, 6H) ppm. ^{13}C NMR (50 MHz, $CDCl_3$) δ = 161.08, 150.00, 139.28, 134.06, 128.66, 128.18, 127.84, 120.98, 120.89, 104.61, 100.12, 72.00, 71.87, 71.73, 70.61 (d, *J* = 3.5 Hz), 70.58, 70.33, 65.09, 59.12,

55.44, 29.09, 26.31, 24.14, 24.02, 23.61 (t, J = 6.0 Hz) ppm. ESI-MS (ion trap): m/z 508 [M+H$^+$].

2.5. REFERENCES

(1) Biasutto, L.; Zoratti, M. *Curr. drug Metab.* **2014**, *15*, 77–95.

(2) Biasutto, L.; Marotta, E.; Bradaschia, A.; Fallica, M.; Mattarei, A.; Garbisa, S.; Zoratti, M.; Paradisi, C. *Bioorganic & Med. Chem. Lett.* **2009**, *19*, 6721–6724.

(3) Biasutto, L.; Marotta, E.; De Marchi, U.; Zoratti, M.; Paradisi, C. *J. Med. Chem.* **2007**, *50*, 241–253.

(4) Biasutto, L.; Marotta, E.; Mattarei, A.; Beltramello, S.; Caliceti, P.; Salmaso, S.; Bernkop-Schnurch, A.; Garbisa, S.; Zoratti, M.; Paradisi, C. *Cell. Physiol. Biochem. : Int. J. Exp. Cell. Physiol. Biochem. Pharmacol.* **2009**, *24*, 557–566.

(5) Mattarei, A.; Azzolini, M.; Carraro, M.; Sassi, N.; Zoratti, M.; Paradisi, C.; Biasutto, L. Acetal Derivatives as Prodrugs of Resveratrol. *Molecular Pharmaceutics*, 2013, *10*, 2781–2792.

(6) Mattarei, A.; Carraro, M.; Azzolini, M.; Paradisi, C.; Zoratti, M.; Biasutto, L. *Molecules* **2014**, *19*, 15900–15917.

(7) Mattarei, A.; Azzolini, M.; Spina, M. L.; Zoratti, M.; Paradisi, C.; Biasutto, L. *Sci. Rep.* **2015**, *5*.

(8) Azzolini, M.; Mattarei, A.; La Spina, M.; Marotta, E.; Zoratti, M.; Paradisi, C.; Biasutto, L. *Mol. Pharm.* **2015**, *12*, 3441–3454.

(9) Mattarei, A.; Azzolini, M.; Zoratti, M.; Biasutto, L.; Paradisi, C. *Molecules* **2015**, *20*, 16085–16102.

(10) Mattarei, A.; Biasutto, L.; Zoratti, M.; Paradisi, C.; Marotta, E.; Garbisa, S.; Azzolini, M.; Bradaschia, A.; Carraro, M.; Sassi, N. New derivatives of resveratrol - EP2774915 A1, January 20, 2016.

(11) Rimando, A. M.; Kalt, W.; Magee, J. B.; Dewey, J.; Ballington, J. R. *J. Agric. Food Chem.* **2004**, *52*, 4713–4719.

(12) Kondratyuk, T. P.; Park, E.-J.; Marler, L. E.; Ahn, S.; Yuan, Y.; Choi, Y.; Yu, R.; van Breemen, R. B.; Sun, B.; Hoshino, J.; Cushman, M.; Jermihov, K. C.; Mesecar, A. D.; Grubbs, C. J.; Pezzuto, J. M. *Mol. Nutr. & Food Res.* **2011**, *55*, 1249–1265.

(13) Mena, S.; Rodríguez, M. L.; Ponsoda, X.; Estrela, J. M.; Jäättela, M.; Ortega, A. L. *PLoS ONE* **2012**, *7*.

(14) McCormack, D.; McFadden, D. *J. Surg. Res.* **2012**, *173*, 53.

(15) Kapetanovic, I.; Muzzio, M.; Huang, Z.; Thompson, T.; McCormick, D. *Cancer Chemother. Pharmacol.* **2010**, *68*, 593–601.

(16) Raunio, H.; Rautio, J.; Huttunen, K. M. *Pharmacol. Rev.* **9AD**, *63*, 750–771.

(17) Majumdar, S.; Sloan, K. B. *Bioorganic & Med. Chem. Lett.* **2007**, *17*, 1447–1450.

(18) Thomas, J. D.; Sloan, K. B. *Tetrahedron Lett.* **2007**, *48*, 109–112.

(19) Thomas, J. D.; Sloan, K. B. *Int. J. Pharm.* **2009**, *371*, 25–32.

(20) Azzolini, M.; La Spina, M.; Mattarei, A.; Paradisi, C.; Zoratti, M.; Biasutto, L. *Mol. Nutr. & Food Res.* **2014**, *58*, 2122–2132.

(21) Férriz, J. M.; Vinsová, J. *Curr. Pharm. Des.* **2010**, *16*, 2033–2052.

(22) Colović, M. B.; Krstić, D. Z.; Lazarević-Pašti, T. D.; Bondžić, A. M.; Vasić, V. M. *Curr. Neuropharmacol.* **2013**, *11*, 315–335.

CHAPTER 3

NEW PSORALEN AND CLOFAZIMINE ANALOGUES AS SELECTIVE TUMOR KILLING AGENTS

Here I report the design and synthesis of 2 new different classes of highly selective anticancer drugs. Our pharmacological target was the mitochondrial Kv 1.3 channel which is expressed in many types of different cancer cell lines. The first group of derivatives were designed starting from 5-hydroxypsoralen, a natural phenolic compound. Despite the fact that such compound and many of its derivatives, like PAP-1, are known inhibitors of the Kv 1.3 channel, it was decided to develop new analogues with better physico-chemical properties and thus hopefully more powerful bioactivity. To do so, the molecular scaffold has been modified trying to improve both the solubility and selectivity in order to target the obtained products specifically and efficiently to mitochondria. The same approach was adopted also for the design and synthesis of the other class of prodrugs, based on the synthetic drug clofazimine.

3.1. INTRODUCTION

3.1.1. PSORALENS AND CLOFAZIMINE AS MITOKV 1.3 INHIBITORS

Psoralen and other furocoumarins are present in vegetables such as figs and parsley. Psoralen is widely used as a photosensitizer, in combination with UVA radiation, to treat skin conditions such as psoriasis (a T-cell mediated inflammatory autoimmune disorder), eczema and mycosis. As first reported in 1994 by Bohuslavizki et al.[1], compounds containing this ring system can inhibit certain K+-selective ion channels. In 2004 the group of H. Wulff and K.G. Chandy characterized the action of Psora-4, PAP-1 (Figure 16) and other similar compounds on K^+ channels, demonstrating a considerable selectivity for Kv1.3[2]. This particular channel is expressed in the plasma membrane of lymphocytes, and it plays a fundamental role in the clonal proliferation of these cells following immunostimulation. Hence, the idea of using psoralens to fight autoimmune disorders[2,3], which however seems now to have been abandoned in favour of derivatives of the membrane-impermeant peptide inhibitor ShK, ShK-186. This is an inhibitor of Kv1.3 (with an IC50 of 69 pM) which has recently been reported to reduce weight gain in mice receiving a fattening diet[4]. However, the psoralen compounds have a proven and excellent safety profile in humans[2]. Other possible applications include occlusive vascular disease, such as atherosclerosis, neointimal hyperplasia[5], restenosis[6]. Methoxypsoralen (5-MOP, Figure 16) is presently in clinical trial for cutaneous T-cell lymphoma.

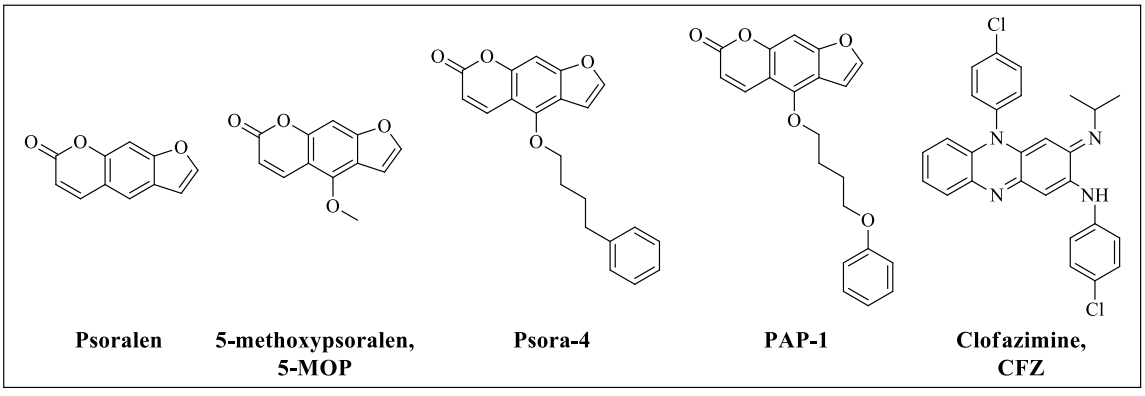

Figure 16. Psoralens and clofazimine currently employed for chemotherapies.

In 2005 Szabò et al. discovered Kv1.3 in the inner membrane of T lymphocyte mitochondria[1]. In several cell types screened subsequently, the presence of a mitochondrial population goes hand in hand with the expression of the same channels in the plasma membrane[2,3] which is high in several cancerous cell lines[4]. Subsequent studies have shown that these mitochondrial channels take part in the process of apoptotic cell death, during

which they interact with and are blocked by the proapoptotic protein Bax after its insertion into the outer mitochondrial membrane[5,6] (Figure 17). Since they can permeate biomembranes, while peptide inhibitors of Kv channels cannot, Psora-4 and PAP-1 can reach and inhibit mitochondrial Kv1.3[3] channels, thus provoking cell death even in the absence of Bax and its homolog Bak[3,7]. These compounds have been tested in studies with cultured lymphocytic cancer cells, primary lymphocytes isolated from the blood of Chronic Lymphocytic Leukemia (CLL) patients, and experimental melanoma in a murine model. While they are effective, concentrations in the range of several μM units are needed (in experiments with cells in suspension), which are hard to reach because of low solubility (a low concentration of an organic co-solvent generally needs to be employed). The chemotherapeutic outcome is thus incomplete.

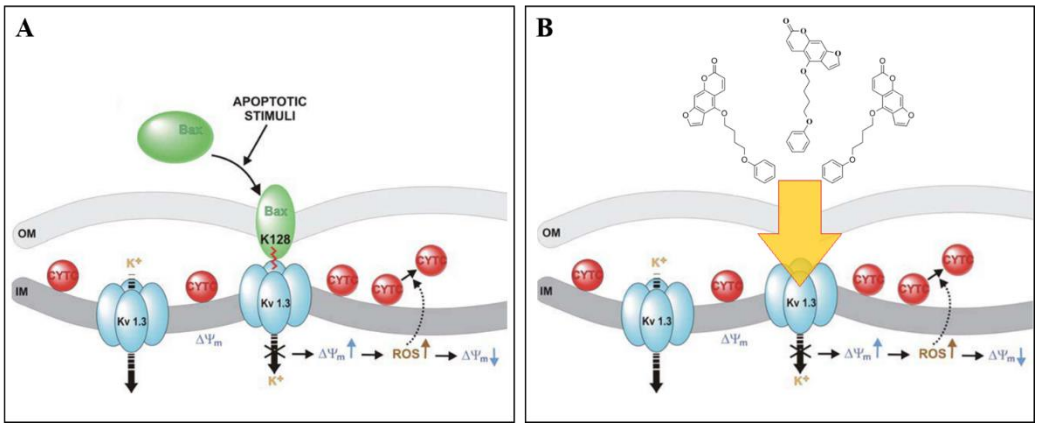

Figure 17. Apoptotic trigger and Kv 1.3 channel blocking by Bax (A) and PAP-1 (B)[9].

Following preliminary evidence[9] from earlier studies conducted with our collaborators (prof. I. Szabò and dr. L. Leanza) I decide to also investigate the activity of clofazimine (**CFZ**, Figure 16) derivatives. Clofazimine is a riminophenazine, and a rather selective Kv1.3 blocker with tenfold higher potency against Kv1.3 than against Kv1.1, Kv1.2, Kv1.5 and Kv3.1[8]. CFZ is already in use for the treatment of various pathologies, including leprosy, psoriasis, chronic graft-versus-host disease, tuberculosis and granulomatous cheilitis. Differently from psoralens, CFZ in addition to being a Kv 1.3 inhibitor, is also a blocker of Multi Drug Resistant (MDR) pumps. This feature might be exploited in the context of a multidrug therapy against tumors – this same characteristic was utilized for the loading on polymeric nanocarrier in Chapter 4.

3.1.2. THE PHARMACOLOGICAL TARGET: THE MITOCHONDRIAL KV 1.3 CHANNEL (MITOKV 1.3)

Several potassium and calcium-selective channels have been identified in the inner mitochondrial membrane (IMM). Most of the IMM K^+ channels identified thus far are considered to be the mitochondrial counterparts of well-known plasma membrane (PM) channels[9].

In particular, the voltage-gated potassium channel Kv1.3 belongs to the Shaker family and is expressed in different tissues, such as brain, kidney, olfactory bulb, lymphocytes, skeletal muscle, adipose tissue[10] In healthy individuals expression occurs mainly in the CNS and in immune cells, but several types of cancer cells also display an increased expression of the protein[10]. Aberrant expression of Kv1.3 has indeed been observed in different types of tumors, such as melanoma, prostate, breast, B-cell lymphoma, chronic lymphocytic leukemia (B-CLL), gastric, pancreatic tumor and in lung cancer[11]. Expression of Kv1.3 in cancer cells may give an advantage to cancer cells enhancing tumorigenic processes such as proliferation, cell migration and metastasis[12].

Kv1.3 is expressed and active both in the plasma membrane (PM) and in the inner mitochondrial membrane (IMM) of lymphocytes, hippocampal neurons and in various tumor cells[2,3]. While the plasma membrane Kv1.3 is required for cell proliferation, the mitochondrial channel regulates apoptosis. A crucial role for mitoKv1.3 in apoptosis became evident because the expression of a mitochondria-targeted Kv1.3 construct was sufficient to induce cell death upon apoptotic stimulation in CTLL-2 T lymphocytes that lack Kv channels and are otherwise resistant to apoptosis. A physical interaction between Bax and mitoKv1.3 taking place via the lysine residue K128 in Bax has been demonstrated in apoptotic cells, and Bax has been shown to inhibit channel activity at nM concentrations[5,6]. Incubation of Kv1.3-positive isolated mitochondria with Bax triggered apoptotic events, including membrane potential changes (hyperpolarization followed by depolarization because of MPTP opening), ROS production and cytochrome c release (Figure 17); however, Kv1.3-deficient mitochondria were resistant.

3.1.3. DESIGN OF SYNTHETIC TARGETS

The current state of the art leaves still unresolved, or only partially/unsatisfactorily resolved, the following major problems: a) low aqueous solubility of available psoralen and clofazimine derivatives, with attendant constraints for administration and dosing; and b)

need for relatively high dosages. The derivatives of psoralen and clofazimine (Figure 18) I developed in this thesis solve these problems providing two new classes of compounds with improved phisico-chemical properties and efficacy comparable or higher than that of Psora-4 or PAP-1 and CFZ, respectively.

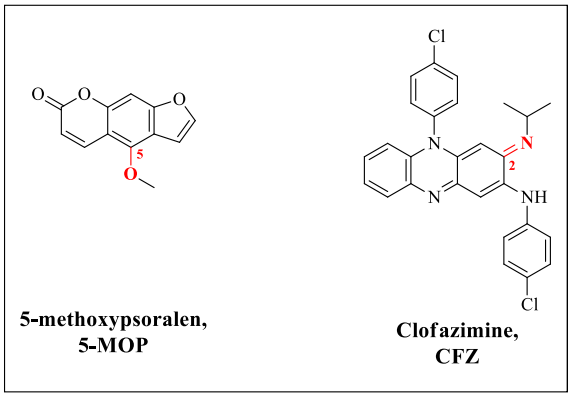

Figure 18. Modification sites in 5-MOP and CFZ.

The psoralen derivative I chose to use as core to be suitably modified, has an oxygen ether bond at position 5 of the psoralen structure (Figure 18). This oxygen can be used to connect the furobenzopyranone ring system to various substituents engineered to provide one or a combination of desirable properties: water solubility, acidity, membrane permeability, concentration in the cell cytoplasm and in mitochondria. The functionalities conferring these properties may be joined to the rest of the molecule by either bio-stable or hydrolizable bond systems. The same approach was adopted in the case of clofazimine which was modified on the imine bond (C2, Figure 18).

More specifically, the approach adopted for mitochondrial targeting was based on the insertion of a triphenylphosphonium group. Indeed, the most commonly used stratagem to target a compound to mitochondria is to link it to a membrane-permeating cation, generally triphenylphosphonium[13–15]. This procedure leads to accumulation in the cell cytoplasm because of the plasma membrane potential, and further into the mitochondria (Figure 19).

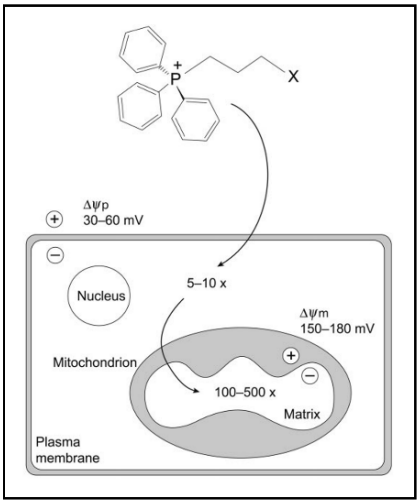

Figure 19. Representation of plasma and mitochondria membrane permeation by TPP cations[21].

Two features of lipophilic cations make them effective at delivering molecules to mitochondria: they can cross phospholipid bilayers without requiring a specific uptake mechanism and they accumulate substantially within mitochondria owing to the large membrane potential. Lipophilic cations are characterized by a delocalized charge and by low-polarity residues. They can easily move through phospholipid bilayers because the energy barrier posed by the hydrocarbon-like inner part of the bilayer is relatively low in their case. During transport, the cations initially adsorb to the membrane in the potential energy well on the outer surface of the membrane. They then pass rapidly through the hydrophobic core of the membrane to the potential energy well on the other membrane surface, followed by desorption[15]. Hence, as it is known that in the case of cancer cells this potential gradient is higher than that in healthy cells, a selective accumulation of mitochondriotropic derivatives in tumor cells is therefore expected. It is important to remark that basing on the pioneering work of Murphy et al.[13–15] our research group has extensively applied that approach, focusing mainly on natural polyphenols delivery to mitochondria. Quercetin and resveratrol were chosen as model polyphenols for those studies[16–18]. In particular, mitochondria-targeted redox-active polyphenol derivatives, were designed to intervene on radical processes in these organelles and as a tool either to protect cells from oxidative insults or to precipitate their death[19,20].

3.2. RESULTS AND DISCUSSION: NEW PSORALEN DERIVATIVES AS SELECTIVE TUMOR KILLING AGENTS

3.2.1. SYNTHETIC STRATEGY

The synthetic approach adopted to functionalize psoralen has focused on a specific site of the molecule, C-5. In particular, we have chosen as starting material not psoralen itself, but one of its natural derivatives, bergapten, 5-MOP (**1**, Figure 20).

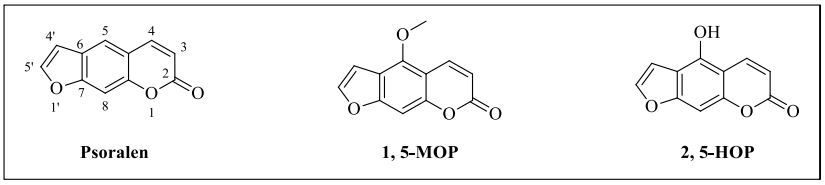

Figure 20. Molecular structure of psoralen, bergapten (1) and bergaptol (2).

Bergapten is a natural linear furocoumarin extracted from many varieties of plants, in particular *Ruta Graveolens* and *Ficus Carica*. Demethylation of bergapten leads to bergaptol (5-HOP, **2,** Figure 20) which served as a very convenient precursor for all the derivatives prepared for this thesis. These are shown in Figure 21 along with the abbreviations and numbers used to identify and cite them in the thesis. All of these derivatives carry on the oxygen at C-5 a 4-carbon saturated chain, which is terminated by either a phosphonium group or a functionalized ether substituent. With the exception of PAP-1, all are new compounds, never reported before in the literature.

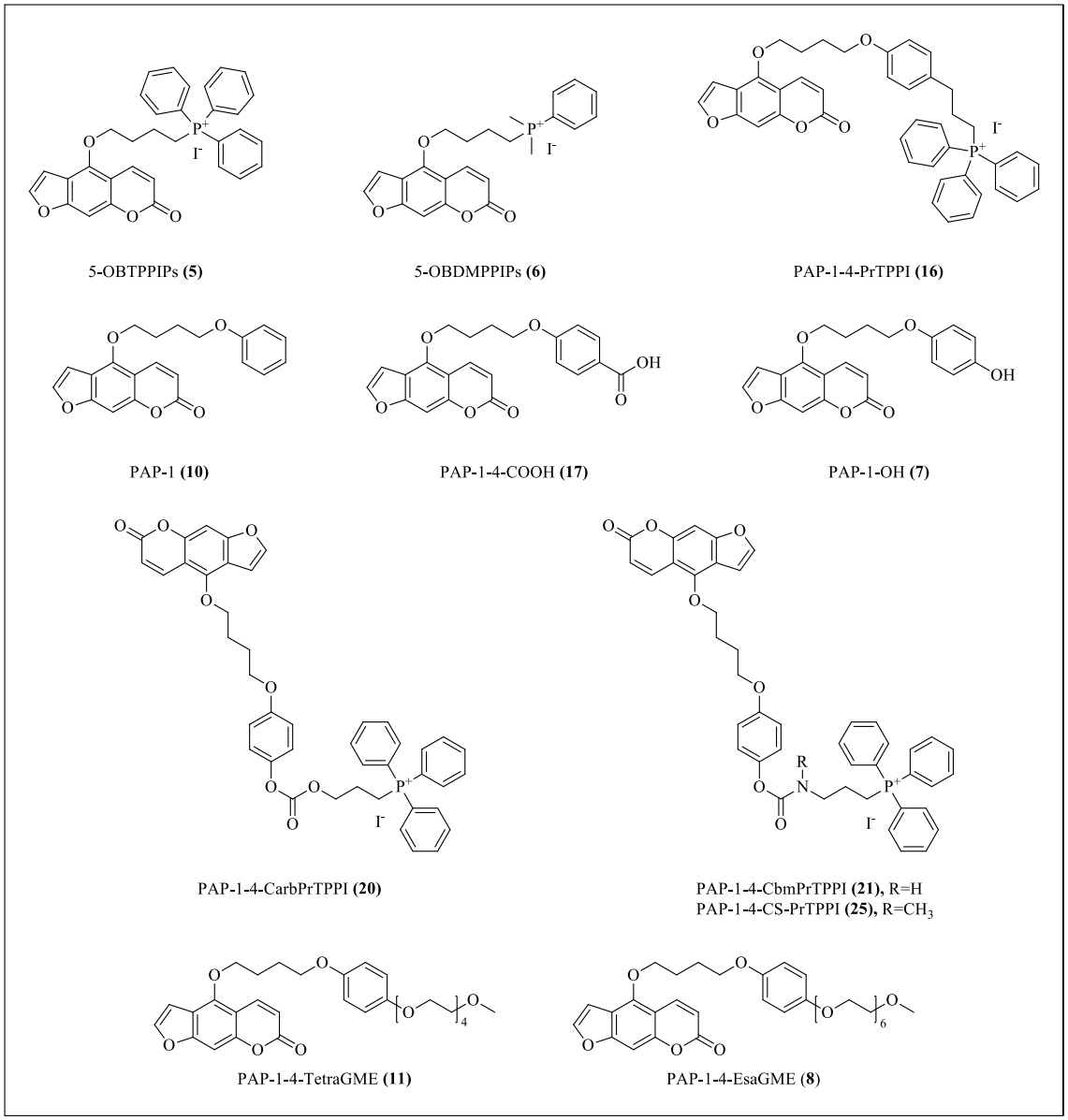

Figure 21. Psoralen derivatives and PAP-1 synthesized in this work.

With the exception of PAP-1 (**10**), all other targets were obtained from a common intermediate, the iodo-substituted compound **4** synthesized from bergapten (**1**) in 3 steps (Figure 22).

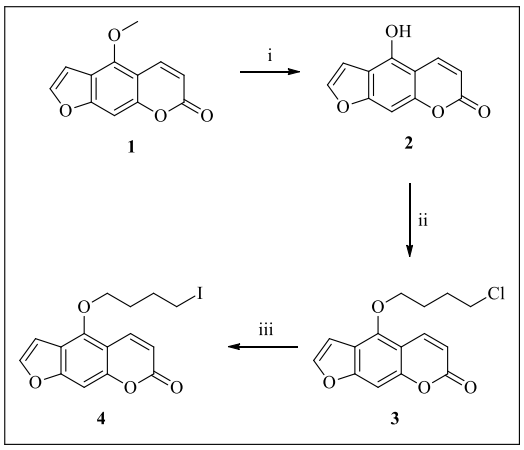

Figure 22. Synthesis of **4**, the common key-intermediate: i) BBr_3 in DCM, rt, 100 min, N_2, quantitative; ii) 1-bromo-4-chlorobutane, Cs_2CO_3, DMF, 50°C, overnight, N_2, 93%; iii) NaI, acetone, reflux, 24h, quantitative.

As shown in Figure 22, the conversion of bergapten (**1**) into the iodo-substituted key intermediate **4** was achieved via demethylation to bergaptol (**2**), already mentioned above, followed by alkylation to the chloro-compound **3** and by a Finkelstein reaction.

All synthetic procedures are described in the Materials and Methods section, except for the three of most promising derivatives PAP-1-4-EsaGME (**8**), PAP-1-4-CbmPrTPPI (**21**) and PAP-1-4-PrTPPI (**16**) which I discuss in the next paragraphs. The choice to modify PAP-1 with the functionalities present in the new derivatives shown in Figure 21 was due to the idea of improving the compounds' polarity and, thus, the solubility in aqueous systems without compromising their ability to permeate biological membranes.

3.2.2. SYNTHESIS OF PAP-1-4-ESAGME (8)

The synthetic approach adopted to synthesize PAP-1-4-EsaGME (**8**) is shown in Figure 23 (for further details see Materials and Methods). Starting from **4**, the derivative **8** was obtained in 2 steps through the other key precursor PAP-1-OH (**7**).

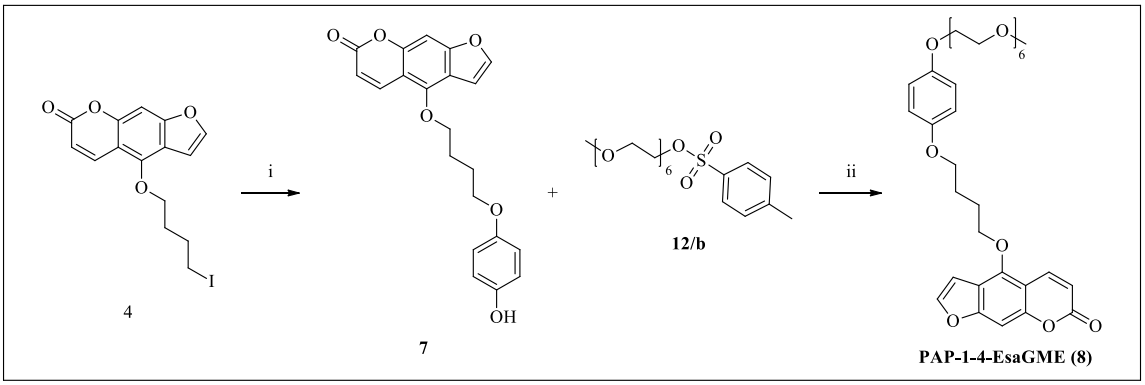

Figure 23. Synthesis of **8**: i) hydroquinone, Cs_2CO_3, DMF, 50°C, overnight, N_2, 84%; ii) Cs_2CO_3, DMF, 50°C, overnight, N_2, 93%.

The choice of modifying the PAP-1 scaffold by linking an oligoethylenglycol chain was made in order to increase the overall solubility in water or in other polar media without altering too much the product molecular weight. This approach is commonly used in pharmacology, but usually higher molecular weight PEGs (2kDa) are employed. In our case, this modest modification result in a satisfactory enhancement of solubility (29.5 ± 2.8 μM). The results obtained with this compound in biological tests will be shown and commented in a dedicated paragraph with the other two promising derivatives PAP-1-4-CbmPrTPPI (**21**) and PAP-1-4-PrTPPI (**16**).

3.2.3. SYNTHESIS OF PAP-1-4-PRTPPI (16)

The synthetic approach adopted to synthesize PAP-1-4-PrTPPI (**16**) is shown in Figure 24 (for further details see Materials and Methods). Starting from **4**, the derivative **16** was obtained in 3 steps.

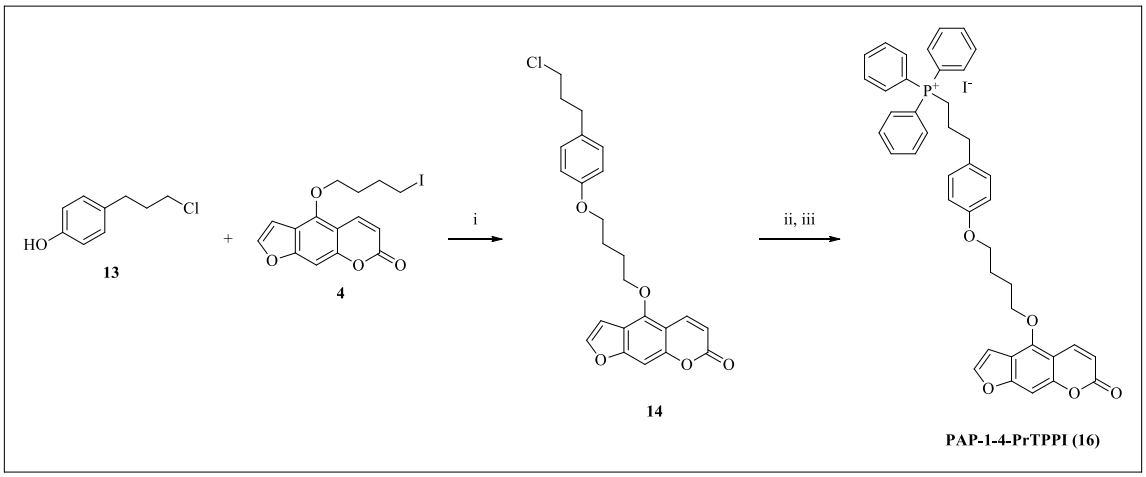

Figure 24. Synthesis of **16**: i) Cs_2CO_3, DMF, 50°C, overnight, N_2, 98%; ii) NaI, acetone, reflux, 24h, 82%; iii) PPh_3, neat, 95°C, 4h, 83%.

Product **16** was the first active mitochondriotropic derivative tested. It presents a PAP-1-like structure in which the lipophilic cation (TPPI) is directly linked to the phenyl group by a covalent (non-bioreversible) C-C bond. This modification slightly enhance the solubility of this derivative up to 2.0 ± 0.3 μM. Also for this case, biological results will be show and commented in a dedicated paragraph with the other two promising derivatives PAP-1-4-CbmPrTPPI (**21**) and PAP-1-4-EsaGME (**8**).

3.2.4. SYNTHESIS OF PAP-1-4-CBMPRTPPI (21)

The synthetic approach adopted to synthesize PAP-1-4-CbmPrTPPI (**21**) is shown in Figure 25 (for further details see Materials and Methods). Starting from **7**, the derivative **21** was obtained in 3 steps. The synthesis was achieved via reaction of PAP-1-OH (**7**) with 4-nitrophenyl (3-chloropropyl) carbamate (**22**), which was synthesized starting from bis(4-nitrophenyl) carbonate (PNPC) as shown in Figure 25.

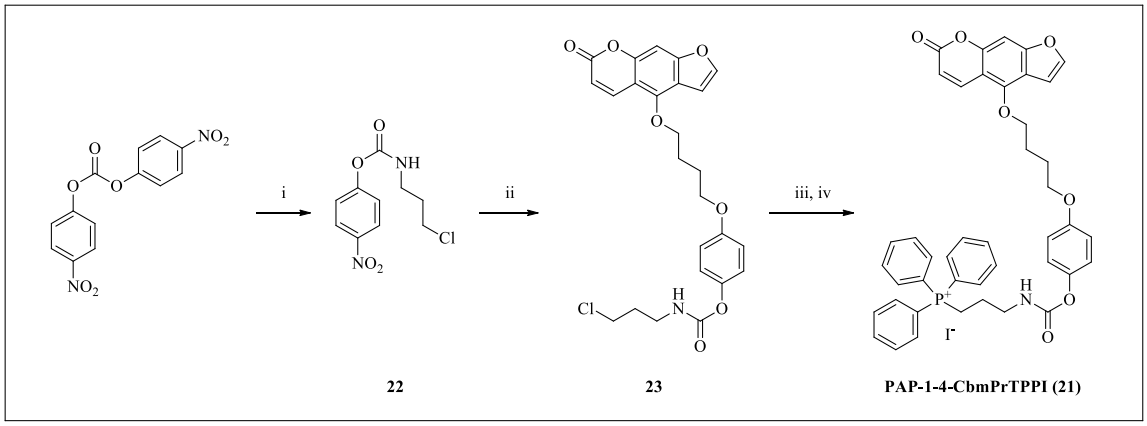

Figure 25. Synthesis of **21**: i) 3-chloropropylamine hydrochloride, DMAP, DCM/THF (1:3), rt, 3h, N2, 70%; ii) PAP-1-OH (**7**), DMAP, DMF, 50°C, overnight, N_2, 80%; iii) NaI, acetone, reflux, 24h, 75%; iv) PPh_3, neat, 95°C, 4h, 82%.

Product **21** was the second active mitochondriotropic derivative tested. It presents a PAP-1-OH-like structure in which the lipophilic cation (TPPI) is linked to the phenolic moiety by a carbamoylic (bioreversible) group. Based on the experience of our research group[22], this kind of bioreversible group is stable under acidic conditions and undergoes very slow hydrolysis at neutral pH, but it can be hydrolyzed by blood enzymes. Enzymatic degradation is not excessively rapid, allowing accumulation into the site of action before the carbamoylic group hydrolysis is completed. Also in this case, biological results will be shown and commented in a dedicated paragraph with the other two promising derivatives PAP-1-4-PrTPPI (**16**) and PAP-1-4-EsaGME (**8**).

3.2.5. BIOLOGICAL *IN VITRO* RESULTS

The compounds synthesized in this thesis work are being tested for efficacy as selective cytotoxic agents by Prof. I. Szabò and associates at the Department of Biology. A summary of the most relevant results obtained is included here to better place my work in its biomedical context. Three out of 13 synthesized compounds were ranked as most efficient ones on the basis of preliminary experiments involving test of their ability to selectively inhibit Kv1.3 and to induce cell death only in cells expressing Kv1.3 (not shown). The next

results are all referred to these three most promising psoralen derivatives: PAP-1-4-EsaGME (**8**), PAP-1-4-PrTPPI (**16**) and PAP-1-4-CbmPrTPPI (**21)**. The following brief discussion on the activity of psoralen derivatives (*in vitro* and *in vivo*) is a summary from the full research article (Romio et al. *in preparation*).

In vitro assays on melanoma cell–model B16F10 (Figure 26) have shown that when the cells express Kv1.3 (Figure 26, blue bars) cell mortality at the tested concentration is practically 100% for compounds **21** and **16**. The killing ability of **8** was very similar to that of PAP-1 and in both these latter cases the required concentration was higher than for the other two derivatives. When the Kv1.3 channel was downregulated (orange bars) in all cases the derivatives and PAP-1 weren't active.

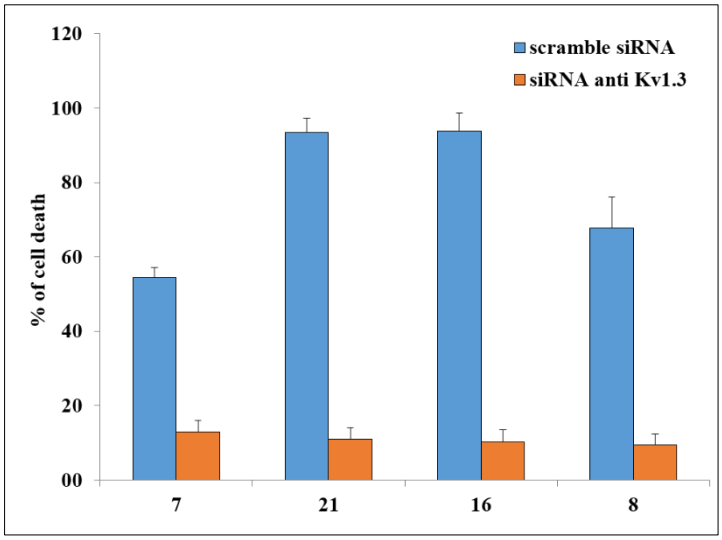

Figure 26. Cytotoxicity depends on the expression of Kv1.3. B16F10 cells were treated as indicated for 24h with indicated concentrations of psoralen derivatives and cell death was evaluated using the Annexin V staining using a fluorescent microscope. Tested concentration: **7** and **8** = 20 μM, **16** and **21** = 10 μM.

It was thus confirmed that for this melanoma cell line the synthesized derivatives show a marked selectivity for Kv1.3-expressing cells.

Figure 27 shows the effects of **8**, **16** and **21** on primary pathological B cells isolated from patients (CD19+/CD5+) versus B lymphocytes obtained from healthy volunteers.

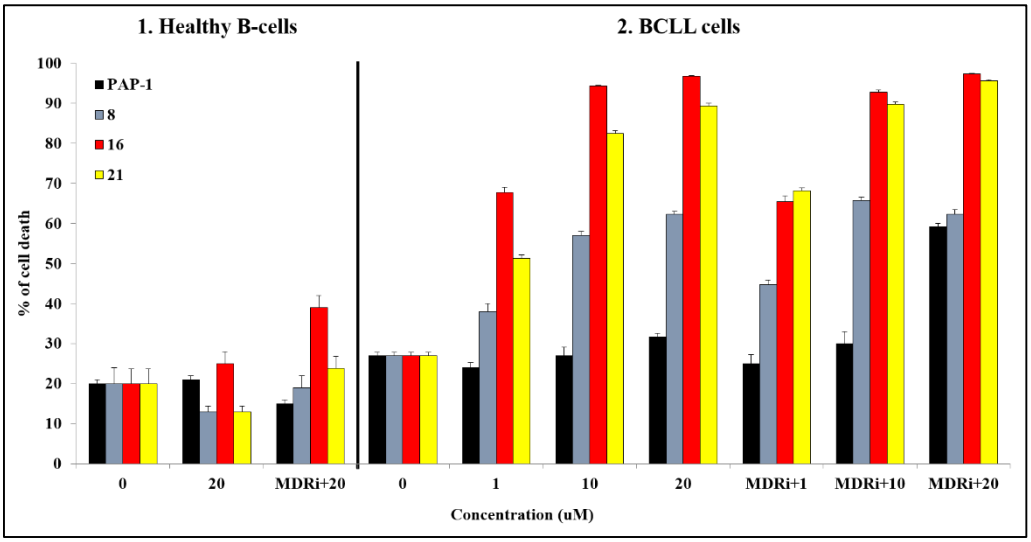

Figure 27. The three PAP-1 derivatives are cytotoxic for leukemic BCLL-2 cells, while sparing healthy B cells.

These experiments further highlight the specificity of the treatment toward pathological cells, while leaving healthy cells alive even when working with ex-vivo primary cells. Experiments were performed according to an already published protocol[13].

All the new derivatives tested showed a higher effectiveness than PAP-1.

3.2.6. BIOLOGICAL *IN VIVO* RESULTS

Some of the i*n vivo* studies on orthotopic murine melanoma are summarized in Figure 28 **I-III**. The administration protocol was as in Leanza et al.[3] As summarized in Figure 28-**I** the effect of the three new derivatives was impressive. Also in these experiments the best results were obtained upon treatment with **16** and **21**; compound **8** to be appreciably effective needed to be co-administered with clofazimine. In order to understand if treatment with **16** may lead to complete tumor regression, this derivative was administered together with cisplatin (0,5 μL/g of mouse), resulting in a reduction of tumor growth estimated at around 95% (Figure 28, **II**).

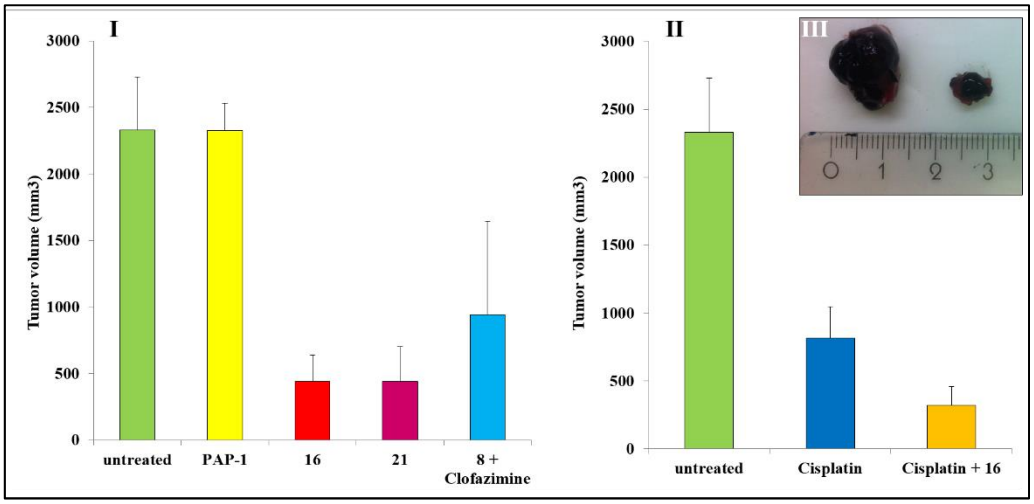

Figure 28. I) Effect of treatment with CFZ+**8** (2 nmol/g + 20 nmol/g), **16** (5 nmol/g), **21** (10 nmol/g) and PAP-1 (20 nmol/g) on murine orthotopic melanoma9. II) Effect of co-administration of **16** with cisplatin on tumor regression volume. III) Tumor volume reduction after treatment with **16**.

To better understand *in vitro* and *in vivo* studies, it was decided to investigate the biodistributions of the two best drug candidates, **16** and **21**, after intraperitoneal administration to healthy mice, comparing them with those PAP-1 (Figure 29). In Figure 29 the results regard PAP-1-OH instead of derivative **21**, because of the labile nature of its carbamoylic bond which undergoes rapid hydrolysis under physiological conditions ($t_{1/2}$ = 20 min (rat) or 10 min (mouse)). As expected, after 2 hours the concentration of all the derivatives (or the hydrolysis product in case of **21**) is higher than after 4 and 8 hours. The liver, the major site of metabolic transformation, was the organ with the highest concentration of derivatives, followed by the kidneys, which have a key role in the elimination of xenobiotics. An important observation is the complete–absence of accumulation in heart. Cardiac tissues express high levels of the Kv 1.5 channel, similar to Kv 1.3, whose possible inhibition would create problems. They were absent also in the brain, presumably because they were blocked by the Blood-Brain-Barrier (BBB).

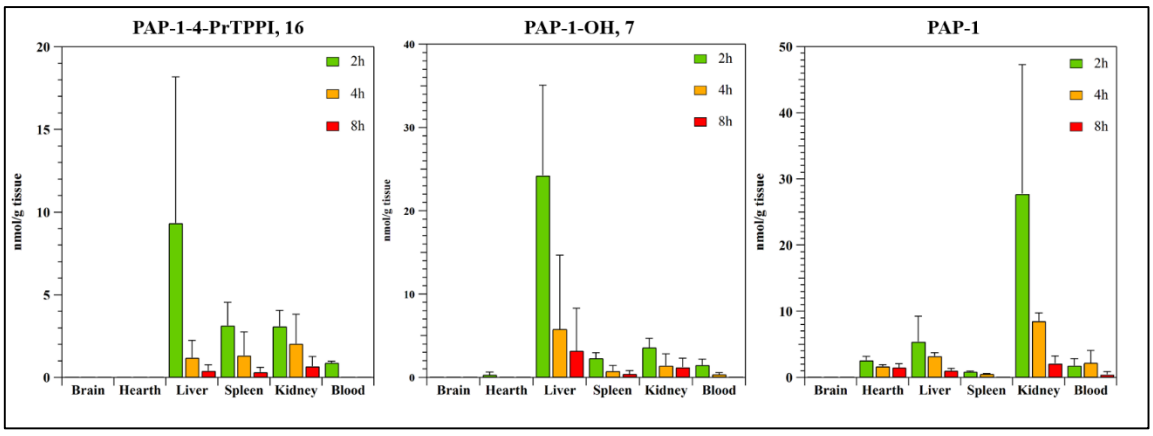

Figure 29. Biodistribution of **16**, **21** hydrolysis product (**7**) and PAP-1.

3.3. CONCLUSIONS ABOUT PSORALEN DERIVATIVES PROJECT

Thirteen new psoralen derivatives were synthesized with the final purpose of improving their activity and selectivity against cancer cells characterized by a strong expression of mitoKv 1.3 channel. If compared with PAP-1 (a commercially available psoralen derivative), three of these new molecular entities (**8**, **16** and **21**, Figure 21) showed interesting activity improvements in various types of assays.

They proved selective in the sense that they were cytotoxic only for cells expressing Kv1.3, in particular in the case of melanoma and leukemia. Differently from PAP-1, they were active even at low μM concentrations.

Finally, preliminary *in vivo* studies on **16**, revealed positive effect against tumor growth in mice after intraperitoneal administration at day 5-7-9-11 after cells injection. Mice were sacrificed after 5 days from the last treatment and tumor volume was determined. In particular, for **16** the synergistic action in combination with cisplatin (Figure 28) afforded a residual tumoral volume of 5% compared to the untreated. Concluding, the work I have done on this part of the PhD project gives encouraging results. I synthesized and successfully tested a new library of selective tumor killing agents with a psoralen-inspired molecular structure. This work has led to a patent application (PD2015A000006) and publication in scientific journals is underway.

3.4. Results and Discussion: New Clofazimine Derivatives as Selective Tumor Killing Agents

3.4.1. Synthesis and Chemical Characterization

The synthetic approach adopted to create clofazimine derivatives has focused on a specific site of the molecule, that on C-2 (Figure 30). In the past, various research groups have synthesized and tested dozens of clofazimine-like derivatives in attempts to increase solubility without decreasing activity [22,23].

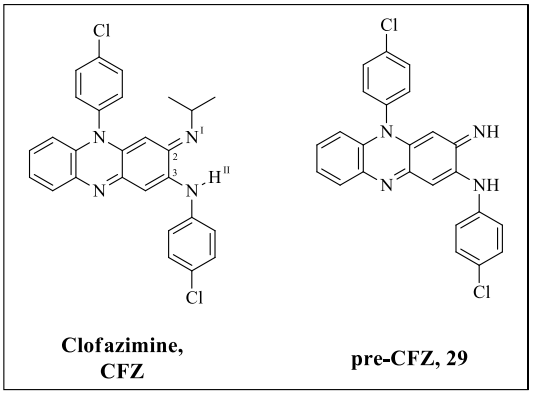

Figure 30. Molecular structure of clofazimine and the derivatives' precursor pre-CFZ.

The approach I have adopted for the synthesis of a new series of derivatives was based on observations reported in the original work by Barry et al.[24]. In particular, one of the most important scaffold characteristics that must be preserved is the co-planarity of the conjugated aromatic rings. More specifically, the possibility to form an intramolecular hydrogen bond between H^{II} and N^{I} (Figure 30) seems to be fundamental to preserve the drug activity. Unfortunately, this characteristic is also the basis of its high lipophilicity and insolubility. Nevertheless, the imine site (C^{2}-N^{I}) remains almost the only site for potentially successful chemical modifications.

In order to create a new family of CFZ-like derivatives, I decide to synthesize the key intermediate pre-CFZ from which all the other structures are easily obtained (Figure 31).

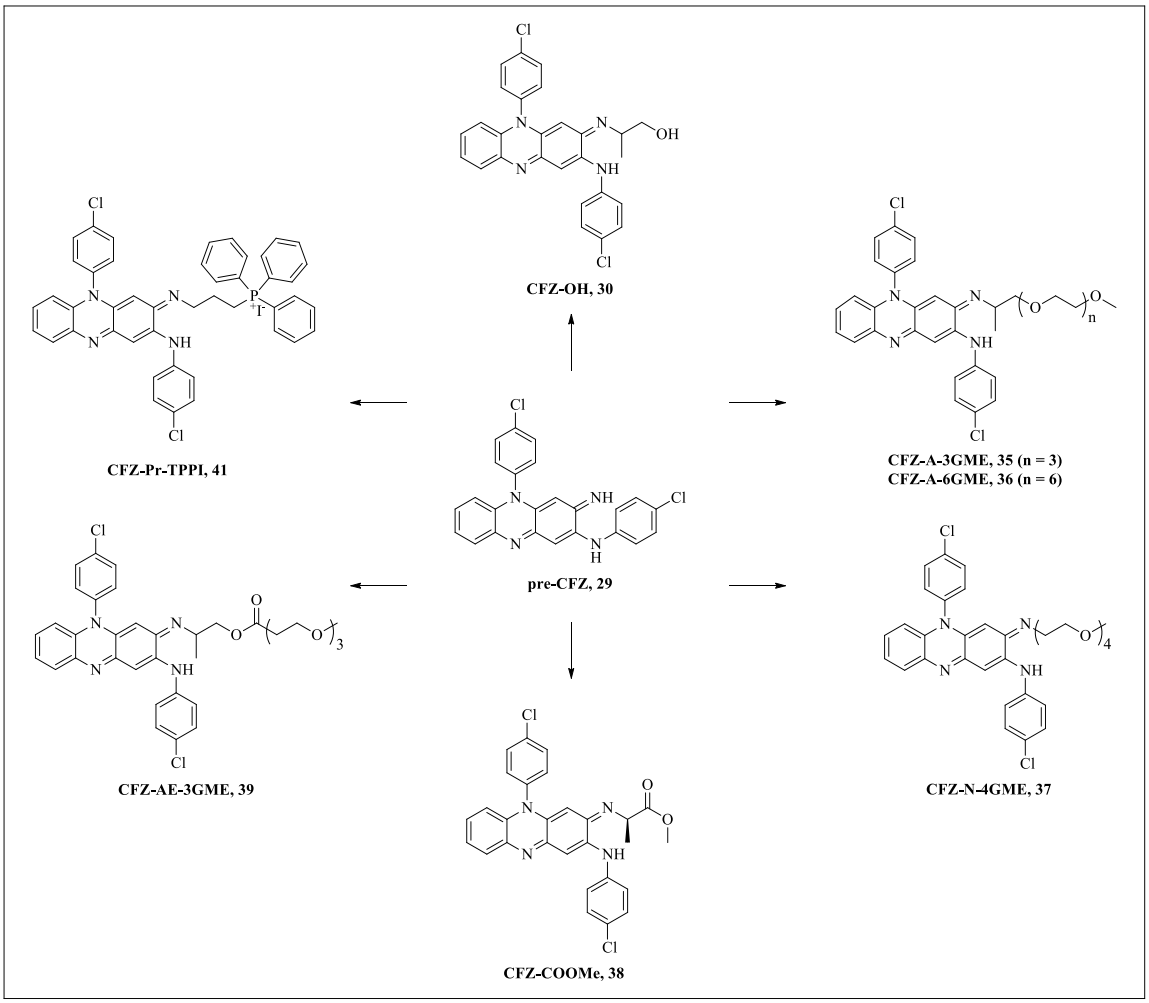

Figure 31. Clofazimine derivatives synthesized in this work starting from the common precursor pre-CFZ.

After a retrosynthetic study performed with the aim to obtain the pre-CFZ compound with high yield, high purity and an easy purification step, I decided to opt for the oxidative dimerization of N-(4-Chlorophenyl)-1,2-benzenediamine shown in Figure 32.

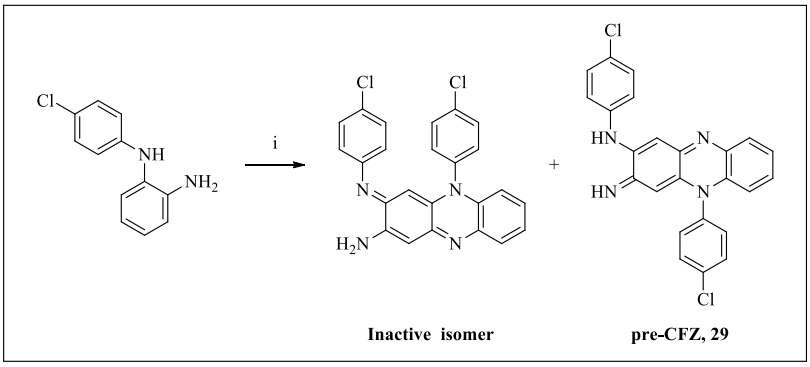

Figure 32. Synthesis of active pre-CFZ isomer: i) $FeCl_3$, HCl, water, rt, 1h, 78% (**pre-CFZ**).

Fortunately, the reaction mechanism favors the formation of the active isomer, pre-CFZ. On the other hand, the isolation and purification of the desired product, pre-CFZ, turned out to be one of the most challenging tasks of the entire project. Eventually, the purification

procedure to obtain pre-CFZ of high purity involved 8 to 10 hours of Soxhlet extraction with chloroform followed by a step of silica gel flash chromatography. However, following this purification strategy I improved the reaction yield from the original 50% (Barry et al.[24]) to the actual 78%. The strong substrate similarity with an already published reaction[25], suggests that the process proceeds via an electrocyclic [4+2] cycloaddition mechanism.
However, once pre-CFZ was obtained, all the other seven derivatives could be synthesized by amination reaction in good yields and under relatively mild conditions of preparation and purification. All synthetic procedures are described in Materials and Methods. In the next paragraphs, I will focus on three derivatives, namely CFZ-N-4GME (**37**), CFZ-Pr-TPPI (**41**) and CFZ-A-6GME (**36**), which gave the best results in terms of solubility and preliminary *in vitro* activity. The choice of promoieties was again based on the desire to improve the compounds aqueous solubility without compromising their ability to permeate biomembranes.

3.4.2. SYNTHESIS OF CFZ-N-4GME (37)

The synthesis of CFZ-N-4GME (**37**) starting from **29** was achieved in one step as shown in Figure 33 (for further details see Materials and Methods).

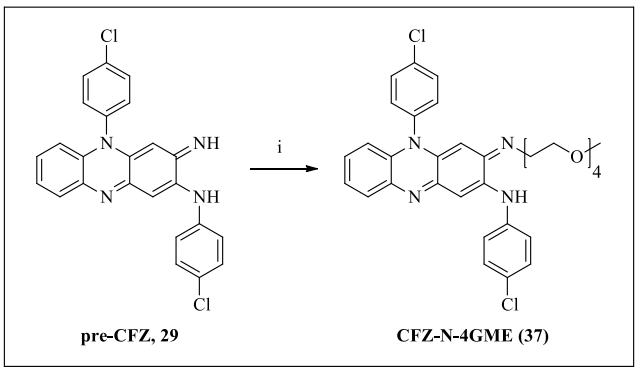

Figure 33. Synthesis of CFZ-N-4GME (**37**): i) 4GME-NH_2, CH_3COONa, dioxane, 100°C, 24h, 85%.

Product **37** was the first oligoethylenglycol derivative obtained. It presents a CFZ-like structure in which the C2 carbon has been decorated with a primary imine-OEG linked to the scaffold via a stable bond. If compared with CFZ, the steric hindrance around the C2-N bond appears to be lower. The modification increased solubility from 0.01 mg/mL (CFZ) to 0.77 mg/mL. The results of bioassays are shown and commented in a dedicated section below, along with those obtained with CFZ-Pr-TPPI (**41**) and CFZ-A-6GME (**36**).

3.4.3. SYNTHESIS OF CFZ-PR-TPPI (41)

The synthesis of CFZ-Pr-TPPI (**41**) starting from **29** was achieved in three steps as shown in Figure 34 (for further details see Materials and Methods).

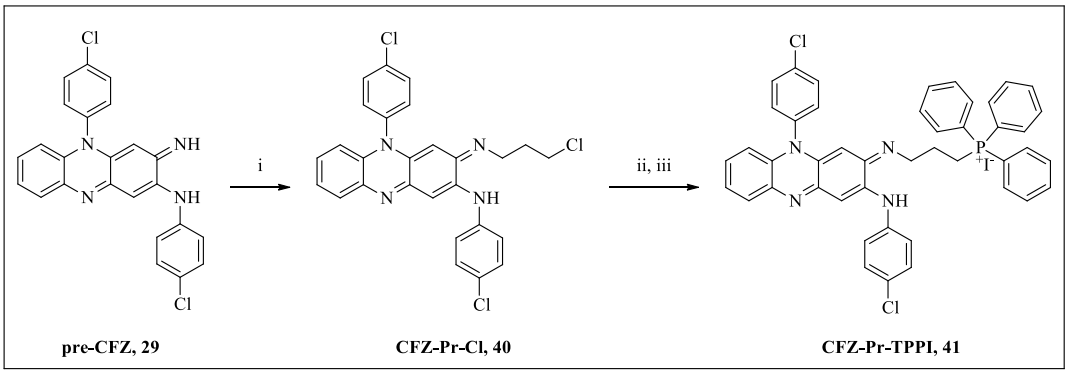

Figure 34. Synthesis of CFZ-Pr-TTPI (**41**): i) 3-chloropropylamine, CH_3COONa, dioxane, 100°C, 24h, 95%; ii) NaI, acetone, reflux, 24h, 85%; iii) PPh_3, neat, 95°C, 4h, 90%.

Product **41** was the first mitochondriotropic derivative obtained. The C2 carbon was decorated with a primary imine-TPPI cation linked to the CFZ scaffold via a stable bond. If compared with CFZ, the steric hindrance around the C2-N bond is increased due to the presence of the TPP cation. The solubility improved from 0.01 mg/mL (CFZ) to 2.66 mg/mL.

3.4.4. SYNTHESIS OF CFZ-A-6GME (36)

The synthetic approach adopted to synthesize CFZ-A-6GME (**36**) is shown in Figure 35 (for further details see Materials and Methods). Starting from **pre-CFZ**, the derivative **36** was obtained in 4 steps including the preparation of **34**.

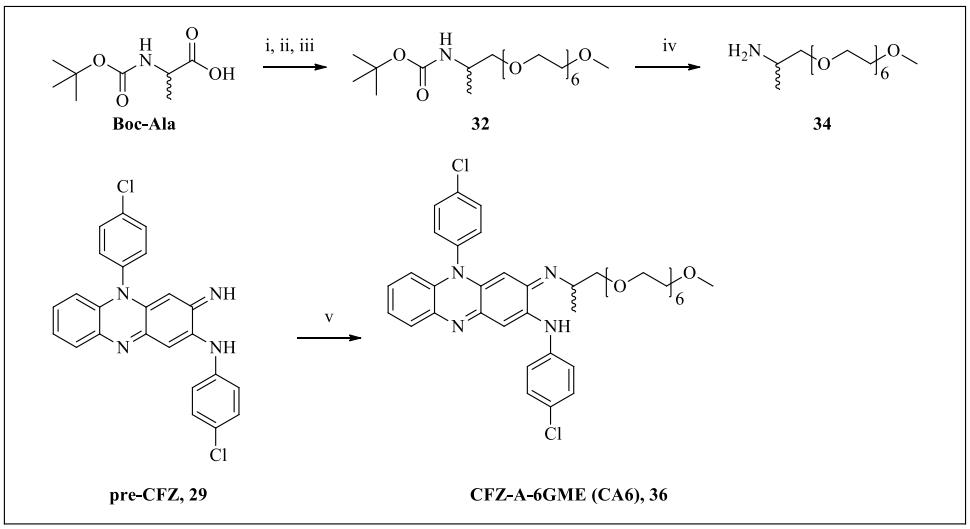

Figure 35. Synthesis of CFZ-A-6GME (**36**): i) 4-N-methylmorpholine, methyl carbonochloridate, THF, 0°C,15 min; ii) $NaBH_4$, H_2O, 0°C to rt, overall 78%; iii) NaH, THF, 0°C, 15 min, then **12/b**, THF, 0°C to rt, 20 h, 95%; iv) TFA, DCM, TIPS, rt, 3h, quantitative; v) **34**, CH_3COONa, dioxane, reflux, 20 h, 55%.

Product **36** was the second oligoethylenglycol derivative obtained. In this case the C2 carbon was decorated with a primary imine-Alanine-OEG construct linked to the scaffold via a stable bond. The steric hindrance neighborhood the C2-N bond should be the same as in clofazimine. The solubility of derivative **36** was determined to be 2.97 mg/mL, i.e. nearly 300 times higher than that of clofazimine. The performance of this compound in bioassays is presented below, along with that of CFZ-Pr-TPPI (**41**) and CFZ-N-4GME (**37**).

3.4.5. Solubility Test of CFZ Derivatives

One of the most problematic characteristics of clofazimine is its extremely low solubility in water. A slight improvement may be obtained varying the pH, because between pH 5 and pH 3 all nitrogen atoms are protonated and this marginally helps drug dissolution. Clofazimine is also poorly soluble in many organic solvents; a satisfactory solubility is reported in DMSO, chloroform, anisole and hot ethanol.

Even at acidic pH values the solubility remains unsatisfactory for an efficient drug formulation and in particular for iv administration, because a co-solvent, surfactants or DMSO are required. Table 2 reports the solubility values of CFZ-derivatives in DMEM. The choice of using DMEM instead of a salt buffer or pure water was made to have a better model to simulate physiological conditions.

Sample	DMEM solubility (mg/L)
CFZ	0.01
CFZ-A-3GME	0.36
CFZ-A-6GME	2.97
CFZ-4GME	0.77
CFZ-COOMe	0.20
CFZ-AE-3GME	0.11
CFZ-Pr-TPPI	2.66

Table 2. Solubility values for CFZ and its derivatives.

The results are significant and encouraging if compared with the CFZ saturation value itself. Specifically, the CFZ-Pr-TPPI and CFZ-A-6GME derivatives have solubilities which are more than 300-fold higher than that of CFZ. Unfortunately, the absolute solubility values remain low, but perhaps this improvement may be sufficient to increase the activity (in terms of biodistribution) of clofazimine or at least, a consequent increased clearance from blood and fat tissues may help to decrease some of the undesired side effects (i.e. changes in skin color).

3.4.6. BIOLOGICAL *IN VITRO* RESULTS

The compounds synthesized in this thesis work are currently being tested for efficacy as selective cytotoxic agents by Prof. I. Szabò and associates at the Department of Biology. A summary of the most relevant *in vitro* results obtained concerning the three derivatives CFZ-A-6GME (**36**), CFZ-4GME (**37**) and CFZ-Pr-TPPI (**41**) is included here to better place my work in its biomedical context.

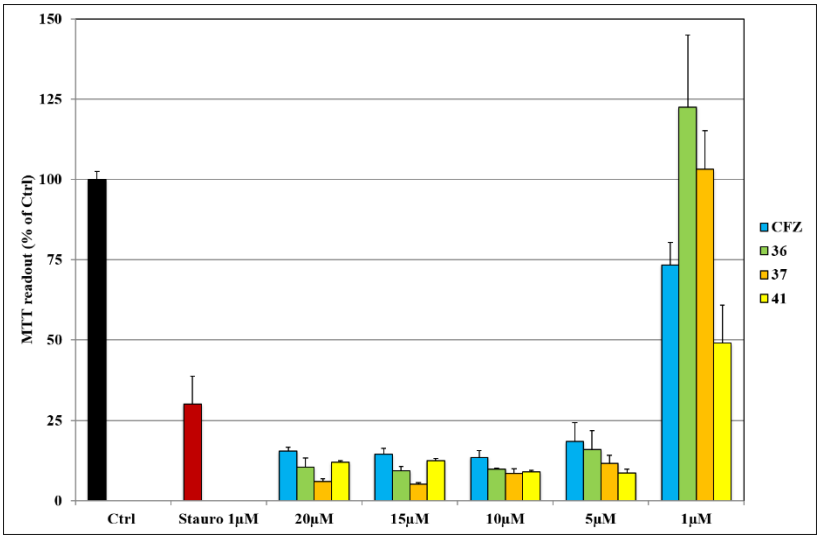

Figure 36. Preliminary MTT results from a screening of the indicated clofazimine derivatives in the range between 1 to 20 µM in murine melanoma B16F10 cells. The results obtained with CFZ (blue) and Staurosporine (red) are reported for comparison purposes. Control (black) intend untreated cells.

Figure 36 summarizes the results of MTT tests carried out with B16F10 cells treated with derivatives **36**, **37** and **41**. Comparing CFZ, Staurosporine (a well-known Kv 1.3 inhibitor[26]) and my derivatives, it is evident how the mitochondriotropic derivative **41** shows a marked activity already at the lowest concentration tested (1 µM) with 50% cell death. This result demonstrates an improved activity in comparison with CFZ itself (25% of cell death). It is important to consider that this derivative is also more soluble than CFZ. On the other hand, it is important to stress that at 5 µM also the other two derivatives **36** and **37** show interesting activity profiles and in both cases these are better than CFZ itself. Figure 37 summarizes *in vitro* results concerning the selectivity of the new derivatives for cells with and without Kv1.3 channel expression. Also in this case Staurosporine was used as a reference cytotoxic agent. The most important result of this test is that the most active derivative **41** seems to lose part of the selectivity for Kv 1.3-expressing cells. **36** and **37** show a lower killing activity at the same concentration of **41**, but at higher concentration still exhibit their activity and seem to maintain a certain selectivity. It should be kept in mind, however, that two different cell lines are being compared, which differ by a multitude

of other factors besides Kv1.3 expression. As mentioned above, these assays are preliminary and the work is still ongoing. These initial observations are considered very encouraging.

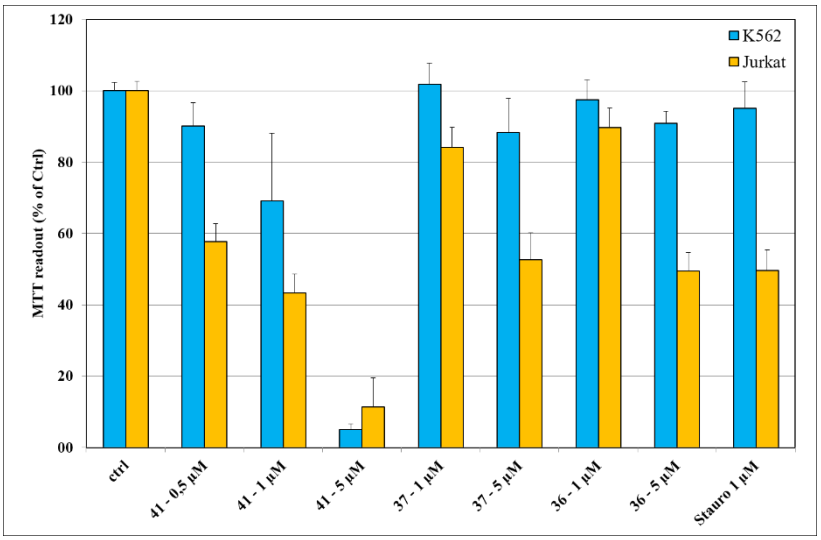

Figure 37. Preliminary MTT results obtained with the most soluble clofazimine derivatives tested at various concentrations and compared Staurosporine. Jurkat cells are human leukemic lymphocytes that express Kv 1.3; K562 cells are human lymphoblasts that do not express the channel.

3.5. Conclusions about Clofazimine Derivatives Project

Seven new clofazimine derivatives were synthesized with the purpose of obtaining analogues with improved solubility, activity and selectivity against cancer cells characterized by a strong expression of mitoKv 1.3 channel. If compared to CFZ, two of the synthesized new compounds (**36** and **41**, Figure 31) show interesting activity improvements from many points of view. First of all, their solubility was about 300-fold higher than that of CFZ itself. Although more *in vitro* and *in vivo* tests need to be done, the preliminary results suggest that the improvement in solubility might be associated with a decrement of the selectivity towards Kv 1.3 channel. It is too early to draw further conclusions, but I am satisfied with regard to the solubility improvements achieved and with the **pre-CFZ** synthesis optimization. In particular, making some modifications to the original procedure published by Barry et al[24], I was able to increase the overall yield from 50% to more than 78% of pure isolated compound. As a concluding remark it is worth mentioning that the possible applications of clofazimine and of its more soluble analogues are potentially huge. Up to now, clofazimine has been used to treat leprosy, tuberculosis and as an antibacterial and antifungal agent. The creation of analogues with improved solubility and activity might possibly extend the scope of pharmacological applications.

3.6. EXPERIMENTAL SECTION

3.6.1. MATERIALS AND METHODS

Starting materials and reagents were purchased from Aldrich, Sigma-Aldrich, TCI, Fluka, Riedel-de Haen (Seelze, German), Prolabo (Fonyenay sous Bois, France), Carbosynth (Compton, Berckshire, UK), and were used as received. The ^{1}H-NMR and ^{13}C-NMR spectra were recorded with a Bruker AC 250F spectrometer operating at 250 MHz for ^{1}H-NMR and 62.9 MHz for ^{13}C-NMR or Bruker 300 UltraShield spectrometer operating at 300 MHz for ^{1}H-NMR and 75 MHz for ^{13}C-NMR or Bruker 500 UltraShield spectrometer operating at 500 MHz for ^{1}H-NMR and 126 MHz for ^{13}C-NMR. Chemical shifts (δ) are given in ppm, and the residual solvent signal was used as an internal standard. TLCs were run on silica gel supported on plastic (Macherey-Nagel Polygram®SIL G/UV254, silica thickness 0.2 mm) and were visualized by UV detection. Flash chromatography was performed on silica gel (Macherey-Nagel 60, 230-400 mesh granulometry (0.063-0.040 mm)) under air pressure. The solvents were of analytical or synthetic grade and were used without further purification. Fluorescence/UV-Vis spectra were recorded at 25°C with a Perkin-Elmer LS-55 spectrofluorimeter cell holder. Quartz cells with an optical pathlenght of 1 cm were used for measurement of both absorption a fluorescence and UV-Vis spectra. Concerning *in vivo* and *in vitro* biological tests, all the work was performed from the collaborators of prof. I. Szabò research group. The protocols and experimental details will be included in an *in preparation* article (Romio et al., *in preparation*).

Synthesis of psoralen derivatives

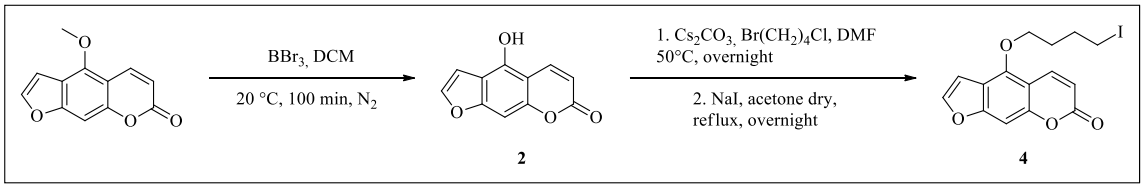

4-Hydroxy-7H-furo-[3,2-g]benzopiran-7-one (5-HOP), [**2**]: compound **1** (501.5 mg, 2.3 mmol, 1 equiv) was dissolved in anhydrous dichloromethane (20 mL) and mixed at room temperature during the slow addition of BBr_3 (10 mL of 1 M solution of DCM, 10 mmol, 10 equiv) under nitrogen. The reaction was stopped after 100 minutes, the product was washed with a saturated solution of $NaHCO_3$ (100 mL) and extracted 3 times with EtOAc (300 mL). The organic phase was dried over $MgSO_4$ and filtered. The solution was concentrated under vacuum until compound **2** precipitate as an off –white solid (467 mg, 2.3 mmol, 99 % yield). ^{1}H-NMR (250 MHz, $CDCl_3$): δ = 8.11 (d, J = 9.8 Hz, 1H; CH), 7.58

(d, J = 2.4 Hz, 1H; CH), 7.10 (t, 1H; CH), 6.93 (dd, J = 2.4, 1.0 Hz, 1H; CH), 6.26 (d, J = 9.8 Hz, 1H; CH), 4.49 (t, J = 5.8 Hz, 2H; CH_2), 3.66 (t, J = 6.0 Hz, 2H; CH_2), 2.21-1.93 ppm (m, 4H; CH_2CH_2); ^{13}C-NMR (62.9 MHz, $CDCl_3$): δ = 161.1 (CO), 158.2, 152.6, 148.6, 144.8, 139.1, 113.0, 112.6, 106.5, 105.0, 93.9, 71.9, 44.5, 29.1, 27.4 ppm; ESI-MS (ion trap): m/z: 203, [M+H$^+$].

4-(4-clorobutoxy)-7H-furo-[3,2-g]chromen-7-one (5-BClOPs), [**3**]: compound **2** (700 mg, 3.5 mmol, 1 equiv) was dissolved in DMF (25 mL) with Cs_2CO_3 (1.69 g, 5.2 mmol, 1.5 equiv) and 1-brom-4-chlorbutane (890 mg, 5.2 mmol, 1.5 equiv) was added to the mixture. The solution was mixed and heated at 50 °C in darkness overnight. The following day, EtOAc (100 mL) was added to the solution and then the mixture was extracted with a 0.5 M solution of HCl (3 x 170 mL). Then, the aqueous phase was extracted with DCM (2 x 70 mL). The organic phase was dehydrated with $MgSO_4$ and filtered. The solvent was stripped off under vacuum and the product was purified by flash chromatography using CH_2Cl_2/EtOAc (98:2) as eluent to afford **3** as a white powder in 87 % yield (878 mg, 3 mmol). ^{1}H-NMR (250 MHz, $CDCl_3$): δ = 8.11 (d, J = 9.8 Hz, 1H; CH), 7.58 (d, J = 2.4 Hz, 1H; CH), 7.10 (t, 1H; CH), 6.93 (dd, J = 2.4, 1.0 Hz, 1H; CH), 6.26 (d, J = 9.8 Hz, 1H; CH), 4.49 (t, J = 5.8 Hz, 2H; CH_2), 3.66 (t, J = 6.0 Hz, 2H; CH_2), 2.21-1.93 ppm (m, 4H; CH_2CH_2); ^{13}C-NMR (62.9 MHz, $CDCl_3$): δ = 161.1 (CO), 158.2, 152.6, 148.6, 144.8, 139.1, 113.0, 112.6, 106.5, 105.0, 93.9, 71.9, 44.5, 29.1, 27.4 ppm; ESI-MS (ion trap): m/z: 293, [M+H$^+$].

4-(4-iodobutoxy)-7H-furo[3,2-g]benzopiran-7-one (5-BIOPs), [**4**]: compound **3** (490 mg, 1.7 mmol, 1 equiv) and NaI (2.47 g, 16.5 mmol, 10 equiv) were added to anhydrous acetone (25 mL) under nitrogen. The solution was mixed and heated at 70 °C in darkness overnight. The following day, an aliquot of EtOAc (30 mL) was added to the solution and then the mixture was washed with deionized water (150 mL). The aqueous phase was discarded and the organic phase was dried over $MgSO_4$ and filtered. The solvent was eliminated under vacuum and the product was purified by flash chromatography using DCM/EtOAc (97:3) as eluent to afford **4** as a yellow powder in 79% yield (512 mg, 1.3 mmol). ^{1}H-NMR (250 MHz, $CDCl_3$): δ = 8.11 (d, J = 9.8 Hz; 1H, CH), 7.58 (d, J = 2.4 Hz; 1H, CH), 6.93 (dd, J = 2.4, 1.0 Hz; 1H, CH), 6.26 (d, J = 9.8 Hz; 1H, CH), 4.47 (t, J = 5.8 Hz; 2H, CH2), 3.29 (t, J = 6.5 Hz; 2H, CH_2), 2.18 – 1.91 ppm (m; 4H, CH_2CH_2); ^{13}C-NMR

(62.9 MHz, $CDCl_3$): δ = 161.1 (CO), 158.2, 152.6, 148.6, 144.8, 139.1, 113.0, 112.6, 106.5, 105.0, 93.9, 71.5, 30.8, 29.9, 5.9 ppm; ESI-MS (ion trap): m/z: 385, $[M+H^+]$.

Synthesis of 5-OBTPIPs (5)

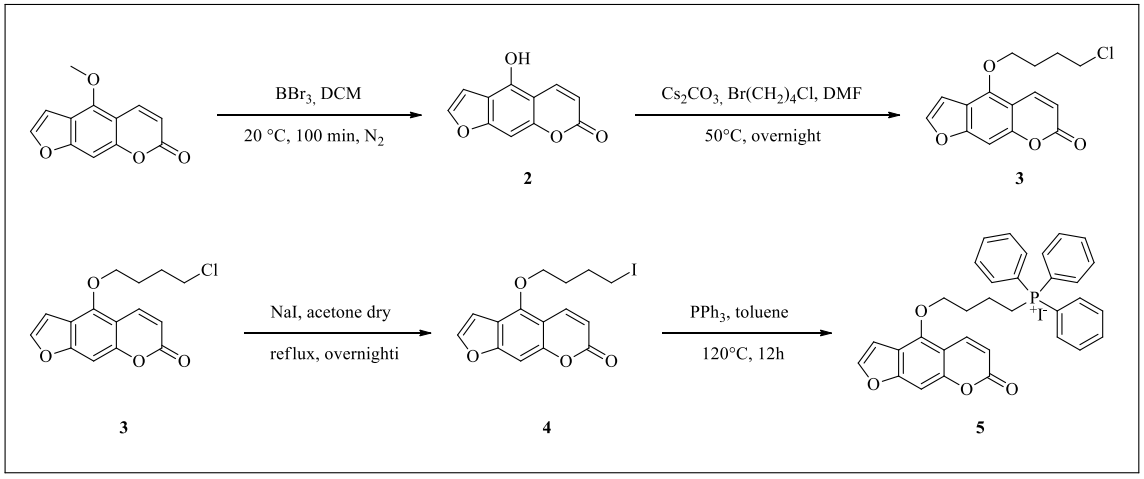

(4-((7-oxo-7H-furo[3,2-g]chromen-4-yl)oxy)butyl)triphenylphosphonium iodide (5-OBTPIPs), [**5**]: a mixture of **4** (200 mg, 0.5 mmol, 1 equiv) and PPh_3 (1.37 g, 5.2 mmol, 10.5 equiv) in HPLC-grade toluene (15 mL), was stirred and heated under nitrogen overnight at 120°C in darkness. The progress of the reaction was monitored by TLC. The following day, the mixture was concentrated by stirring under vacuum and the residue was diluted in a minimal volume of DCM (2 mL) and precipitated with diethyl ether (150 mL). The solvent was decanted and the product was filtered under vacuum and washed with Et_2O (3 x 50 mL); residual solvent was removed under reduced pressure to afford **5** as white powder in 87% yield (292 mg, 0.45 mmol). ^{1}H-NMR (250 MHz, $CDCl_3$): δ = 7.98 – 7.61 (m; 16H, Ar), 7.56 (d, J = 2.4 Hz; 1H, CH), 7.13 (dd, J = 2.4, 0.9 Hz; 1H), 7.03 (s; 1H), 6.12 (d, J = 9.8 Hz; 1H), 4.63 (t, J = 5.9 Hz; 2H, OCH_2), 3.94 (t, J = 14.7 Hz; 2H, CH_2), 2.50 – 2.31 (m; 2H, CH_2P^+), 2.08 – 1.84 ppm (m; 2H, CH_2);); ^{13}C-NMR (62.9 MHz, $CDCl_3$): δ = 161.1 (CO), 158.2, 152.4, 148.6, 145.0, 143.0, 139.3, 135.1, 135.0 133.7, 133.5, 130.6, 130.4, 118.6, 117.2, 112.7, 112.1, 105.9, 105.7, 93.4, 71.2, 30.3, 30.0, 22.9, 22.1, 19.3, 19.2 ppm.

Synthesis of 5-OBDMPPIPs (6)

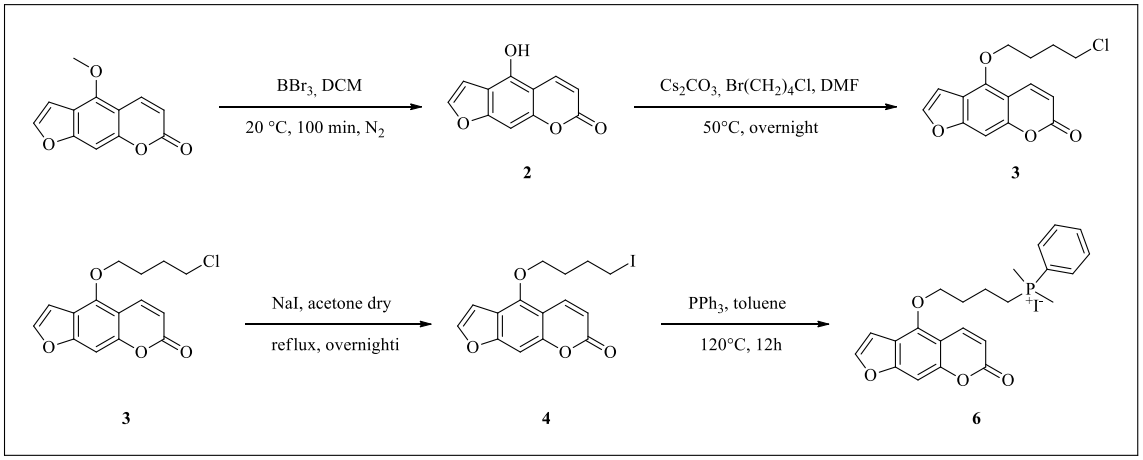

Dimethyl(4-((7-oxo-7H-furo[3,2-g]chromen-4-yl)oxy)butyl)(phenyl)phosphonium iodide (5-OBDMPPIPs), [**6**]: a mixture of **4** (202 mg, 0.5 mmol, 1 equiv) and $P(CH_3)_2Ph$ (923 mg, 6.7 mmol, 13.5 equiv) in HPLC-grade toluene (15 mL), was stirred and heated under nitrogen at 110°C in darkness. The progress of the reaction was monitored by TLC. After 5 hours, the mixture was concentrated by stirring under vacuum and then the residue was diluted in the minimal volume MeOH (2-3 mL) and precipitated with diethyl ether (150 mL). The solvent was decanted and the product was filtered under vacuum and washed with Et_2O (3 x 50 mL); residual solvent was removed under reduced pressure to afford **6** in 72% yield (197 mg, 0.38 mmol). ^{1}H-NMR (250 MHz, acetone d-6): δ = 8.10 (dd, J = 9.8, 0.6 Hz), 7.78 (s), 7.75 (d, J = 2.4 Hz), 7.16 (dd, J = 2.4, 1.0 Hz), 7.07 – 6.98 (m), 6.67 (d, J = 2.2 Hz), 6.12 (d, J = 9.8 Hz), 4.55 (t, J = 6.0 Hz), 3.93 (t, J = 6.0 Hz), 2.08 – 1.80 (m); ^{13}C-NMR (62.9 MHz, acetone d-6): δ = 160.8 (CO), 159.1, 153.7, 153.1, 152.1, 150.0, 146.16, 139.9, 116.6, 116.3, 113.9, 113.2, 107.2, 106.4, 93.8, 73.5, 68.6, 27.5, 26.7 ppm.

Synthesis of PAP-1-OH (7)

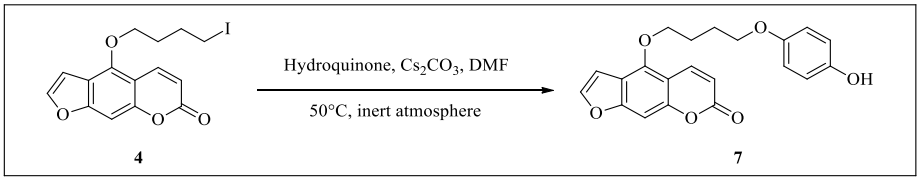

4-(4-(4-hydroxyphenoxy)butoxy)-7H-furo[3,2-g]benzopiren-7-one (PAP-1-OH), [**7**]: a mixture **4** (100 mg, 0.26 mmol, 1 equiv) and Cs_2CO_3 (128 mg, 2 mmol, 2 equiv) were dissolved in anhydrous DMF (15 mL), and hydroquinone (434 mg, 3.9 mmol, 15 equiv) was added to the mix. The solution was stirred and heated at 45 °C in darkness overnight. The following day EtOAc (90 mL) was added to the solution and the mixture was washed

with 0.5 M HCl (5 x 50 mL). The organic phase was dried over $MgSO_4$ and filtered. The solvent was stripped off under vacuum and the crude product was purified by flash chromatography using $CHCl_3$/acetone (90:10) as eluent to afford **7** as a white powder in 84 % yield (81 mg, 0.2 mmol). ^{1}H-NMR (250 MHz, $CDCl_3$): δ = 8.10 (dd, J = 9.8, 0.6 Hz), 7.75 (d, J = 2.4 Hz), 7.16 (dd, J = 2.4, 1.0 Hz), 7.07 – 6.98 (m), 6.67 (d, J = 2.2 Hz), 6.12 (d, J = 9.8 Hz), 4.55 (t, J = 6.0 Hz), 3.93 (t, J = 6.0 Hz), 2.08 – 1.80 (m). ^{13}C-NMR (62.9 MHz, $CDCl_3$): δ = 160.83, 159.11, 153.73, 153.13, 152.15, 150.06, 146.16, 139.99, 116.59, 116.27, 113.89, 113.19, 107.16, 106.39, 93.82, 73.46, 68.59, 27.50, 26.68 ppm. ESI+-MS (ion trap): m/z: 367, [M+H$^+$].

Synthesis of PAP-1-4-TetraGME

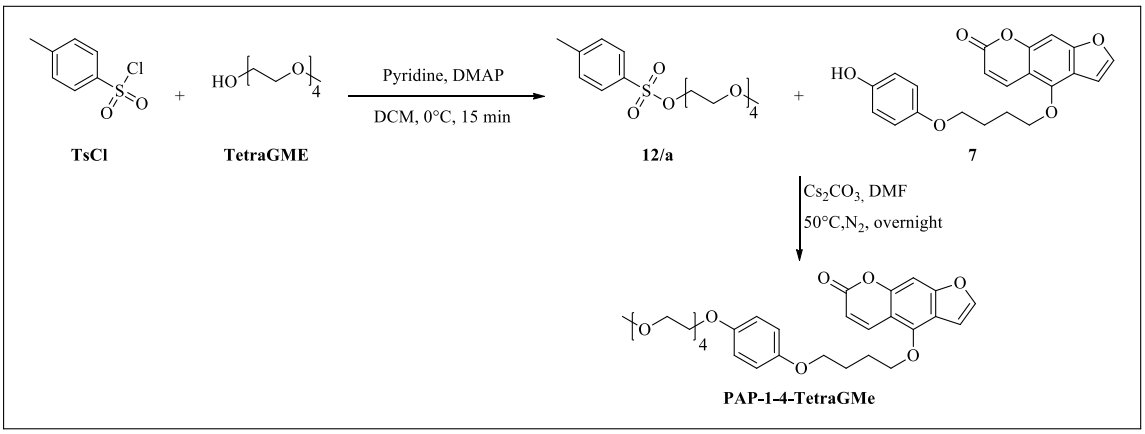

Methoxy tetra-(ethylenglicol)-(p-toluensulfonate) (TetraGME-OTs), [**12/a**] : pyridine (5.32 g, 33.6 mmol, 2 eq.) and DMAP (8.21 g, 67.2 mmol, 2 eq.) were added to a solution of methoxy-tetra-(ethylene glycol) TetraGME (7g, 33.6 mmol, 1 eq.) in DCM (15 mL), and the mixture was stirred at 0°C for 15 min. A solution of tosyl chloride (9.61 g, 50.4 mmol, 1.5 eq.) in DCM (15 mL) was then added dropwise and the mixture was stirred at room temperature for 4 hours. The mixture was diluted in DCM (150 mL) and washed with 0.5 M HCl (100 mL). The aqueous layer was washed with DCM (5 x 75 mL) and all organic fractions were collected, dried over MgSO4, filtered and the solvent removed in vacuo. The residue was purified by flash chromatography using DCM/EtOAc 8:2 as eluent to afford 11.95 g of **12/a** (100 %) as a colorless oil. ^{1}H NMR (300 MHz, $CDCl_3$) δ = 8.12 (d, J = 9.8 Hz, 1H), 7.88 – 7.70 (m, 1H), 7.57 (d, J = 2.4 Hz, 1H), 7.38 – 7.24 (m, 1H), 7.11 (s, 1H), 6.95 (dd, J = 2.4, 1.0 Hz, 1H), 6.88 – 6.72 (m, 1H), 6.23 (d, J = 9.8 Hz, 1H), 4.53 (t, J = 6.0 Hz, 2H), 4.20 – 4.11 (m, 2H), 4.10 – 4.04 (m, 2H), 4.01 (t, J = 5.8 Hz, 2H), 3.87 – 3.78 (m, 2H), 3.77 – 3.44 (m, 12H), 3.36 (s, 3H), 2.44 (s, 3H); ^{13}C NMR (75 MHz, $CDCl_3$) δ =

162.92, 160.02, 154.47, 147.90, 142.10, 139.92, 134.76, 132.59, 130.72, 130.45, 128.61, 118.50, 118.13, 118.07, 116.28, 115.36, 113.06, 96.60, 94.39, 74.22, 73.62, 72.28, 70.95, 70.56, 70.36, 61.63, 59.76, 24.16, 22.47 ppm.

4-(4-(4-(2,5,8,11-tetraoxatridecan-13-yloxy)phenoxy)butoxy)-7H-furo[3,2-g] benzopiren-7-one (PAP-1-4-TetraGME), [**11**]: compound **7** (185 mg, 0.50 mmol, 1 equiv) was dissolved in DMF (15 mL) with Cs_2CO_3 (328 mg, 1.1 mmol, 2 equiv) and **12/a** (282 mg, 0.75 mmol, 1.5 equiv) was added to the mixture. The solution was stirred and heated at 50 °C in darkness overnight. The following day EtOAc (100 mL) was added to the solution and then the mixture was washed with 0.5 M HCl (5 x 70 mL). The organic phase was dehydrated with $MgSO_4$ and filtered. The solvent was removed under vacuum and the crude product was purified by flash chromatography using DCM/acetone (70:30) as eluent to afford **11** as a colorless oil in 93 % yield (261 mg, 0.47 mmol). ^{1}H NMR (300 MHz, $CDCl_3$) δ = 8.12 (d, J = 9.8 Hz, 1H), 7.88 – 7.70 (m, 1H), 7.57 (d, J = 2.4 Hz, 1H), 7.38 – 7.24 (m, 1H), 7.11 (s, 1H), 6.95 (dd, J = 2.4, 1.0 Hz, 1H), 6.88 – 6.72 (m, 1H), 6.23 (d, J = 9.8 Hz, 1H), 4.53 (t, J = 6.0 Hz, 2H), 4.20 – 4.11 (m, 2H), 4.10 – 4.04 (m, 2H), 4.01 (t, J = 5.8 Hz, 2H), 3.87 – 3.78 (m, 2H), 3.77 – 3.44 (m, 12H), 3.36 (s, 3H), 2.44 (s, 3H) ppm. ^{13}C NMR (75 MHz, $CDCl_3$) δ = 162.92, 160.02, 154.47, 147.90, 142.10, 139.92, 134.76, 132.59, 130.72, 130.45, 128.61, 118.50, 118.13, 118.07, 116.28, 115.36, 113.06, 96.60, 94.39, 74.22, 73.62, 72.28, 70.95, 70.56, 70.36, 61.63, 59.76, 24.16, 22.47 ppm. ESI+-MS (ion trap): m/z: 558, [M+H$^+$].

Synthesis of PAP-1-4-EsaGME

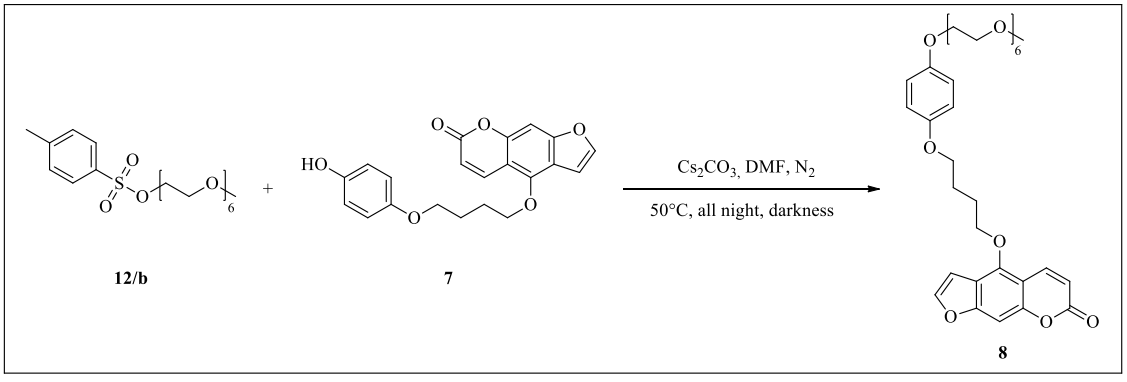

Methoxy-esa(ethylene glycol)-p-toluenesulfonate (EsaGME-OTs), [**12/b**]: pyridine (1.09 mL, 13.5 mmol, 2 eq.) and DMAP (1.65 g, 13.5 mmol, 2 eq.) were added to a solution of EsaGME (2.0 g, 6.75 mmol, 1 eq.) in dichloromethane (10 mL), and the mixture was

stirred at 0 °C for 15 min. A solution of tosyl chloride (1.93 g, 10.1 mmol, 1.5 eq.) in dichloromethane (10 mL) was then added dropwise and the mixture was stirred at room temperature for 4 hours. The mixture was diluted in dichloromethane (150 mL) and washed with 0.5N HCl (100 mL). The aqueous layer was washed with dichloromethane (5 × 75 mL) and all the organic fractions were collected, dried over $MgSO_4$ and filtered. The solvent was evaporated under reduced pressure and the residue was purified by flash chromatography using DCM/Acetone 6.5:3.5 as eluent. 98% yield as a colorless oil. ^{1}H-NMR (250 MHz, $CDCl_3$) δ (ppm) = 2.35 (s, 3H, Ar-CH_3), 3.27 (s, 3H, -O-CH_3), 3.42-3.60 (m, 22H, 2 × -O-CH_2-CH_2-O- + -O-CH_2-), 4.05 (t, 2H, Ts-CH_2-, ^{3}J = 5.00 Hz), 7.25 (d, 2H, 2 × Ar-H, ^{3}J = 7.93 Hz), 7.70 (d, 2H, 2 × Ar-H, ^{3}J = 8.34 Hz). ^{13}C-NMR (62.9 MHz, $CDCl_3$) δ (ppm) = 144.6, 132.7, 129.6, 127.7, 71.7, 70.5, 70.4, 70.4, 70.3, 70.3, 70.3, 69.1, 68.4, 58.8, 21.4; ESI-MS (ion trap): m/z 451 [M+H$^+$].

4-(4-(4-(2,5,8,11,14,17-hexaoxanonadecan-19-yloxy)phenoxy)butoxy)-7H-furo[3,2-g]chromen-7-one (PAP-1-4-EsaGME), [**8**]: compound **7** (200 mg, 0.54 mmol, 1 equiv) was dissolved in DMF (25 mL) with Cs_2CO_3 (352 mg, 1.1 mmol, 2 equiv) and **12/b** (365 mg, 0.81 mmol, 1.5 equiv) was added to the mixture. The solution was stirred and heated at 50 °C in darkness overnight under nitrogen. The following day, EtOAc (100 mL) was added to the solution and then the mixture was extracted with 0.5 M HCl (5 x 70 mL). The aqueous phase was discarded and the organic phase was dehydrated with $MgSO_4$ and filtered. The solvent was evaporated under vacuum and the crude product was purified first by flash chromatography using CH_2Cl_2/acetone (70:30, R_f = 0.5) as eluent and then using preparative HPLC to afford **8** as a colorless oil in 93 % yield (261 mg, 0.47 mmol). ^{1}H NMR (300 MHz, $CDCl_3$) δ = 8.09 (d, J = 9.8 Hz, 1H), 7.55 (d, J = 2.4 Hz, 1H), 7.07 (s, 1H), 6.92 (d, J = 2.3 Hz, 1H), 6.86 – 6.73 (m, 4H), 6.20 (d, J = 9.8 Hz, 1H), 4.50 (t, J = 5.9 Hz, 2H), 4.09 – 4.02 (m, 2H), 3.99 (t, J = 5.7 Hz, 2H), 3.86 – 3.75 (m, 2H), 3.74 – 3.56 (m, 18H), 3.52 (dd, J = 5.6, 3.3 Hz, 2H), 3.34 (s, 3H), 2.18 – 1.85 (m, 4H) ppm. ^{13}C NMR (75 MHz, CD_2Cl_2) δ = 161.24, 158.28, 153.11, 153.09, 152.70, 148.94, 144.86, 139.34, 115.69, 115.34, 113.18, 112.49, 106.67, 105.18, 95.60, 93.80, 77.58, 77.16, 76.74, 72.57, 71.93, 70.80, 70.62, 70.58, 70.49, 69.87, 68.12, 67.89, 59.02, 26.99, 26.00 ppm. ESI-MS (ion trap): m/z 646 [M+H]$^+$.

Synthesis of PAP-1-4-PrTPPI (16)

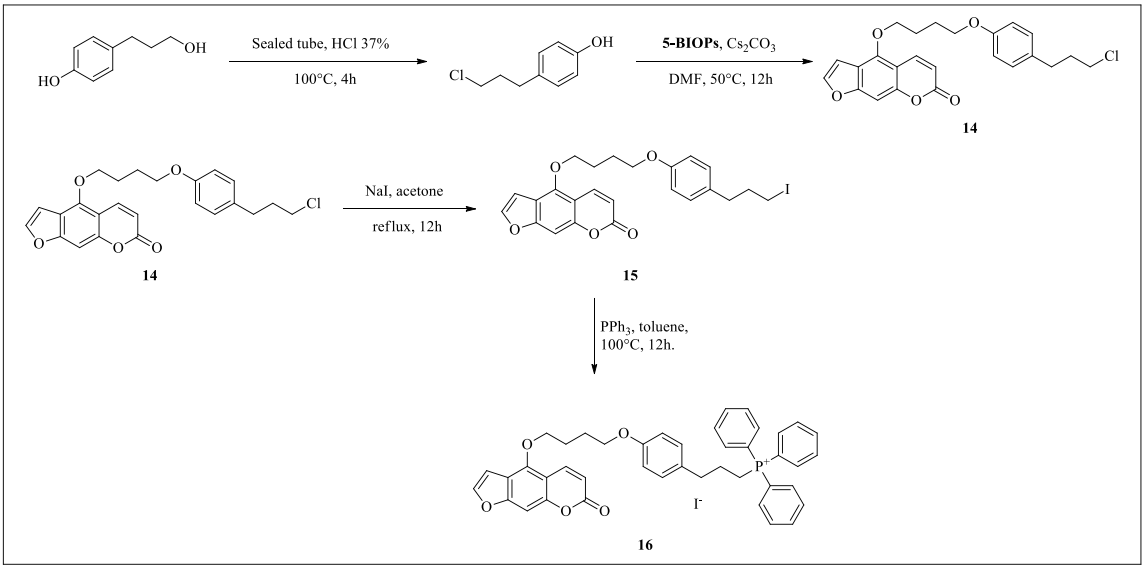

4-(3-chloropropyl)phenol, [**13**]: 4-(3-hydroxypropyl)phenol (500 mg, 3.4 mmol) and conc. HCl (4.5 mL) were heated in a Carius tube at 100°C for 4 h. After cooling, the reaction mixture was poured into water (150 mL) and extracted with ether (100 mL). The extract was dried over sodium sulfate and concentrated under vacuum to give a brown oil. The product was purified by flash chromatography (DCM) to afford **13** as a pale brown oil (457 mg, 2.7 mmol) in 82% yield. ^{1}H NMR (300 MHz, $CDCl_3$) δ (ppm) = 7.09 (d, J = 8.6 Hz, 1H), 6.81 (d, J = 8.6 Hz, 1H), 5.40 (s, 1H; Ar-OH), 3.55 (t, J = 6.5 Hz, 2H), 2.74 (t, J = 7.4 Hz, 2H), 2.18 – 1.95 (m, 2H); ^{13}C NMR (75 MHz, $CDCl_3$) δ = 153.59, 132.92, 129.61, 115.31, 44.18, 34.11, 31.74 ppm.

4-(4-(4-(3-chloropropyl)phenoxy)butoxy)-7H-furo[3,2-g]chromen-7-one (PAP-1-4-propCl), [**14**]: compound **4** (560 mg, 1.5 mmol, 2.5 equiv) was dissolved in DMF (20 mL) with Cs_2CO_3 (586 mg, 1.2 mmol, 2 equiv) and **13** (150 mg, 0.6 mmol, 1 equiv) was added to the mixture. The solution was stirred and heated at 50 °C in darkness overnight. The following day, EtOAc (250 mL) was added to the solution and then the mixture was extracted with 0.5 M HCl (5 x 70 mL). The aqueous layer was washed with dichloromethane (100 mL) and all the organic fractions were collected, dried over $MgSO_4$ and filtered. The solvent was eliminated under vacuum and the crude product was purified by flash chromatography using DCM/petroleumether (95:5) to afford **14** as a solid white powder in 97% yield (372 mg, 0.87 mmol). ^{1}H NMR (300 MHz, CD_2Cl_2) δ (ppm) = 8.12 (d, J = 9.8 Hz, 1H), 7.60 (t, J = 2.1 Hz, 1H), 7.18 – 7.04 (m, 3H), 6.98 (dd, J = 5.4, 2.4 Hz, 1H), 6.87 – 6.74 (m, 2H), 6.29 – 6.11 (m, 1H), 4.50 (dt, J = 17.8, 5.6 Hz, 2H), 4.05 (t, J =

5.7 Hz, 2H), 3.53 (t, J = 6.5 Hz, 2H, C-Cl), 3.32 (t, J = 6.4 Hz, 2H), 2.75 – 2.65 (m, 2H), 2.17 – 1.91 (m, 4H).

4-(4-(4-(3-iodopropyl)phenoxy)butoxy)-7H-furo[3,2-g]chromen-7-one (PAP-1-4-propI), [**15**]: compound **14** (400 mg, 0.9 mmol, 1 equiv) and NaI (1.82 g, 12 mmol, 13 equiv) were added to anhydrous acetone (25 mL) under nitrogen. The solution was stirred and heated at 70 °C in darkness overnight. The next day, EtOAc (150 mL) was added to the solution and the mixture was washed with deionized water (150 mL). Then, the aqueous layer was re-washed with DCM (70 mL). In the end, the aqueous phase was discarded and the organic phase was dried over with $MgSO_4$ and filtered. The solvent was stripped off under vacuum and the crude product was purified by flash chromatography using DCM/petroleumether/EtOAc (50:45:5) as eluent to afford **15** as a yellow powder in 65 % yield (317 mg, 0.6 mmol). ^{1}H NMR (500 MHz, CD_2Cl_2) δ (ppm) = 8.15 (d, J = 9.8 Hz, 1H), 7.62 (dd, J = 4.5, 2.4 Hz, 1H), 7.11 (t, J = 6.9 Hz, 3H), 6.99 (d, J = 8.5 Hz, 1H), 6.87 – 6.75 (m, 2H), 6.22 (dd, J = 19.1, 9.8 Hz, 1H), 4.52 (dt, J = 28.7, 5.9 Hz, 2H), 4.05 (t, J = 5.9 Hz, 2H), 3.31 (t, J = 6.7 Hz, 2H), 3.17 (t, J = 6.9 Hz, 2H, C-I), 2.65 (t, J = 7.3 Hz, 2H), 2.14 – 1.96 (m, 4H). ^{13}C NMR (126 MHz, CD_2Cl_2) δ (ppm) = 160.77, 158.29, 157.36, 152.83, 149.06, 144.91, 139.16, 132.69, 129.48, 114.37, 113.20, 112.55, 106.71, 105.17, 93.54, 93.47, 72.71, 67.43, 35.23, 30.86, 26.90, 25.94, 6.48, 6.16.

(3-(4-(4-((7-oxo-7H-furo[3,2-g]chromen-4-yl)oxy)butoxy)phenyl)propyl)triphenyl phosphonium iodide (PAP-1-4-propTPPI) , [**16**]: a mixture of **15** (290 mg, 0.6 mmol, 1 equiv) and PPh_3 (1.47 g, 5.6 mmol, 10 equiv) in HPLC-grade toluene (20 mL), was mixed and heated under nitrogen at 120°C in darkness overnight. The progress of the reaction was monitored by TLC. The following day, the solvent was eliminated under vacuum and then the residue was diluted in minimal volume DCM (2 mL) and precipitated with diethyl ether (150 mL). The solvent was decanted and the product was filtered under vacuum and washed with Et_2O (6 x 50 mL); residual solvent was removed under reduced pressure to afford **17** as pale yellow powder in 61% yield (267 mg, 0.34 mmol). ^{1}H NMR (300 MHz, $CDCl_3$) δ (ppm) = 8.11 (d, J = 9.8 Hz, 1H), 7.98 – 7.59 (m, 9H), 7.57 (d, J = 2.4 Hz, 1H), 7.16 – 7.04 (m, 1H), 6.98 – 6.92 (m, 1H), 6.76 (d, J = 8.6 Hz, 1H), 6.14 (dd, J = 22.1, 9.8 Hz, 1H), 4.56 (dt, J = 26.2, 5.8 Hz, 1H), 4.01 (t, J = 5.7 Hz, 1H), 3.96 – 3.81 (m, 1H), 3.66 (td, J = 12.8, 8.2 Hz, 1H), 2.94 (t, J = 7.2 Hz, 1H), 2.17 – 1.78 (m, 2H) ppm. ^{13}C NMR (126 MHz, $CDCl_3$) δ =161.24, 158.27, 157.43, 152.63, 148.95, 144.94, 139.43, 135.15, 133.81, 133.69, 133.61,

132.07, 130.60, 130.50, 129.99, 129.23, 128.66, 128.60, 118.36, 117.68, 114.55, 113.19, 112.38, 106.61, 105.23, 93.73, 72.56, 67.36, 65.83, 34.80, 34.66, 30.93, 26.94, 25.93, 24.64, 22.07, 21.67, 15.26 ppm.

Synthesis of PAP-1-4-COOH (17)

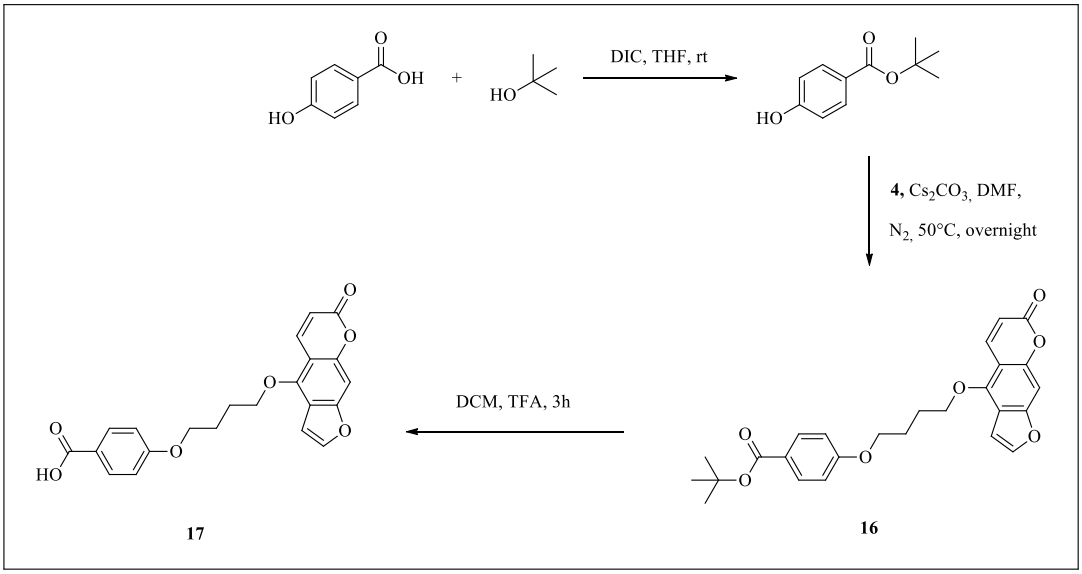

tert-Butyl 4-hydroxybenzoate. A mixture of 4-hydroxybenzoic acid (300 mg, 2.2 mmol, 1 eq), tert-butanol (2 mL, 22 mmol, 10 eq) and N,N′-diisopropylcarbodiimide (DIC) (550 mg, 4.3 mmol, 2 eq) in THF (20 mL) was stirred at room temperature overnight. The following day, the mixture was washed with brine (100 mL) and extracted with EtOAc (3 x 100 mL). The aqueous phase was discarded and the organic phase was dehydrated with $MgSO_4$ and filtered. The solvent was evaporated off under vacuum; the solid precipitate was removed by filtration and the product obtained was purified by flash chromatography using DCM /EtOAc (95:5) as eluent to afford tert-butyl 4-hydroxybenzoate as a white powder in 61% yield (317 mg, 0.6 mmol). ^{1}H NMR (300 MHz, $CDCl_3$) δ (ppm) = 7.93 – 7.84 (m, 2H, Ar), 6.93 – 6.84 (m, 2H, Ar), 1.59 (s, 9H); ^{13}C NMR (75 MHz, CD_2Cl_2) δ (ppm) = 166.87, 160.62, 131.86, 123.71, 115.33, 81.39, 28.37 (-CH_3).

tert-butyl 4-(4-((7-oxo-7H-furo[3,2-g]chromen-4-yl)oxy)butoxy)benzoate (PAP-1-4-TBE), [**16**]: compound **4** (560 mg, 1.5 mmol, 2.5 equiv) was dissolved in DMF (20 mL) with Cs_2CO_3 (586 mg, 1.2 mmol, 2 equiv) and tert-butyl 4-hydroxybenzoate (150 mg, 0.6 mmol, 1 equiv) was added to the mixture. The solution was stirred and heated at 50 °C in darkness overnight. The next day, EtOAc (250 mL) was added to the solution and then the

mixture was extracted with 0.5 M HCl (3 x 75 mL). The aqueous layer was washed with dichloromethane (80 mL) and all the organic fractions were collected, dried over $MgSO_4$ and filtered. The solvent was eliminated under vacuum and the crude product was purified by flash chromatography using DCM/petroleumether/EtOAc (80:15:5) to afford **16** as a solid white powder in 85% yield (230 mg, 0.51 mmol). ^{1}H NMR (300 MHz, $CDCl_3$) δ (ppm) = 8.11 (d, J = 9.8 Hz, 1H), 7.98 – 7.86 (m, 2H), 7.57 (d, J = 2.4 Hz, 1H), 7.11 (s, 1H), 6.94 (dd, J = 2.3, 0.8 Hz, 1H), 6.91 – 6.82 (m, 2H), 6.23 (d, J = 9.8 Hz, 1H), 4.53 (t, J = 5.8 Hz, 2H), 4.12 (t, J = 5.5 Hz, 2H), 2.16 – 1.98 (m, 4H), 1.58 (s, 9H). ^{13}C NMR (75 MHz, CD_2Cl_2) δ (ppm) = 165.57, 162.21, 161.16, 158.29, 152.71, 148.88, 144.89, 139.23, 131.45, 124.67, 113.89, 113.15, 112.55, 106.63, 105.17, 93.83, 80.61, 72.44, 67.52, 28.31, 26.94, 25.85.

4-(4-((7-oxo-7H-furo[3,2-g]chromen-4-yl)oxy)butoxy)benzoic acid (PAP-1-4-COOH), [**17**]: compound **16** (230 mg, 0.5 mmol, 1 equiv) was dissolved in anhydrous dichloromethane (20 mL) and trifluoroacetic acid (3.4 mL, 50 mmol, 100 equiv) was added to the mixture. The solution was stirred at room temperature for 2 hours. The solvent was removed on a rotary evaporator. The residue was diluted with toluene and evaporated again (repeating three times); in the end, it was dried under vacuum to afford **17** as a solid white-grey powder in 97 % yield (191 mg, 0.48 mmol). ^{1}H NMR (250 MHz, d_6-DMSO) δ (ppm) = 8.18 (d, J = 9.8 Hz, 1H), 8.04 (d, J = 2.5 Hz, 1H), 7.87 (d, J = 8.8 Hz, 2H), 7.35 (s, 2H), 7.00 (d, J = 8.8 Hz, 2H), 6.29 (d, J = 9.8 Hz, 1H), 4.58 (s, 2H), 4.15 (s, 2H), 1.98 (s, 4H) ppm. ^{13}C NMR (63 MHz, d_6-DMSO) δ (ppm) = 218.31, 167.01, 162.16, 160.15, 157.69, 152.15, 148.74, 145.96, 139.51, 131.36, 122.87, 114.27, 112.87, 112.32, 105.93, 105.75, 93.21, 72.20, 67.46, 26.13, 25.16 ppm.

Synthesis of PAP-1-4-CarbPrTPPI (20)

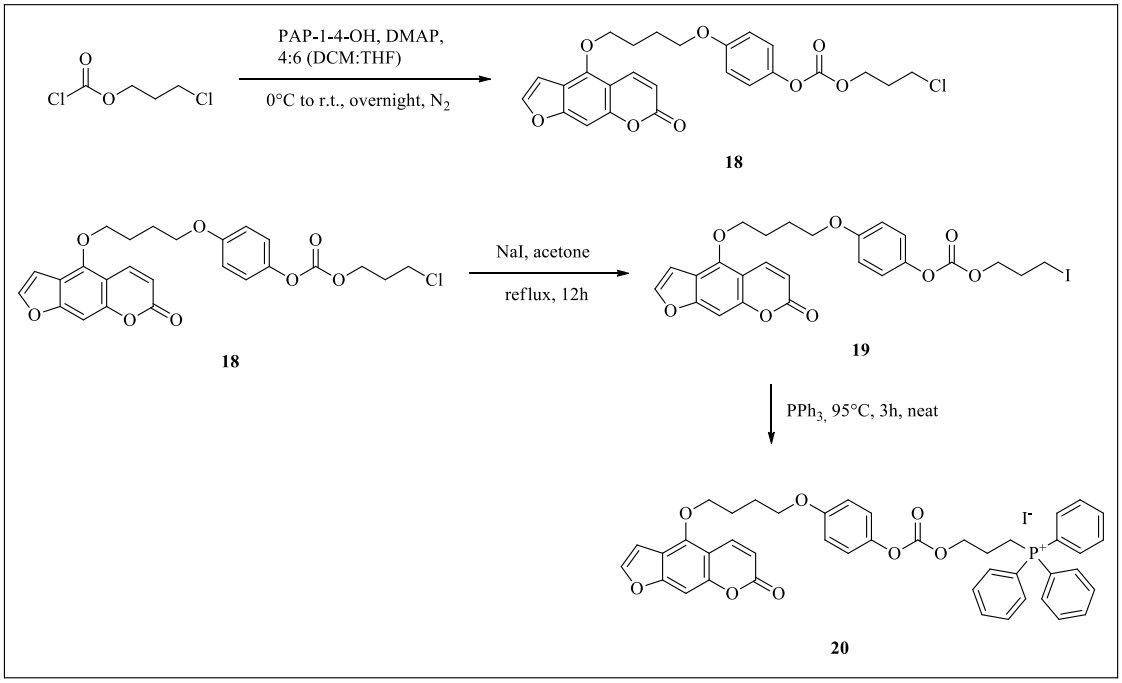

3-chloropropyl (4-(4-((7-oxo-7H-furo[3,2-g]chromen-4-yl)oxy)butoxy)phenyl) carbonate (PAP-1-4-CarbPrCl), [**18**]: compound **7** (150 mg, 0.4 mmol, 1 equiv) was dissolved in anhydrous THF (15 mL) with DMAP (60 mg, 0.5 mmol, 1.2 equiv) at 0°C. After a few minutes, a solution of 3-chloropropyl chloroformate (49 uL, 0.4 mmol, 1 equiv) in anhydrous dichloromethane (10 mL) was added dropwise ~~at~~ to the reaction mixture. The system was stirred under inert atmosphere overnight. Subsequently, EtOAc (100 mL) was added to the solution and then the mixture was extracted with 0.5 M HCl (5 x 70 mL). The aqueous phase was discarded and the organic phase was dried over $MgSO_4$ and filtered. The solvent was eliminated under vacuum and the crude product was purified by flash chromatography using DCM /EtOAc (97:3, R_f = 0.31) as eluent to afford **18** as white powder in 94 % yield (188 mg, 0.38 mmol). ^{1}H NMR (500 MHz, $CDCl_3$) δ = 8.12 (d, J = 9.8 Hz, 1H), 7.57 (d, J = 2.3 Hz, 1H), 7.16 – 7.01 (m, 3H), 6.94 (d, J = 1.7 Hz, 1H), 6.87 (d, J = 9.0 Hz, 2H), 6.24 (d, J = 9.8 Hz, 1H), 4.53 (t, J = 5.9 Hz, 2H), 4.40 (t, J = 6.0 Hz, 2H), 4.05 (t, J = 5.7 Hz, 2H), 3.68 (t, J = 6.3 Hz, 2H), 2.20 (p, J = 6.2 Hz, 2H), 2.14 – 1.96 (m, 4H) ppm. ^{13}C NMR (126 MHz, $CDCl_3$) δ = 161.28, 158.37, 156.76, 154.02, 152.81, 148.97, 144.95, 144.86, 139.32, 122.02, 115.12, 113.30, 112.70, 106.79, 105.21, 94.00, 72.58, 67.82, 65.39, 40.94, 31.60, 27.03, 25.99 ppm. ESI-MS (ion trap): m/z 487 $[M+H]^+$.

3-iodopropyl (4-(4-((7-oxo-7H-furo[3,2-g]chromen-4-yl)oxy)butoxy)phenyl) carbonate (PAP-1-4-CarbPrI), [**19**]: compound **18** (188 mg, 3.8 mmol, 1 equiv) was

dissolved in anhydrous acetone (30 mL) satured with NaI, under nitrogen. The solution was stirred and heated at 70 °C in darkness overnight. The next day, EtOAc (100 mL) was added to the solution and then the mixture was washed with water (4 x 75 mL). Then, the aqueous layer was re-washed with DCM (70 mL). In the end, the aqueous phase was discarded and the organic phases were dehydrated with $MgSO_4$ and filtered. The solvent was evaporated off under vacuum and the crude product was purified by flash chromatography using DCM/EtOAc (97:3, R_f = 0.7) as eluent to afford **19** as light yellow powder in 80 % yield (176 mg, 0.3 mmol). ^{1}H NMR (300 MHz, $CDCl_3$) δ = 8.09 (d, J = 9.8 Hz, 1H), 7.56 (d, J = 2.4 Hz, 1H), 7.17 – 7.01 (m, 3H), 6.93 (d, J = 2.4 Hz, 1H), 6.89 – 6.80 (m, 2H), 6.22 (d, J = 9.8 Hz, 1H), 4.51 (t, J = 5.8 Hz, 2H), 4.30 (t, J = 6.0 Hz, 2H), 4.04 (t, J = 5.6 Hz, 2H), 3.27 (t, J = 6.8 Hz, 2H), 2.23 (p, J = 6.4 Hz, 2H), 2.14 – 1.92 (m, 4H) ppm. ^{13}C NMR (75 MHz, $CDCl_3$) δ = 161.17, 158.26, 156.68, 153.89, 152.70, 148.89, 144.88, 144.77, 139.25, 121.94, 115.06, 113.18, 112.58, 106.67, 105.17, 93.86, 72.50, 68.22, 67.77, 32.28, 26.95, 25.92, 1.04 ppm. ESI-MS (ion trap): m/z 577 $[M+H]^+$.

(3-(((4-(4-((7-oxo-7H-furo[3,2-g]chromen-4-yl)oxy)butoxy)phenoxy)carbonyl)oxy) propyl) triphenyl phosphonium iodide (PAP-1-4-CarbPrTPPI), [**20**]: a mixture (neat) of **19** (176 mg, 0.3 mmol, 1 equiv) and PPh_3 (1.60 g, 5.6 mmol, 20 equiv), was mixed and heated under nitrogen at 95°C in darkness for 3 hours. After this time, the residue was dissolved in the minimal volume of DCM (5 mL) and the solute was precipitated with diethyl ether (150 mL). The solvent was decanted and the product was filtered under vacuum and washed with Et_2O (5 x 15 mL); residual solvent was removed under reduced pressure to afford **20** as light yellow powder in 98% yield (193 mg, 0.3 mmol). ^{1}H NMR (300 MHz, $CDCl_3$) δ = 8.08 (d, J = 9.8 Hz, 1H), 7.91 – 7.60 (m, 15H), 7.56 (d, J = 2.4 Hz, 1H), 7.05 (s, 1H), 7.00 (d, J = 9.0 Hz, 2H), 6.94 (d, J = 2.4 Hz, 1H), 6.81 (d, J = 9.1 Hz, 2H), 6.18 (d, J = 9.8 Hz, 1H), 4.52 (q, J = 6.0 Hz, 4H), 4.01 (t, J = 5.6 Hz, 2H), 3.87 (td, J = 13.3, 8.0 Hz, 2H), 2.29 – 1.77 (m, 6H) ppm. ^{13}C NMR (75 MHz, $CDCl_3$) δ = 161.27, 158.28, 156.65, 153.48, 152.64, 148.94, 144.98, 144.62, 139.41, 135.39, 133.80, 133.67, 130.81, 130.64, 121.91, 118.23, 117.08, 115.07, 113.20, 112.43, 106.62, 105.24, 93.76, 72.52, 67.81, 42.88, 26.89, 25.87, 22.30, 20.37, 19.66 ppm.

Synthesis of PAP-1-4-CP-PrTPPI (21)

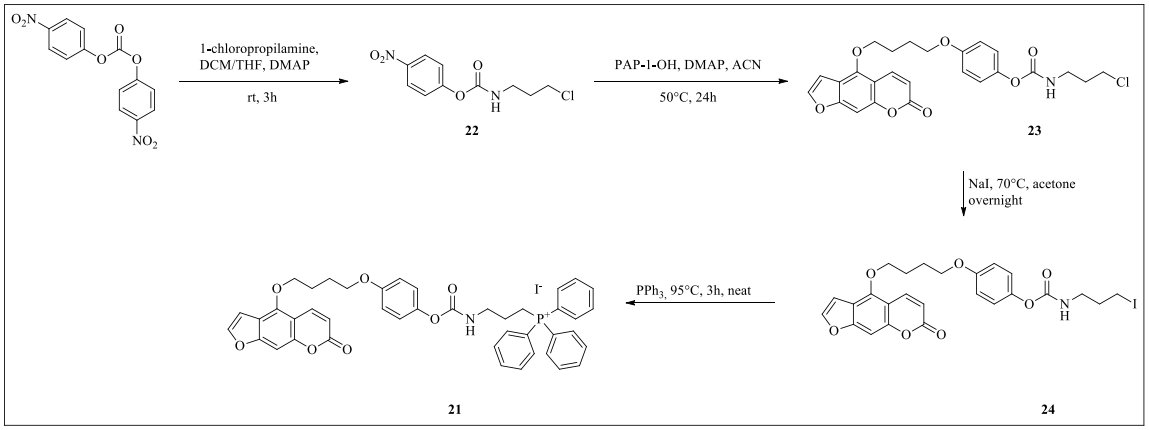

4-nitrophenyl (3-chloropropyl)carbamate (PNPCbmPrCl), [**22**]: 300 mg (2.31 mmol, 1 equiv) of 3-chloropropylamine hydrochloride were dissolved in 10 mL of anhydrous DCM after the addiction of 564 mg (4.61 mmol, 2 equiv) of DMAP. This solution was added dropwise to a solution of BPNPC (775 mg, 2.54 mmol, 1.1 equiv) in anhydrous THF (20 mL) while stirring under nitrogen at room temperature. After 3 hours, EtOAc (150 mL) was added to the solution and then the mixture was washed with ~~a~~ 0.5 M HCl (3 x 75 mL). The aqueous layer was washed with dichloromethane (80 mL) and all the organic fractions were collected, dried over $MgSO_4$ and filtered. The solvent was eliminated under vacuum and the crude product was purified by flash chromatography using DCM/EtOAc (98:2) to afford **22** as white-yellow powder in 75% yield (448 mg, 1.73 mmol). ^{1}H NMR (300 MHz, Acetone) δ = 8.28 (d, J = 9.1 Hz, 2H), 7.44 (d, J = 9.1 Hz, 2H), 7.19 (s, 1H), 3.74 (t, J = 6.5 Hz, 2H), 3.43 (dd, J = 12.8, 6.5 Hz, 2H), 2.10 (dd, J = 13.2, 6.6 Hz, 2H) ppm. ^{13}C NMR (75 MHz, $CDCl_3$) δ = 157.48, 154.22, 145.49, 125.75, 123.05, 43.09, 39.27, 33.33, 29.84 ppm.

4-(4-((7-oxo-7H-furo[3,2-g]chromen-4-yl)oxy)butoxy)phenyl (3-chloropropyl) carbamate (PAP-1-4-CbmPrCl), [**23**]: a mixture of **22** (282 mg, 1.1 mmol, 2 equiv), **7** (200 mg, 0.5 mmol, 1 equiv) and DMAP (133 mg, 1.1 mmol, 2 equiv) were added to ACN (20 ml) and stirred under nitrogen at 50°C for 48 hours. After this time, 0.5 M HCl (150 mL) was added to the solution and then the mixture was extracted with chloroform (3 x 100 mL). The organic layer was collected, dried over $MgSO_4$ and filtered. The solvent was eliminated under vacuum and the crude product was purified by flash chromatography using $CHCl_3$/Et_2O/petroleum ether (60:10:30, R_f = 0.15) to afford **23** as white powder in 70% yield (194 mg, 0.4 mmol). ^{1}H NMR (500 MHz, $CDCl_3$) δ = 8.10 (d, J = 9.8 Hz, 1H),

7.56 (d, J = 2.3 Hz, 1H), 7.10 (s, 1H), 7.01 (d, J = 9.0 Hz, 2H), 6.93 (dd, J = 2.3, 0.8 Hz, 1H), 6.84 (d, J = 9.0 Hz, 2H), 6.23 (d, J = 9.8 Hz, 1H), 4.52 (t, J = 6.0 Hz, 2H), 4.04 (t, J = 5.8 Hz, 2H), 3.62 (t, J = 6.3 Hz, 2H), 3.41 (q, J = 6.4 Hz, 2H), 2.15 – 1.90 (m, 6H) ppm. ^{13}C NMR (126 MHz, $CDCl_3$) δ = 161.40, 158.33, 156.19, 155.26, 152.73, 148.95, 144.93, 144.67, 139.42, 122.59, 114.99, 113.22, 112.56, 106.71, 105.22, 93.89, 77.16, 72.53, 67.75, 42.36, 38.69, 32.32, 26.98, 25.92 ppm. ESI-MS (ion trap): m/z 488 $[M+H]^+$.

4-(4-((7-oxo-7H-furo[3,2-g]chromen-4-yl)oxy)butoxy)phenyl (3-iodopropyl) carbamate (PAP-1-4-CbmPrI), [**24**]: compound **23** (183 mg, 0.4 mmol, 1 equiv) was dissolved in anhydrous acetone (30 mL) satured ~~in~~ with NaI, under nitrogen. The solution was stirred and heated at 70 °C in darkness overnight. The following day, EtOAc (100 mL) was added to the solution and then the mixture was washed with water (4 x 75 mL). Then, the aqueous layer was re-washed with DCM (50 mL). In the end, the aqueous phase was discarded and the organic phases were dehydrated with $MgSO_4$ and filtered. The solvent was eliminated under vacuum and the crude product was purified by flash chromatography using $CHCl_3$/MeOH (95:5) as eluent to afford **24** as a yellow powder in 72 % yield (155.6 mg, 0.27 mmol). ^{1}H NMR (300 MHz, $CDCl_3$) δ = 8.11 (d, J = 9.8 Hz, 1H), 7.57 (d, J = 2.3 Hz, 1H), 7.11 (s, 1H), 7.02 (d, J = 8.9 Hz, 2H), 6.94 (d, J = 2.0 Hz, 1H), 6.84 (d, J = 8.9 Hz, 2H), 6.24 (dd, J = 9.8, 2.6 Hz, 1H), 4.52 (t, J = 5.8 Hz, 2H), 4.04 (t, J = 5.6 Hz, 2H), 3.35 (q, J = 6.3 Hz, 2H), 3.22 (t, J = 6.8 Hz, 2H), 2.19 – 1.91 (m, 6H) ppm. ^{13}C NMR (75 MHz, CD_2Cl_2) δ = 161.41, 158.37, 156.24, 155.25, 152.78, 150.24, 148.99, 144.93, 144.70, 139.42, 122.60, 116.21, 115.64, 115.05, 113.30, 112.63, 106.79, 105.23, 93.97, 77.16, 72.59, 67.80, 41.80, 33.17, 27.03, 25.96, 2.81 ppm.

(3-(((4-(4-((7-oxo-7H-furo[3,2-g]chromen-4-yl)oxy)butoxy)phenoxy)carbonyl) amino) propyl) triphenylphosphonium iodide (PAP-1-4-CbmPrTPPI), [**21**]: a mixture of **24** (156 mg, 0.27 mmol, 1 equiv) and PPh_3 (1.50 g, 5.6 mmol, 20 equiv) (neat), was mixed and heated under nitrogen at 95°C in darkness for 3 hours. After this time, the mixture was dissolved in the minimal volume of DCM (5 mL) and the solute precipitated with diethyl ether (150 mL). The solvent was decanted and the product was filtered under vacuum and washed with Et_2O (5 x 15 mL); residual solvent was removed under reduced pressure to afford **21** as white powder in 82% yield (186 mg, 0.22 mmol). ^{1}H NMR (300 MHz, $CDCl_3$) δ = 8.11 (d, J = 9.8 Hz, 1H), 7.72 (m, 15H), 7.56 (d, J = 2.1 Hz, 1H), 7.36 (d, J = 4.3 Hz, 1H), 7.08 (s, 1H), 6.96 (d, J = 9.0 Hz, 2H), 6.78 (d, J = 8.8 Hz, 2H), 6.22 (d, J = 9.8 Hz,

1H), 4.51 (t, J = 5.7 Hz, 2H), 4.01 (t, J = 5.4 Hz, 2H), 3.73 (dd, J = 15.5, 13.0 Hz, 2H), 3.55 (d, J = 4.9 Hz, 2H), 2.20 – 1.80 (m, 6H) ppm. ^{13}C NMR (75 MHz, CD_2Cl_2) δ = 161.33, 158.33, 155.96, 155.64, 152.73, 149.00, 144.92, 139.44, 135.33, 133.73, 133.60, 130.78, 130.62, 122.65, 118.65, 117.51, 114.86, 113.28, 112.57, 106.73, 105.26, 93.86, 77.16, 72.61, 67.78, 65.89, 26.98, 25.93 ppm.

Synthesis of PAP-1-4-CS-PrTPPI (25)

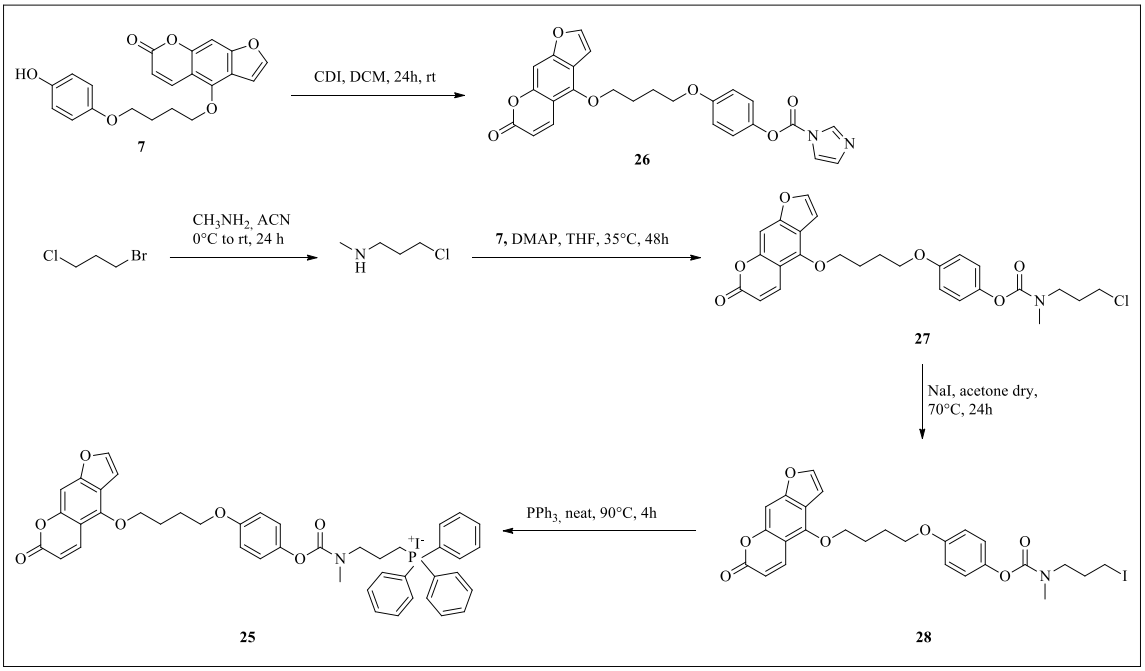

4-(4-((7-oxo-7H-furo[3,2-g]chromen-4-yl)oxy)butoxy)phenyl 1H-imidazole-1-carboxylate (PAP-1-CI), [**26**]: a solution of **7** (142.2 mg, 0.39 mmol, 1 equiv) and CDI (95 mg, 0.58 mmol, 1.5 equiv) in DCM (10 mL) was stirred under nitrogen at room temperature for 24 hours. After this time, DCM was added (100 mL) and the solution was washed with brine (3 x 75 mL); the organic phase was dried over $MgSO_4$ and filtered. The solvent was evaporated under vacuum to give PAP-1-CI (164.4 mg, 0.36 mmol, 92%) as a white powder that was used for the next steps without any further purification. ^{1}H NMR (300 MHz, $CDCl_3$) δ = 8.29 (s, 1H), 8.14 (d, J = 9.8 Hz, 1H), 7.63 – 7.52 (m, 2H), 7.23 – 7.10 (m, 4H), 6.94 (d, J = 9.0 Hz, 3H), 6.25 (d, J = 9.8 Hz, 1H), 4.55 (t, J = 5.7 Hz, 2H), 4.10 (t, J = 5.5 Hz, 2H), 2.09 (s, 4H) ppm. ^{13}C NMR (75 MHz, $CDCl_3$) δ = 161.25, 158.39, 157.42, 152.83, 148.95, 147.69, 144.98, 143.49, 139.27, 137.55, 131.20, 122.07, 117.53, 115.39, 113.34, 112.75, 106.83, 105.19, 94.07, 72.58, 67.92, 27.04, 26.01 ppm. ESI+-MS (ion trap): m/z: 461, [M+H$^+$].

3-chloro-N-methylpropan-1-amine (MeNHPrCl): a solution of 1-bromo-3-chloropropane (628 μL, 3.2 mmol, 1 equiv) in ACN (5 mL) was added dropwise to a solution of methylamine (40% w/w in water, 5.6 mL, 32 mmol, 10 equiv) in ACN (15 mL), at 0° C and under stirring. After the addition the ice-cooled bath was removed and the reaction was allowed to proceed for 24 hours. After this time, Et_2O (100 mL) was added to the mixture and the resulting solution was washed with 30% NaOH solution (2 x 100 mL); the organic phase was dried over $MgSO_4$ and filtered. The organic solvent was evaporated under reduced pressure and the obtained pale yellow oil was diluted with Et_2O and acidified with HCl (4.0 M in dioxane) under stirring. After 1 hour, when almost all the ammonium salt precipitate was formed, the suspension was filtered and the solid was washed 3 times with cold Et_2O. Then it was recovered and dried under nitrogen flux to give the desired product as a white powder (464.5 mg, 3.22 mmol) in quantitative yield. ^{1}H NMR (300 MHz, MeOD) δ = 4.81 (s, 1H), 3.70 (t, J = 6.3 Hz, 2H), 3.21 – 3.12 (m, 2H), 2.73 (s, 3H), 2.24 – 2.11 (m, 2H) ppm. ^{13}C NMR (75 MHz, MeOD) δ = 48.00, 42.18, 33.75, 30.03, 23.92 ppm. ESI+-MS (ion trap): m/z: 108, [M+H$^+$].

4-(4-((7-oxo-7H-furo[3,2-g]chromen-4-yl)oxy)butoxy)phenyl (3-chloropropyl) (methyl) carbamate (PAP-1-4-CS-Pr-Cl) , [**27**]: a mixture of DMAP (87 mg, 0.71 mmol, 2 equiv) and MeNHPrCl (61 mg, 0.43 mmol, 1.2 equiv) in THF (10 mL) was added dropwise to a solution of PAP-1-4-CI (164.4 mg, 0.36 mmol, 1 equiv) in THF. The mixture was stirred at 35°C for 48 hours. After this time, it was diluted with DCM (100 mL) and washed with 0.5 M HCl (2 x 100 mL). The organic phase was filtered and dried over $MgSO_4$. After evaporation of the solvent the residue was purified using FSGC (DCM/EtOAc (95:5, R_f = 0.3) as eluent to afford PAP-1-4-CS-Pr-Cl as a white powder in 50 % yield (89.4 mg, 0.2 mmol) as a milky oil. ^{1}H NMR (300 MHz, $CDCl_3$) δ = 8.10 (d, J = 9.8 Hz, 1H), 7.56 (d, J = 2.3 Hz, 1H), 7.09 (s, 1H), 7.01 (d, J = 8.9 Hz, 2H), 6.93 (d, J = 1.4 Hz, 1H), 6.84 (d, J = 9.0 Hz, 2H), 6.23 (d, J = 9.8 Hz, 1H), 4.51 (t, J = 5.8 Hz, 2H), 4.04 (t, J = 5.5 Hz, 2H), 3.60 (d, J = 5.8 Hz, 3H), 3.48 (t, J = 6.6 Hz, 1H), 3.05 (d, J = 28.2 Hz, 3H), 2.18 – 1.94 (m, 6H) ppm. ^{13}C NMR (75 MHz, $CDCl_3$) δ = 161.25, 158.32, 156.16, 152.75, 148.95, 145.11, 144.91, 139.32, 122.65, 114.99, 113.24, 112.61, 106.73, 105.20, 93.89, 72.56, 67.78, 47.34, 46.73, 42.43, 42.11, 35.28, 31.15, 30.67, 27.00, 25.94 ppm. ESI+-MS (ion trap): m/z: 522, [M+Na$^+$].

4-(4-((7-oxo-7H-furo[3,2-g]chromen-4-yl)oxy)butoxy)phenyl (3-iodopropyl)(methyl) carbamate (PAP-1-4-CS-Pr-I), [**28**]: PAP-1-4-CS-Pr-Cl (89.4 mg, 0.2 mmol, 1 equiv) was dissolved in anhydrous acetone (15 mL) satured with NaI, under nitrogen. The solution was stirred at 70 °C in darkness for 24 hours. The following day, the mixture was filtered and the solvent was removed under vacuum. The residue was diluted in DCM (100 mL) and the mixture was filtered again; the organic phase was washed with brine (100 mL) and water (25 mL). The organic phase was dried over $MgSO_4$, filtered and the solvent was removed under vacuum. The residue was dried under vacuum and next it was purified by flash chromatography using DCM/EtOAc (95:5) as eluent to afford PAP-1-4-CS-Pr-I as a yellow powder in 90 % yield (95.7 mg, 0.16 mmol). ^{1}H NMR (300 MHz, $CDCl_3$) δ = 8.11 (d, J = 9.8 Hz, 1H), 7.56 (d, J = 2.2 Hz, 1H), 7.10 (s, 1H), 7.01 (d, J = 8.9 Hz, 2H), 6.93 (d, J = 2.1 Hz, 1H), 6.84 (d, J = 8.9 Hz, 2H), 6.23 (d, J = 9.8 Hz, 1H), 4.52 (t, J = 5.8 Hz, 2H), 4.04 (t, J = 5.5 Hz, 2H), 3.46 (dt, J = 31.6, 6.5 Hz, 2H), 3.20 (dd, J = 15.8, 7.1 Hz, 2H), 3.05 (d, J = 27.8 Hz, 3H), 2.16 (dd, J = 13.0, 6.6 Hz, 2H), 2.11 – 1.95 (m, 4H) ppm. ^{13}C NMR (75 MHz, $CDCl_3$) δ = 171.17, 161.24, 158.33, 156.17, 152.77, 148.96, 145.10, 144.91, 139.31, 122.67, 115.00, 113.26, 112.64, 106.76, 105.20, 93.92, 72.57, 67.79, 50.29, 49.70, 35.26, 32.08, 31.68, 27.01, 25.95, 21.12 ppm. ESI+-MS (ion trap): m/z: 614, [M+Na^+].

(3-(methyl((4-(4-((7-oxo-7H-furo[3,2-g]chromen-4-yl)oxy)butoxy)phenoxy)carbonyl) amino) propyl) triphenylphosphonium iodide (PAP-1-4-CS-Pr-TPPI), [**25**]: PAP-1-4-CS-Pr-I (96 mg, 0.16 mmol, 1 equiv) was mixed with PPh_3 (850 mg, 3.24 mmol, 20 equiv) in neat conditions. The mixture was stirred for 4 hours at 95 °C. After this time, the residue was dissolved in DCM (2 mL) and the solute was precipitated in Et_2O. This procedure was repeated for a total of 5 times. The white solid obtained was recovered and characterized (100 mg, 0.12 mmol, 72%). ^{1}H NMR (300 MHz, $CDCl_3$) δ = 8.12 (d, J = 9.9 Hz, 1H), 7.94 – 7.64 (m, 15H), 7.59 (d, J = 2.2 Hz, 1H), 7.27 (s, 1H), 7.12 (s, 1H), 6.98 (d, J = 11.2 Hz, 2H), 6.82 (d, J = 11.7 Hz, 2H), 6.25 (d, J = 10.1 Hz, 1H), 4.55 (t, J = 5.2 Hz, 2H), 4.05 (t, J = 4.8 Hz, 2H), 4.00 – 3.60 (m, 4H), 3.12 (d, J = 47.2 Hz, 3H), 2.17 – 1.96 (m, 6H) ppm. ^{13}C NMR (75 MHz, $CDCl_3$) δ = 161.24, 158.28, 156.06, 152.65, 148.94, 144.95, 139.38, 135.28, 135.25 (d, J = 3.0 Hz), 133.79 (d, J = 10.1 Hz), 133.66, 130.72, 130.55 (d, J = 12.6 Hz), 122.56, 118.49, 117.34, 114.93, 112.45, 105.22, 93.74, 72.53, 67.75, 65.83, 36.05, 26.90, 25.86, 20.94, 20.24, 15.28 ppm. ESI+-MS (ion trap): m/z: 726, [M-I-+H^+].

Synthesis of CFZ-OH (30)

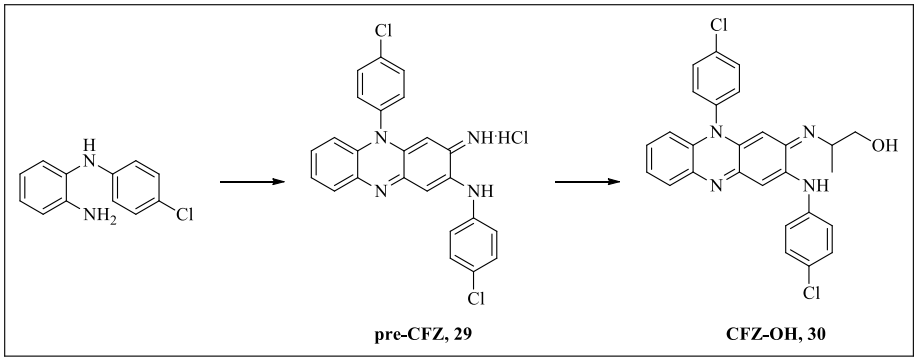

N,5-bis(4-chlorophenyl)-3-imino-3,5-dihydrophenazin-2-amine, (pre-CFZ), [**29**]: N^1-(4-chlorophenyl) benzene-1,2-diamine (500 mg, 2.3 mmol, 1 equiv.) was suspended in H_2O (50 mL) and stirred for 10 minutes. TFA (261 mg, 2.3 mmol, 1 equiv.) was then slowly added followed by the addiction of $FeCl_3$ (1.1 g, 6.9 mmol, 3 equiv.). After 1 hour, the reaction was quenched with 10 mL of a 0.1 M solution of NaOH in EtOH. The solvent was removed and the residue was suspended in 25 mL of chloroform, then the mixture was extracted with a Soxhlet extractor for 8 hours. Successively, the solvent was removed under vacuum and the residue was purified by flash chromatography using $CHCl_3$/Petroleum spirit/MeOH (8:1:1) + 1% CH_3COOH as eluent (R_f = 0.45) to afford **29** as a dark red power in 78% yield (389 mg, 0.9 mmol). ^{1}H NMR (500 MHz, TFA-d) δ = 7.98 (d, *J* = 8.1 Hz, 1H), 7.77 (t, *J* = 7.5 Hz, 1H), 7.74 (d, *J* = 7.5 Hz, 2H), 7.67 (t, *J* = 7.8 Hz, 1H), 7.46 (d, *J* = 7.5 Hz, 2H), 7.39 – 7.21 (m, 5H), 7.13 (d, *J* = 8.7 Hz, 1H), 6.55 (s, 1H), 3.90 (s, 1H) ppm. ^{13}C NMR (126 MHz, $CDCl_3$+ TFA) δ = 154.56, 145.87, 139.94, 139.43, 135.13, 133.88, 132.98, 132.48, 132.37, 130.80, 130.67, 128.02, 125.38, 121.91, 117.84, 117.81, 115.54, 113.27, 111.00, 96.43, 96.19, 76.97 ppm. ESI-MS (ion trap): 431 m/z $[M+H]^+$.

(Z)-2-((10-(4-chlorophenyl)-3-((4-chlorophenyl)amino)phenazin-2(10H)-ylidene) amino) propan-1-ol, (CFZ-OH), [**30**]: compound **29** (150 mg, 0.35 mmol, 1 equiv), 2-aminopropanol (600 mg, 8.00 mmol, 23 equiv) and sodium acetate (125 mg, 1.55 mmol, 17 equiv) were dissolved in dioxane. The mixture was stirred at 110°C overnight, then diluted with 100 mL of DCM and washed twice with HCl 0.5M (1 x 50 mL) and brine (1 x 50 mL). The organic phase was dried over $MgSO_4$, filtered and the solvent was evaporated under vacuum. The crude product was purified by SGFC using $CHCl_3$/EtP/MeOH (8:1:1+1%CH_3COOH, R_f = 0.35) as eluent to afford **CFZ-OH** (**30**, 128 mg, 0.26 mmol) as a dark red powder in 75% yield. ^{1}H NMR (500 MHz, $CDCl_3$) δ = 8.13 (d, *J* = 8.2 Hz, 1H), 7.84 (t, *J* = 8.5 Hz, 2H), 7.65 (t, *J* = 7.5 Hz, 1H), 7.57 (t, *J* = 7.6 Hz,

1H), 7.45 (d, *J* = 8.6 Hz, 2H), 7.40 - 7.36 (m, 5H), 6.98 (d, *J* = 8.5 Hz, 1H), 5.80 (s, 1H), 4.05 – 3.97 (m, 1H), 3.78 (m, 1H), 3.66 – 3.57 (m, 1H), 1.26 (s, 1H), 1.11 (d, J = 6.5 Hz, 3H) ppm. ^{13}C NMR (126 MHz, $CDCl_3$) δ = 153.50, 146.42, 142.19, 138.71, 138.05, 137.97, 135.18, 134.50, 132.47, 131.91, 131.30, 130.52, 130.39, 129.90, 129.55, 129.27, 128.90, 127.31, 124.84, 116.29, 104.29, 90.07, 64.05, 54.54, 14.95 ppm. ESI-MS (ion trap): 489 m/z $[M+H]^+$.

Synthesis of CFZ-A-3GME (35) and CFZ-A-6GME (36)

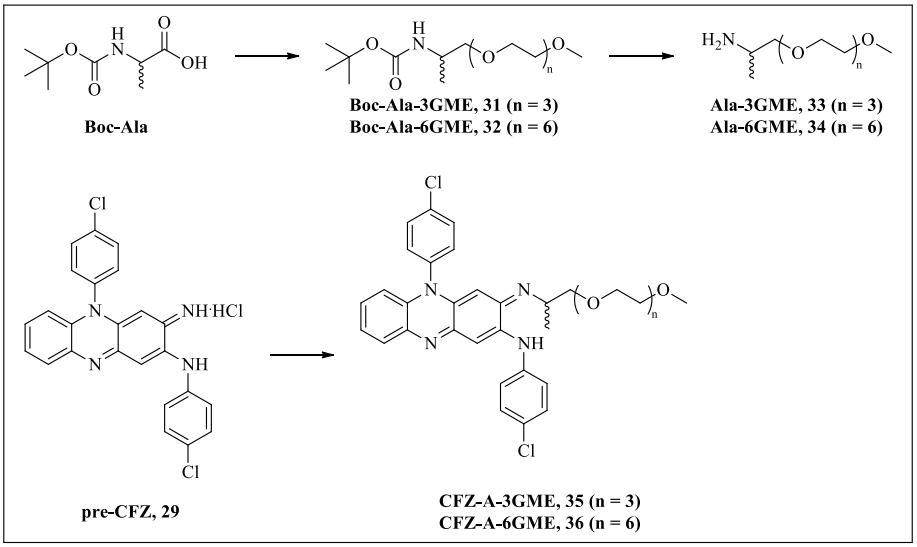

tert-butyl (1-hydroxypropan-2-yl)carbamate (Boc-Ala-OH): a solution of methyl carbonochloridate (1.8 mL, 23.3 mmol, 1.2 equiv.) in THF was added dropwise to a solution of N-methyl-morpholine (2.6 mL, 23.3 mmol, 1.2 equiv.), Boc-Alanine (4.0 g, 21.2 mmol, 1 equiv.) in anhydrous THF (70 mL) at 0°C. After 15 minutes, the solution was filtered and the filtrate was washed twice with THF (2 x 30 mL). A solution of $NaBH_4$ (1.1 g, 26.5 mmol) in water (8 mL) was added dropwise over 30 minutes to the THF solution at room temperature. The solvent was evaporated under vacuum and the residue was solubilized in EtOAc (100 mL). The organic phase was washed with brine until neutrality. The organic phase was dried using $MgSO_4$, filtered and the solvent was evaporated under vacuum. The residue was purified with FSGC using DCM/Acetone (93:7) as eluent to afford **Boc-Ala-OH** (2.93 g, 16.7 mmol) as colorless oil in 78% yield.^{1}H NMR (300 MHz, $CDCl_3$) δ = 4.78 (s, 1H), 3.81 – 3.71 (m, 1H), 3.66 – 3.57 (m, 1H), 3.54 – 3.45 (m, 1H), 2.98 (s, 1H), 1.45 (s, 9H), 1.15 (d, *J* = 6.8 Hz, 3H) ppm. ^{13}C NMR (75 MHz, $CDCl_3$) δ = 158.05, 81.35, 68.83, 50.26, 30.26, 30.12, 30.02, 18.95 ppm. ESI-MS (ion trap): 198 m/z $[M+Na]^+$.

Methoxy-tri(ethylene glycol)-p-toluenesulfonate (3GME-OTs), [**12/c**]: pyridine (1.09 mL, 13.5 mmol, 2 eq.) and DMAP (1.65 g, 13.5 mmol, 2 eq.) were added to a solution of 3GME (2.0 g, 6.75 mmol, 1 eq.) in dichloromethane (10 mL), and the mixture was stirred at 0 °C for 15 min. A solution of tosyl chloride (1.93 g, 10.1 mmol, 1.5 eq.) in dichloromethane (10 mL) was then added dropwise and the mixture was stirred at room temperature for 4 hours. The mixture was diluted in dichloromethane (150 mL) and washed with 0.5 N HCl (100 mL). The aqueous layer was washed with dichloromethane (5 × 75 mL) and all the organic fractions were collected, dried over $MgSO_4$ and filtered. The solvent was evaporated under reduced pressure and the residue was purified by flash-chromatography using CH_2Cl_2:EtOAc 8:2 as eluent. 95 % yield as a colorless oil. ^{1}H-NMR (250 MHz, $CDCl_3$) δ (ppm): 2.43 (s, 3H, Ar-C*H*$_3$), 3.35 (s, 3H, -O-C*H*$_3$), 3.49-3.66 (m, 10H, 2 × -O-C*H*$_2$-C*H*$_2$-O- + -O-C*H*$_2$-), 4.14 (t, 2H, Ts-C*H*$_2$-, $^3J_{H\text{-}H}$ = 5.75 Hz), 7.32 (d, 2H, 2 × Ar-*H*, $^3J_{H\text{-}H}$ = 8.25 Hz), 7.77 (d, 2H, 2 × Ar-*H*, $^3J_{H\text{-}H}$ = 8.25 Hz); ^{13}C-NMR (62.9 MHz, $CDCl_3$) δ (ppm): 144.7, 132.9, 129.7, 127.9, 71.8, 70.6, 70.5, 70.4, 69.2, 68.6, 58.9, 21.6. ESI-MS (ion trap): m/z 337 $[M+H_2O+H]^+$.

tert-butyl 2,5,8,11-tetraoxatetradecan-13-ylcarbamate (Boc-Ala-3GME), [**31**]: a solution of **12/c** (1 g, 3.14 mmol, 1.5 equiv.) in THF (5 mL) was added dropwise to a solution of Boc-Ala-OH (367 mg, 2.09 mmol, 1.0 equiv.) and NaH (108 mg, 2.7 mmol, 1.3 equiv.) in dry THF (20 mL), and the mix was allowed to react overnight at room temperature. The solvent was removed under vacuum and the residue was dissolved with DCM (75 mL) and washed with brine (10 mL). The organic phase was dried over $MgSO_4$ and filtered. The solvent was evaporated under reduced pressure and the residue was purified by FSGC using DCM/Acetone/MeOH (6.5:3.5:0.1, R_f = 0.16) as eluent to afford the product as colorless oil (420 mg, 1.31 mmol) in 62% yield. ^{1}H NMR (300 MHz, $CDCl_3$) δ = 4.88 (s, 1H), 3.85 – 3.39 (m, 15H), 3.37 (s, 3H), 1.43 (s, 9H), 1.15 (d, *J* = 6.7 Hz, 3H) ppm. ^{13}C NMR (75 MHz, $CDCl_3$) δ = 158.16, 71.88, 70.49, 70.43, 70.25, 69.23, 69.12, 58.92, 51.83, 41.26, 18.03, 17.92 ppm. ESI-MS (ion trap): 344 m/z $[M+Na]^+$.

tert-butyl 2,5,8,11,14,17,20-heptaoxatricosan-22-ylcarbamate (Boc-Ala-6GME), [**32**]: a solution of **12/b** (1 g, 2.2 mmol, 1.5 equiv.) in THF (5 mL) was added dropwise to a solution of Boc-Ala-OH (260 mg, 1.47 mmol, 1.0 equiv.) and NaH (76 mg, 1.9 mmol, 1.3 equiv.) in dry THF (20 mL), and the mix was allowed to react overnight at room

temperature. The solvent was removed under vacuum and the residue was dissolved with DCM (75 mL) and washed with brine (10 mL). The organic phase was dried over $MgSO_4$ and filtered. The solvent was evaporated under reduced pressure and the residue was purified by FSGC using EtOAc/ACN/EtP (7:2:1, R_f = 0.22) as eluent to afford the product **32** as colorless oil (270 mg, 1.2 mmol) in 40% yield. ^{1}H NMR (300 MHz, $CDCl_3$) δ = 4.93 (s, 1H), 3.92 – 3.50 (m, 25H), 3.43 (d, *J* = 4.5 Hz, 2H), 3.38 (s, 3H), 1.44 (s, 9H), 1.16 (d, *J* = 6.7 Hz, 3H) ppm.^{13}C NMR (50 MHz, $CDCl_3$) δ = 155.46, 79.01, 74.44, 71.94, 70.59, 59.00, 46.24, 28.44, 17.97 ppm. ESI-MS (ion trap): 476 m/z $[M+Na]^+$.

2,5,8,11,14,17,20-heptaoxatricosan-22-amine (NH_2-Ala-6GME), [**34**]: TFA (1.52 mL, 19.8 mmol, 22 equiv.) was added to a solution of **32** (410 mg, 0.9 mmol, 1.0 equiv) in anhydrous DCM (5 mL) . The solution was stirred at room temperature for 15 hours. The solution was quenched with 30% NaOH solution and extracted three times with DCM (3 x 90mL). The organic phase was dried over $MgSO_4$ and filtered. The solvent was evaporated under reduced pressure to afford the product **34** as a colorless oil (270 mg, 0.76 mmol) in 84% yield. The product was used for the next steps without any further purification. ^{1}H NMR (200 MHz, $CDCl_3$) δ = 3.82 (s, 2H), 3.70 – 3.49 (m, 27H), 3.38 (s, 3H), 1.13 (d, *J* = 6.2 Hz, 3H) ppm. ^{13}C NMR (50 MHz, $CDCl_3$) δ = 76.15, 71.86, 70.50, 70.39, 70.34, 70.28, 58.96, 46.89, 18.15 ppm. ESI-MS (ion trap): 354 m/z $[M+H]^+$.

2,5,8,11-tetraoxatetradecan-13-amine (NH_2-Ala-3GME), [**33**]: TFA (5 mL) and TIPS (0.5 mL) were added to a solution of **31** (240 mg, 0.75 mmol, 1.0 equiv) in anhydrous DCM (5 mL). The solution was stirred at room temperature for 15 hours. The solution was quenched with 30% NaOH solution and extracted three times with DCM (3 x 90mL). The organic phase was dried over $MgSO_4$ and filtered. The solvent was evaporated under reduced pressure to afford the product as a colorless oil (60 mg, 0.27 mmol) in 40% yield. The product was used for the next steps without any further purification. ^{1}H NMR (300 MHz, $CDCl_3$) δ = 3.71 – 3.37 (m, 14 H), 3.35 (s, 3 H), 3.22 – 3.08 (m, 1H), 2.51 (s, 2 H), 1.02 (d, *J* = 6.0 Hz, 3 H) ppm. ^{13}C NMR (50 MHz, $CDCl_3$) δ = 77.44, 72.03, 70.62, 70.53, 59.07, 46.70, 19.06 ppm. ESI-MS (ion trap): 222 m/z $[M+H]^+$.

3-(2,5,8,11-tetraoxatetradecan-13-ylimino)-N,5-bis(4-chlorophenyl)-3,5-dihydro phenazin-2-amine (CFZ-Ala-3GME), [**35**]: a solution of **29** (20 mg, 0.05 mmol, 1 equiv),

33 (60 mg, 0.27 mmol, 6 equiv) and CH_3COOH (3 μL, 0.05 mmol, 1 equiv) in dioxane (5 mL) was stirred at reflux overnight. The solvent was removed under reduced pressure and the residue was purified using preparative HPLC (0% to 90%B in 30 min; flux = 17 mL/min; A: water+0.05% TFA, B: ACN+0.05% TFA) to afford the desired product as a dark red solid (8.3 mg, 0.01 mmol) in 30 % yield. ^{1}H NMR (500 MHz, $CDCl_3$) δ = 9.61 (s, 1H), 8.15 (d, *J* = 8.2, 1.0 Hz, 1H), 7.83 (dd, *J* = 11.1, 8.4 Hz, 2H), 7.67 (t, *J* = 7.3 Hz, 1H),7.59 (t, *J* = 7.3 Hz,1H), 7.46 – 7.35 (m, 7H), 6.99 (d, *J* = 8.4 Hz, 1H), 6.00 (s, 1H), 3.85 – 3.41 (m, 15H), 3.30 (s,3H), 1.31 (d, *J* = 6.0 Hz, 3H) ppm. ^{13}C NMR (126 MHz, $CDCl_3$) δ = 153.28, 146.09, 142.02, 138.79, 138.06, 137.93, 135.24, 134.32, 132.38, 132.05, 131.62, 130.57, 130.44, 129.92, 129.64, 129.35, 128.85, 127.54, 124.76, 116.52, 105.24, 90.52, 73.79, 71.92, 70.63, 70.44, 70.37, 59.07, 53.57, 51.90, 16.13 ppm. ESI-MS (ion trap): 635 m/z $[M+H]^+$.

3-(2,5,8,11,14,17,20-heptaoxatricosan-22-ylimino)-N,5-bis(4-chlorophenyl)-3,5-dihydro phenazin-2-amine (CFZ-Ala-6GME): a solution of **29** (38 mg, 0.09 mmol, 1 equiv), **34** (270 mg, 0.76 mmol, 8.5 equiv) and CH_3COOH (5.3 μL, 0.09 mmol, 1 equiv) in dioxane (5 mL) was stirred at reflux overnight. The solvent was removed under reduced pressure and the residue was purified using preparative HPLC (0% to 90%B in 30 min; flux = 17 mL/min; A: water+0.05% TFA, B: ACN+0.05% TFA) to afford the desired product as a dark red solid (45 mg, 0.06 mmol) in 65 % yield. ^{1}H NMR (500 MHz, $CDCl_3$) δ = 9.61 (s, 1H), 8.15 (d, *J* = 8.2 Hz, 1H), 7.90 – 7.79 (m, 2H), 7.68 (t, *J* = 7.5 Hz, 1H), 7.61 (t, *J* = 7.4 Hz, 1H), 7.49 – 7.34 (m, 5H), 7.00 (d, *J* = 8.5 Hz, 1H), 5.99 (s, 1H), 3.80 – 3.45 (m, 27H), 3.36 (s, 3H), 1.27 (d, *J* = 6.3 Hz, 3H) ppm. ^{13}C NMR (126 MHz, $CDCl_3$) δ = 153.09, 145.81, 138.78, 138.01, 137.96, 135.09,134.13, 132.26, 131.89, 131.84, 130.38, 130.32, 129.81, 129.55, 129.18, 128.64, 127.56, 124.44, 116.51, 105.78, 90.48, 77.04, 73.34, 71.72, 70.33, 70.25, 70.18, 70.14, 70.09, 58.85, 51.23, 29.70, 15.73 ppm. ESI-MS (ion trap): 765 m/z $[M+H]^+$.

Synthesis of CFZ-N-4GME (37)

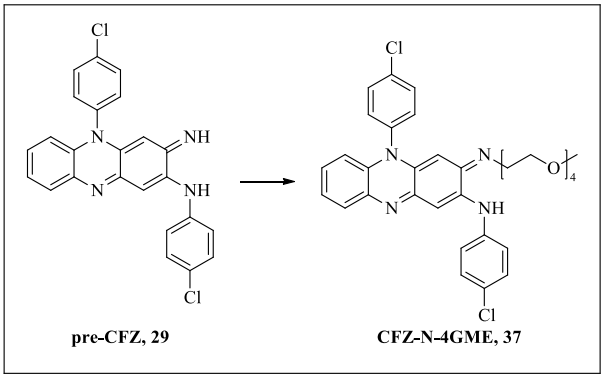

3-(2,5,8,11-tetraoxatridecan-13-ylimino)-N,5-bis(4-chlorophenyl)-3,5-dihydrophenazin-2-amine, (CFZ-N-4GME), [**37**]: compound **29** (50 mg, 0.11 mmol, 1 equiv) was suspended in dioxane (5 mL) and an aliquot of acetic acid (7 μL, 0.11 mmol, 1 equiv) was added under magnetic stirring. NH_2-4GME (360 mg, 1.74 mmol, 15 equiv) was added slowly to the refluxing mix; the solution was stirred overnight at 110 °C and the reaction was monitored by TLC using Petroleum ether/EtOAc (65:35), R_f = 0.35. The solution was cooled to room temperature, diluted with chloroform (25 mL), washed with brine (1 x 50 mL) and extracted with chloroform (3 x 50 mL). The organic phase was dried with $MgSO_4$ and filtered. The solvent was evaporated and the crude powder obtained was purified by preparative HPLC (40 %B to 70%B in 11.2 min – A = H_2O + 0.05% TFA and B = ACN) to afford **37** as a dark purple powder in 81% yield (45 mg, 0.09 mmol). ^{1}H NMR (500 MHz, $CDCl_3$) δ = 10.03 (s, 1H), 8.13 (d, J = 7.1 Hz, 1H), 7.83 (d, J = 8.6 Hz, 2H), 7.66 (t, J = 7.1 Hz, 1H), 7.59 (t, J = 7.2 Hz, 1H), 7.44 – 7.34 (m, 7H), 6.98 (d, J = 8.0 Hz, 1H), 6.02 (s, 1H), 3.81 (t, J = 5.4 Hz, 2H), 3.60 – 3.49 (m, 12H), 3.46 (dd, J = 5.7, 3.6 Hz, 2H), 3.31 (s, 3H) ppm. ^{13}C NMR (126 MHz, $CDCl_3$) δ = 154.46, 146.26, 142.02, 138.76, 138.25, 137.95, 135.17, 134.36, 132.20, 131.50, 130.42, 130.25, 129.83, 129.59, 129.02, 127.43, 124.54, 116.46, 104.99, 90.49, 71.94, 70.64, 70.57, 70.50, 70.47, 70.43, 68.81, 59.07, 45.21 ppm. ESI-MS (ion trap): 517 - 519 m/z $[M+H]^+$.

Synthesis of CFZ-COOMe (38)

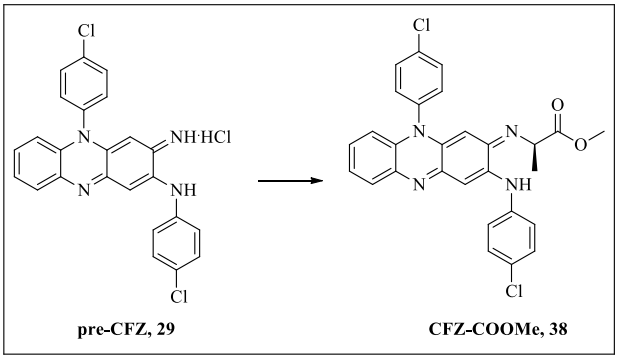

(Z)-methyl 2-((10-(4-chlorophenyl)-3-((4-chlorophenyl)amino)phenazin-2(10H)-ylidene)amino) propanoate, (CFZ-COOMe), [**38**]: compound **29** (40 mg, 0.09 mmol, 1 equiv), Alanine methyl ester (200 mg, 1.40 mmol, 15 equiv) and sodium acetate (130 mg, 1.60 mmol, 17 equiv) were dissolved in dioxane (8 mL). The mixture was stirred at 70°C overnight. The mixture was diluted with 100 mL of DCM and washed twice with HCl 0.5M (1 x 50 mL) and brine (1 x 50 mL). The organic phase was evaporated under vacuum. The crude product was purified by SGFC using $CHCl_3$/Acetone (9:1, R_f = 0.35) as eluent to afford **38** (20 mg, 0.04 mmol) as a orange powder in 68% yield. ^{1}H NMR (300 MHz, $CDCl_3$) δ = 7.65 (t, *J* = 7.1 Hz, 3H), 7.40 (d, *J* = 8.7 Hz, 2H), 7.33 – 7.07 (m, 9H), 6.49 (d, *J* = 8.1 Hz, 2H), 6.14 (s, 2H), 5.42 (s, 2H), 3.72 (d, *J* = 12.8 Hz, 7H), 1.72 (s, 3H), 1.59 (s, 3H). ESI-MS (ion trap): 515 m/z $[M+H]^+$.

Synthesis of CFZ-AE-3GME

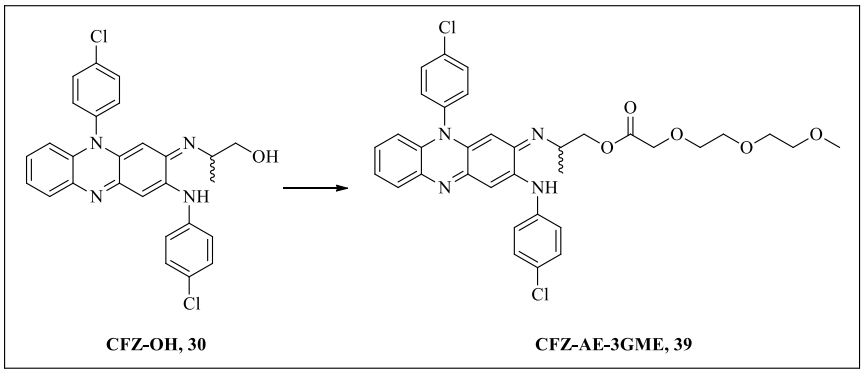

(Z)-2-((10-(4-chlorophenyl)-3-((4-chlorophenyl)amino)phenazin-2(10H)-ylidene)amino) propyl 2-(2-(2-methoxyethoxy)ethoxy)acetate, (CFZ-AE-3GME), [**39**]: a mixture of 3GME-COOH (30 mg, 0.17 mmol, 1 equiv), **30** (99.4 mg, 0.2 mmol, 1.2 equiv), DCC (38.6 mg, 0.19 mmol, 1.1 equiv) and DMAP (4 mg, 0.03 mmol, 0.2 equiv) in dry DCM (10 mL) was stirred at room temperature for 15 hours. The mixture was washed with brine (1 x 100 mL), the organic phase was concentrated to dryness under vacuum and

the product was purified by FSGC using DCM/Et_2O/Acetone (9:3:1, R_f = 0.25) as eluent to afford **4** (56.4 mg, 0.087 mmol) as a dark red powder in 55 % yield. ^{1}H NMR (300 MHz, $CDCl_3$) δ = 8.14 (d, *J* = 8.2 Hz, 1H), 7.85 (dd, *J* = 24.6, 8.4 Hz, 2H), 7.62 (dt, *J* = 25.7, 7.6 Hz, 2H), 7.51 – 7.41 (m, 4H), 7.40 – 7.29 (m, 3H), 6.97 (d, *J* = 8.3 Hz, 1H), 5.98 (s, 1H), 4.33 (ddd, *J* = 17.1, 11.2, 6.6 Hz, 2H), 4.08 (s, 2H), 3.87 (dd, *J* = 13.4, 7.0 Hz, 1H), 3.74 (d, *J* = 7.0 Hz, 1H), 3.69 – 3.55 (m, 5H), 3.53 – 3.46 (m, 2H), 3.32 (s, 3H), 1.47 (d, *J* = 6.4 Hz, 3H) ppm. ^{13}C NMR (75 MHz, $CDCl_3$) δ = 170.37, 153.20, 142.09, 135.33, 132.76, 132.05, 131.46, 130.38, 129.84, 129.41, 128.57, 124.67, 116.55, 89.78, 71.98, 71.05, 70.73, 70.59, 68.46, 66.00, 59.11, 50.11, 20.84, 16.38 ppm. ESI-MS (ion trap): 649 m/z $[M+H]^+$.

Synthesis of CFZ-Pr-TPPI (41)

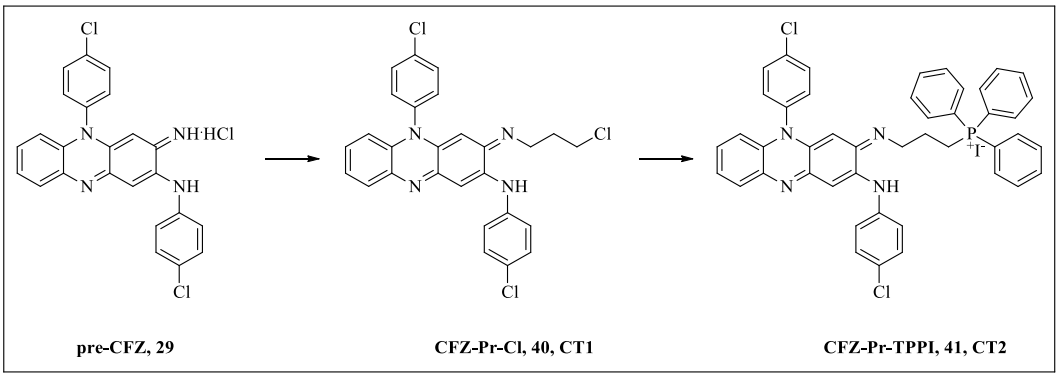

(Z)-N,5-bis(4-chlorophenyl)-3-((3-chloropropyl)imino)-3,5-dihydrophenazin-2-amine (CFZ-Pr-Cl, CT1), [**40**]: a solution of **29** (70 mg, 0.14 mmol, 1 equiv), 1-chloropropilamine (280 mg, 2.14 mmol, 15 equiv) and CH_3COONa (235 mg, 2.86 mmol, 20 equiv) in dioxane (25 mL) was stirred at 50°C for 20 hours. The solvent was removed under reduced pressure and the residue was diluited with DCM (100 mL) and washed with a mixture of brine and 0.5M HCl (80:20). The organic phase was dried over $MgSO_4$ and filtered. The solvent was removed under reduced pressure and the residue was purified by FSGC using DCM/Et_2O/MeOH (90:20:5, R_f =0.35) to afford **40** as a dark red solid (66 mg, 0.13 mmol) in 91% yield. ^{1}H NMR (500 MHz, $CDCl_3$) δ = 8.01 (d, *J* = 8.0 Hz, 1H), 7.79 (d, *J* = 8.5 Hz, 2H), 7.49 (dt, *J* = 15.5, 7.4 Hz, 2H), 7.42 (d, *J* = 8.7 Hz, 2H), 7.36 (d, *J* = 8.7 Hz, 4H), 7.26 (s, 1H), 6.84 (d, *J* = 8.3 Hz, 1H), 5.79 (s, 1H), 3.63 (t, *J* = 5.8 Hz, 2H), 3.48 (t, *J* = 7.1 Hz, 2H), 2.23 – 2.16 (m, 2H) ppm. ^{13}C NMR (126 MHz, $CDCl_3$) δ = 153.44, 142.41, 138.12, 137.48, 135.27, 134.84, 132.23, 130.37, 129.75, 129.36, 124.22, 115.77, 102.87, 89.38, 42.93, 35.88, 32.04, 31.65, 29.83 ppm. ESI-MS (ion trap): 509 m/z $[M+H]^+$.

(Z)-N,5-bis(4-chlorophenyl)-3-((3-iodopropyl)imino)-3,5-dihydrophenazin-2-amine (CFZ-Pr-I): a solution of CFZ-Pr-Cl (57 mg, 0.11 mmol, 1 equiv) and NaI (420 mg, 2.81 mmol, 25 equiv) in anhydrous acetone (15 mL) was stirred for 24 hours at 70°C. The mixture was filtered and the solvent was removed under reduced pressure. The residue was diluted in DCM (75 mL) and washed with brine (20 mL). The organic phase was concentrated and the residue was purified by FSGC using DCM/Et_2O/MeOH (90:10:2.5, R_f =0.25) to afford the product as a dark red solid (30 mg, 0.05 mmol) in 50% yield. ^{1}H NMR (300 MHz, $CDCl_3$) δ = 8.16 (d, *J* = 8.3 Hz, 1H), 7.84 (d, *J* = 8.7 Hz, 2H), 7.68 (t, *J* = 7.1 Hz, 1H), 7.60 (t, *J* = 7.8 Hz, 1H), 7.49 – 7.33 (m, 7H), 7.00 (d, *J* = 8.0 Hz, 1H), 3.57 – 3.47 (m, *J* = 13.3, 7.3 Hz, 2H), 3.22 (t, *J* = 6.0 Hz, 2H), 2.24 – 2.09 (m, 2H) ppm. ^{13}C NMR (75 MHz, $CDCl_3$) δ = 146.25, 142.05, 138.91, 138.14, 135.43, 134.38, 132.62, 132.40, 131.64, 130.55, 129.90, 129.59, 128.99, 128.89, 127.60, 124.58, 116.50, 105.26, 89.59, 45.30, 30.86, 3.77 ppm. ESI-MS (ion trap): 599 m/z $[M+H]^+$.

(Z)-(3-((10-(4-chlorophenyl)-3-((4-chlorophenyl)amino)phenazin-2(10H)-ylidene)amino) propyl) triphenylphosphonium iodide (CFZ-Pr-TPPI), [**41**]: a mixture of **CFZ-Pr-I** (69.2 mg, 0.12 mmol, 1 equiv) and PPh_3 (755 mg, 2.8 mmol, 25 equiv) in HPLC-grade toluene (20 mL), was stirred overnight under nitrogen 120°C in darkness. The solvent was evaporated off under vacuum and then the residue was diluted in the minimal volume of CH_2Cl_2 (2 mL) and precipitated with diethyl ether (150 mL). The solvent was decanted and the product was filtered under vacuum and washed with Et_2O (6 x 50 mL); residual solvent was removed under reduced pressure to afford **41** as dark red powder in 30% yield (26.7 mg, 0.04 mmol). ^{1}H NMR (300 MHz, $CDCl_3$) δ = 8.10 (d, *J* = 8.2 Hz, 1H), 7.90 (td, *J* = 7.1, 3.3 Hz, 8H), 7.81 – 7.57 (m, 14H), 7.50 – 7.33 (m, 6H), 6.96 (d, *J* = 9.7 Hz, 1H), 6.13 (s, 1H), 4.15 (t, *J* = 14.4 Hz, 2H), 4.03 – 3.91 (m, 2H), 2.51 – 2.34 (m, 2H) ppm. ^{13}C NMR (75 MHz, $CDCl_3$) δ = 138.08, 135.02, 134.41, 134.28, 132.62, 130.60, 130.43, 129.79, 124.96, 116.86, 104.28, 91.42 ppm. ESI-MS (ion trap): 733 m/z $[M+H]^+$.

3.7. REFERENCES

(1) Szabò, I.; Bock, J.; Jekle, A.; Soddemann, M.; Adams, C.; Lang, F.; Zoratti, M.; Gulbins, E. J. Biol. Chem. 2005, 280, 12790–12798.

(2) Gulbins, E.; Sassi, N.; Grassmè, H.; Zoratti, M.; Szabò, I. Biochim. et Biophys. Acta 2010, 1797, 1251–1259.

(3) Leanza, L.; Henry, B.; Sassi, N.; Zoratti, M.; Chandy, K. G.; Gulbins, E.; Szabò, I. EMBO Mol Med 2012, 4, 577–593.

(4) Leanza, L.; O'Reilly, P.; Doyle, A.; Venturini, E.; Zoratti, M.; Szegezdi, E.; Szabo, I. Curr. Pharm. Des. 2014, 20, 189–200.

(5) Szabò, I.; Soddemann, M.; Leanza, L.; Zoratti, M.; Gulbins, E. Cell death Differ. 2011, 18, 427–438.

(6) Szabó, I.; Bock, J.; Grassmé, H.; Soddemann, M.; Wilker, B.; Lang, F.; Zoratti, M.; Gulbins, E. Proc. Natl. Acad. Sci. United States Am. 2008, 105, 14861–14866.

(7) Leanza, L.; Trentin, L.; Becker, K. A.; Frezzato, F.; Zoratti, M.; Semenzato, G.; Gulbins, E.; Szabo, I. Leukemia 2013, 27, 1782–1785.

(8) Ren, Y. R.; Pan, F.; Parvez, S.; Fleig, A.; Chong, C. R.; Xu, J.; Dang, Y.; Zhang, J.; Jiang, H.; Penner, R.; Liu, J. O. PloS one 2008, 3.

(9) Szabo, I.; Zoratti, M. Physiol. Rev. 2014, 94, 519–608.

(10) Comes, N.; Bielanska, J.; Vallejo-Gracia, A.; Serrano-Albarrás, A.; Marruecos, L.; Gómez, D.; Soler, C.; Condom, E.; Ramón Y Cajal, S.; Hernández-Losa, J.; Ferreres, J. C.; Felipe, A. Front. Physiol. 2013, 4.

(11) Arcangeli, A.; Crociani, O.; Lastraioli, E.; Masi, A.; Pillozzi, S.; Becchetti, A. Curr. Med. Chem. 2009, 16, 66–93.

(12) Pardo, L. A.; Stühmer, W. Nat. Rev. Cancer 2014, 14, 39–48.

(13) Hoye, A. T.; Davoren, J. E.; Wipf, P.; Fink, M. P.; Kagan, V. E. Accounts Chem. Res. 2008, 41, 87–97.

(14) Smith, R. A. J.; Hartley, R. C.; Murphy, M. P. Antioxidants & redox Signal. 2011, 15, 3021–3038.

(15) Murphy, M. P.; Smith, R. A. J. Annu. Rev. Pharmacol. Toxicol. 2007, 47, 629–656.

(16) Biasutto, L.; Mattarei, A.; Paradisi, C. Methods Mol. Biol. 2015, 1265, 161–179.

(17) Biasutto, L.; Mattarei, A.; Marotta, E.; Bradaschia, A.; Sassi, N.; Garbisa, S.; Zoratti, M.; Paradisi, C. Bioorganic & Med. Chem. Lett. 2008, 18, 5594–5597.

(18) Mattarei, A.; Biasutto, L.; Marotta, E.; De Marchi, U.; Sassi, N.; Garbisa, S.; Zoratti, M.; Paradisi, C. Chembiochem : Eur. J. Chem. Biol. 2008, 9, 2633–2642.

(19) Biasutto, L.; Dong, L.-F.; Zoratti, M.; Neuzil, J. Mitochondrion 2010, 10, 670–681.

(20) Biasutto, L.; Mattarei, A.; Sassi, N.; Azzolini, M.; Romio, M.; Paradisi, C.; Zoratti, M. Anti-cancer agents Med. Chem. 2014, 14, 1332–1342.

(21) Mattarei, A.; Azzolini, M.; Spina, M. L.; Zoratti, M.; Paradisi, C.; Biasutto, L. Sci. Rep. 2015, 5.

(22) Levy, L. Lepr. Rev. 1981, 52, 23–26.

(23) Kamal, A.; Babu, A. H.; Ramana, A. V.; Sinha, R.; Yadav, J. S.; Arora, S. K. Bioorganic & Med. Chem. Lett. 2005, 15, 1923–1926.

(24) Barry, V. C.; Belton, J. G.; Conalty, M. L.; Denneny, J. M.; Edward, D. W.; O'Sullivan, J. F.; Twomey, D.; Winder, F. Nature 1957, 179, 1013–1015.

(25) Stöckner, F.; Beckert, R.; Gleich, D.; Birckner, E.; Günther, W.; Görls, H.; Vaughan, G. Eur. J. Org. Chem. 2007, 2007, 1237–1243.

(26) Choi, J. S.; Hahn, S. J.; Rhie, D. J.; Jo, Y. H.; Kim, M. S. Naunyn-Schmiedeberg's Arch. Pharmacol. 1999, 359, 256–261.

CHAPTER 4

NEW BIOACTIVE AND BIOCOMPATIBLE AMPHIPHILIC COPOLYMER SYSTEMS FOR ANTICANCER DRUG DELIVERY

In this last chapter I describe and discuss the results of studies in which I applied the prodrug approach to a macromolecular contest. By using resveratrol and pterostilbene as models, I have synthesized two different kinds of amphiphilic copolymers capable of self-assembling in water forming stable core-shell aggregates. These can hopefully be used for the delivery of anticancer drugs to solid tumors by exploiting the EPR (Enhanced Permeability and Retention) effect. During the time I spent at the ETH in Zürich, I have developed a novel class of polymethyloxazoline-pterostilbene copolymers. These constructs, definitely more performing than resveratrol-based ones, stably self-assemble in water remaining in suspension for several weeks without aggregating. Additionally, I observed that they become more stable when loaded with highly lipophilic drugs such as clofazimine. This drug was chosen both because once released in the cells it is expected to exhibit its known ability to inhibit the MDR pumps that are responsible for resistance to anticancer drugs, and because it was found to stabilize, even at very low concentration, the core of the polymeric micelles, probably thanks to hydrophobic interactions with pterostilbene units. Finally, these nanostructures have been preliminarily tested on macrophages to assess the toxicity and uptake using fluorescence microscopy techniques. The results of these very preliminary experiments are encouraging.

4.1. INTRODUCTION

Targeted delivery of therapeutic molecules is the most desirable feature of an effective chemotherapy. Low molecular weight traditional chemotherapeutic agents easily accumulate into the tumoral tissues, but also in other healthy organs, cells and subcellular organelles. In many cases, this feature creates a series of problematic side effects that requires the interruption of treatment. Additionally, low molecular weight drugs are rapidly eliminated from the body requiring frequent or higher dosing. Moreover, many new chemotherapeutic agents (i.e. taxanes) suffer of a very low water solubility and require the co-administration of ethanol or organic surfactants (Kolliphor EL™ or Tween-80™) that are not devoid of side effects[1]. Several approaches have been developed to circumvent the problems associated with non-specific drug delivery. One of the most promising is represented by the macromolecular drug delivery design. In particular, even if during the past 20 years liposomes-based drug nanocarrier systems have achieved considerable success in the field of drug delivery[2], more recently, the scientific community focused its attention on the development of more modular systems like, for example, polymeric nanoparticles[3].

4.1.1. AMPHIPHILIC POLYMERS AND CORE-SHELL NANOPARTICLES

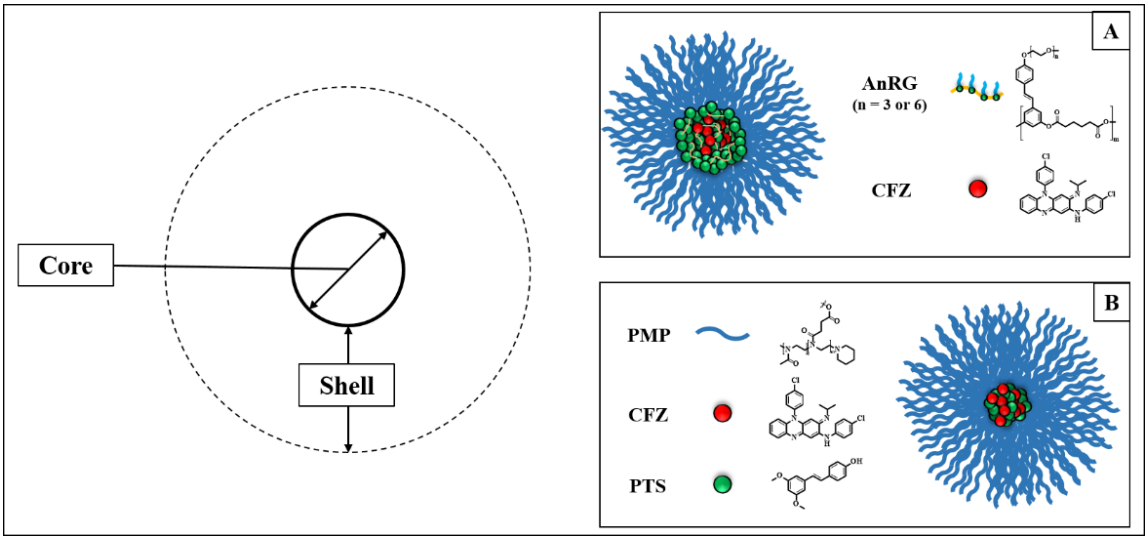

Figure 38. Schematic representation of core-shell polymeric micelles obtained from AnRG, PMPs and loaded with CFZ.

Amphiphilic copolymers are a class of macromolecules with amphiphilic character, having a large solubility difference between hydrophilic and hydrophobic segments. They are able to assemble in water giving polymeric micelles with a fairly narrow size distribution and

characterized by a core–shell structure (Figure 38). The water-insoluble block forms the hydrophobic core, which incorporates hydrophobic molecules (i.e. anticancer drugs), and the water-soluble block forms the hydrophilic shell to stabilize the micelles in aqueous media, ideally shielding the core and drugs from degrading interactions with the environment. Core segregation from water is the direct driving force for micellization and proceeds through a combination of intermolecular forces, including hydrophobic interaction[4] and hydrogen bonding[5] of constituent block copolymers.

The distribution of drug-loaded polymeric micelles in the body is strictly related to their size, shape and surface characteristics. A major obstacle to targeting by colloidal carrier systems, is the non-specific uptake by reticuloendothelial systems (RES), and the ability to avoid recognition by the RES is required for these systems to achieve longevity in the blood circulation[6]. In order to achieve these features the nanocarrier shell composition choice is fundamental: highly hydrophilic polymers like polyethylene glycol (PEG) and polyoxazolines (POXs) are able to confer stealth properties ensuring a prolonged blood life-time. Notably, the majority of investigators employ PEG as the hydrophilic and non-ionic component of the amphiphilic block copolymers to ensure stealth behavior and safety. Unfortunately, at the same time, because of the extensive use of PEG-containing cosmetics and other body contact products, a considerable portion of human population bear antibodies against PEG. There is increasing evidence that antibody response against PEG can affect the efficacy of PEG-conjugated drugs and drug nano-formulations in a subset of patients[7,8]. This provides the rationale for selecting a new different polymer platform for the design of the polymeric micelle shell.

4.1.2. NEW AMPHIPHILIC COPOLYMERS BASED ON PTEROSTILBENE AND RESVERATROL

During the last year of my PhD, I have designed, synthesized and tested two different platforms of novel bioactive copolymers:

1. A3RG and A6RG are two copolymers based on a polyester scaffold made of resveratrol-monoOEG (where the glycol side chain ha a length of 3 and 6 constitutive units respectively) and adipic acid (Figure 38, A and Figure 39).
2. PMP-1/4 are a series of four new amphiphilic polymethyloxazoline-co-pterostilbene based polymers (Figure 38, B and Figure 39).

Both these systems are able to assemble in water giving polymeric micelles loadable with CFZ and their hydrolysis products are not toxic (Figure 39).

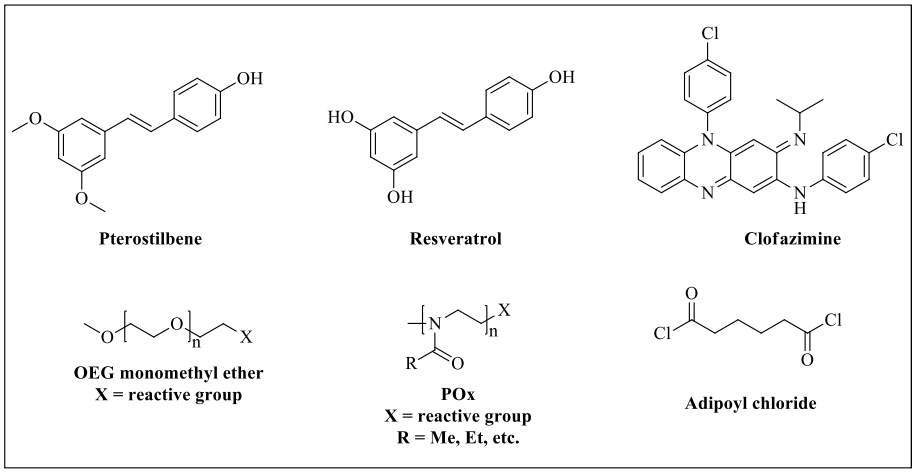

Figure 39. Molecular components of designed polymers.

The aims of this work are conceptually ambitious; on the one hand, to develop a new class of fully biocompatible and highly modular resveratrol-monoOEG and polymethyloxazoline amphiphilic copolymer able to assemble giving stable core-shell nanocarrier for anticancer drug delivery; on the other hand, to prove that core stabilization could be obtained by loading a highly hydrophobic drug called clofazimine (CFZ). This is a very well-study anti-leprosy and antimicrobial drug with many other potential therapeutically effects (i.e. specific anticancer agent)[9]. For our purposes, we will exploit the inhibitory activity against multidrug resistance pump (MDRP) property performed by CFZ[10]. In the future, by decorating the copolymer scaffold directly with anticancer drugs (i.e. etoposide, mitomycin c, doxorubicin, etc.) and loading the core with CFZ, it could be possible to obtain a nanocarrier capable of conveying the drug into solid tumor tissue compartments by exploiting the EPR effect[11] and of releasing, at the same time, the anticancer agent and CFZ. In this way, by inhibiting the MDR pumps CFZ will allow the drug to achieve its therapeutic effects without the danger of being blocked by these chemo-resistant systems. To the best of our knowledge, this is the first time that a dual delivery nanocarrier-based system was used, comprising both an anticancer drug and CFZ, as MDRP inhibitor (see Chapter 3)[9]. In order to achieve these ambitious goals, we need to obtain stable nanoparticles with a small PDI value and an average diameter lower than 200 nm. In particular, this last parameter is fundamental in order to exploit unique characteristics of tumor microenvironment, such as drain failure of lymphatic vessels, elevated interstitial fluid pressure (IFP)[12], and accumulation of collagen in the interstitial space[13]. All these characteristics limit the ability of the nanoformulations with sizes above 60 nm to penetrate

through the tumor[14]. It was shown that after extravasating from the leaky tumor vessel, these particles could not diffuse and remained in the perivascular region[15], which resulted in reduced efficacy.

4.2. Results and Discussion on Resveratrol-OEG Copolymers

4.2.1. Synthesis of AnRG Copolymers

As it was remarked in the previous section, the employed phenolic compounds are natural substances that our body can easily recognize and metabolize[16–18]. Resveratrol (RSV) and pterostilbene (PTS) shown in Figure 39, are common polyphenols that everybody usually assumes regularly with the diet, while adipic acid is a constituent of the Krebs cycle. Moreover, the above mentioned polyphenols are being studied since a long time due to their potential role on tumor angiogenesis[19].

Concerning the creation of hydrophilic side chains of the AnRG copolymer, I employed two oligoethylenglycols (OEG) of two different chain lengths, 3 and 6. This choice was made in order to prevent micellar aggregation in aqueous solutions and to exploit the well-known OEG stealth properties against immune system.

In Figure 40, are represented the two amphiphilic copolymers A3RG and A6RG. The OEG side chain was linked to RSV by an ether bond formed with the hydroxyl group either at position 4' or 3 of resveratrol. In this way, I synthesized a monomer that could later be used for the polycondensation reaction with adipoyl chloride.

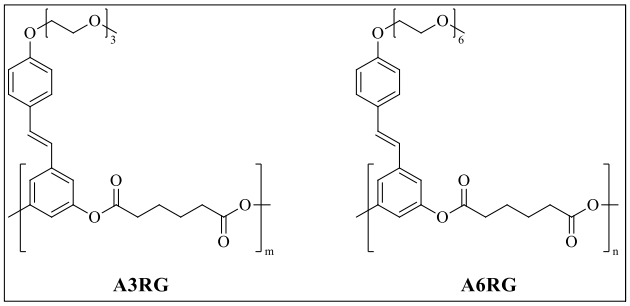

Figure 40. RSV copolymers with OEG side chains link by an ether with the polyester scaffold.

The monomer synthesis is summarized in the upper part of Figure 41, while the polymerization reaction is shown in the lower part of the same figure.

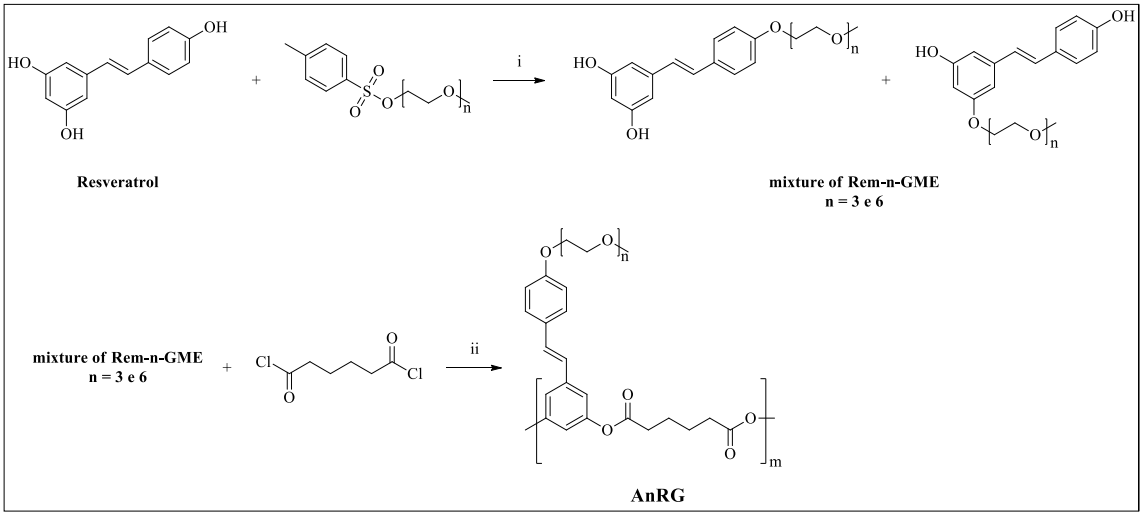

Figure 41. Synthesis of resveratrol monomer and AnRG: i) Cs_2CO_3, DMF, 50°C, 5h; ii) TEA•HCl, 1,2-dichlorobenzene, 200°C, 48h, N_2.

The optimization of the synthesis and the purification of these macromolecules required months of attempts. The monomer was easy to purify by silica flash chromatography, but the two isomers (3 and 4') could not be separated. Finally, the AnRG copolymers were purified by precipitation in cold methanol and then dialyzed against acetone for 2 days (membrane MWCO 1 kDa). The final polymeric product appears as a very viscous dark brown oil. The color is probably due to oxidation processes occurring when the RSV is deprotonated during the polycondensation reaction. Only a few percent fraction of oxidized product is sufficient to make the final product colored. Fortunately, however, these side products didn't affect the product final properties. The reaction time was a fundamental parameter to control the final molecular weight and the features of the copolymer: after 48 h, the obtained product showed good properties and it was easy to purify and characterize. FT-IR spectroscopy revealed the presence of ester bonds with a characteristic band at 1760 cm^{-1}. ^{1}H-NMR analysis allowed to estimate the average molecular weight that was 3300 Da in the case of A3RG and 7900 Da in the case of A6RG; both values were in good agreement with the results of GPC analysis using THF as eluent and polystyrene (PS) standards used for calibration.

4.2.2. PREPARATION OF DRUG LOADED POLYMERIC MICELLES

Drug loaded AnRG micelles were prepared using the nanoprecipitation method[20,21]. This technique offers numerous advantages, in that it is straightforward, rapid and easy to perform. The nanoparticle formation is practically instantaneous and the entire procedure is carried out in only one step. The copolymer (AnRG) was dissolved in acetone at a

concentration of 10 mg/mL and, in the same solution, CFZ drug was dissolved at a concentration of 0.1 mg/mL to form the diffusing phase. This phase was then added to 25 mL of distilled water (the dispersing phase) by means of a syringe positioned with the needle directly in the medium under high magnetic stirring for 24 hours at room temperature. The freshly formed nanoparticles were then centrifuged 2 times for 10-min cycles at 4300 × g to precipitate all aggregates and unloaded CFZ. The precipitate was analyzed using UV-Vis in order to quantify the drug loading percentage.

Unfortunately, it was observed that the A3RG (with the shortest hydrophilic OEG side chain) micelles tend to irreversibly aggregate after few hours. To overcome this inconvenient, 0.2% (w/w) of the commercial surfactant Tween-40™ was added to the distilled water used during the micelles preparation in order to increase the nanoparticles stability. Obviously, this alteration of the system surfactant properties was made only in order to consent a complete characterization of the A3RG copolymers and its shape and PDI. Certainly, this system wasn't stable enough to be employed as polymeric loaded nanocarrier but it was still interesting to be studied and compered with the more stable A6RG.

4.2.3. Size Distribution and Stability of CFZ-loaded AnRG Micelles

The water nanosuspension was used for DLS size distribution quantification and stability assays; all these data are summarized in Table 3.

NPs	Average diameter (nm)	PDI	LC (%)	LE (%)	DL (%)
A3RG*	99 ± 1	0.10	-	-	-
Loaded A3RG*	147 ± 6	0.16	-	-	-
A6RG	216 ± 7	0.26	-	-	-
Loaded A6RG	281 ± 5	0.36	1.09	100	1.10

Table 3. AnRG NPs characterization by DLS measurements on water diluted solutions. *: water content of Tween-20™ was 0.2% (w/w), for this reason LC, LE and DL couldn't be calculated correctly. For LC, LE and DL equations see Materials and Methods.

From the data reported in Table 3 it is evident that once the systems were loaded with clofazimine, their hydrodynamic diameter increased. The loading efficiency (LE) was quantitative and the A6RG obtained nanosuspension was stable for over 15 days. On the contrary, empty and loaded A3RG even in the presence of 0.2% Tween-20™ weren't stable for more than 2 days.

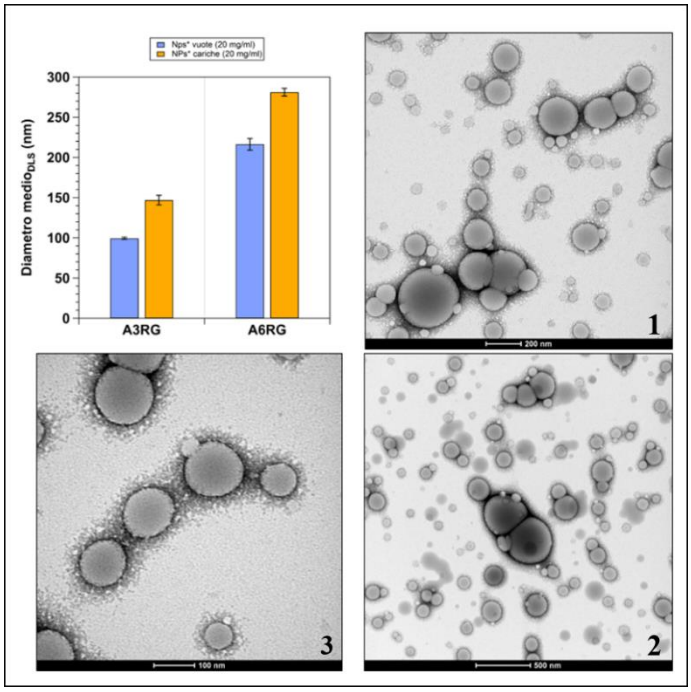

Figure 42. Average diameter from DLS of A3RG and A6RG. TEM images (**1** to **3**) recorded on stained (uranyl acetate) CFZ loaded A3RG sample with 0.2% of Tween-20^{TM}.

TEM images of both AnRG systems shows spherical micellar structures (Figure 42). The size distribution was in very good agreement with the DLS one. In order to study also the tridimensional structure and shape of these nanostructure, I performed some AFM analysis on silica surfaces (Figure 43).

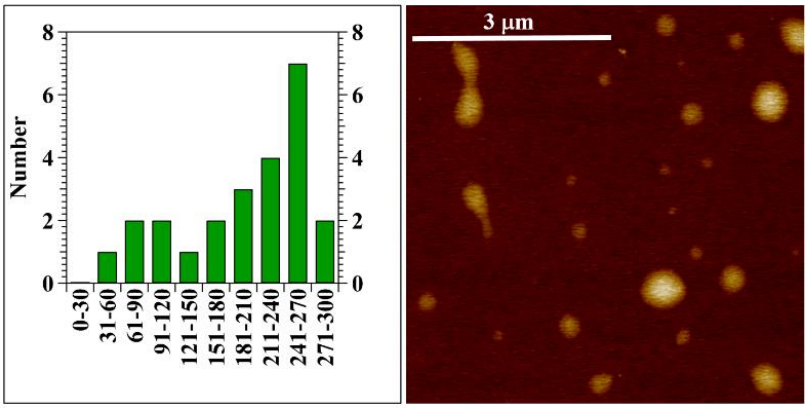

Figure 43. AFM image and size distribution analysis of CFZ-loaded A6RG polymer.

The AFM analysis confirms the spherical micellar nature of A6RG nanostructures. In Figure 43, there are many structures that look like elongated drops. This might be due to the soft nature of these micelles. When the AFM tip passes over the nanostructures, they are deformed and scraped on the silica surface. This is an undesirable feature for a polymeric micelle, because this feeble nature could hinder the spread and extravasation through the endothelial cells of blood vessels. This fragility could also be a problem for micelle production, storage and administration.

4.3. CONCLUSIONS ON ANRG COPOLYMERS PROJECT

I designed and synthesized two new resveratrol-OEG based copolymers able to assemble in water giving polymeric micelles by nanoprecipitation technique. One of these structures (A6RG) could be successfully loaded with clofazimine. In contrast, CFZ-loaded A3RG showed marked instability and tendency to aggregate within few hours. A6RG micelles showed a spherical shape when observed by TEM, with a size between 50 and 300 nm and relatively acceptable PDI values. These structures were stable in water for 2 weeks, then they precipitated irreversibly. These systems represent the first tentative of making bioactive resveratrol-OEG copolymers able to self-assemble in water giving new drug delivery nanocarriers. Unfortunately, preliminary tests and AFM structure characterization suggested that these systems couldn't be promising for the design of drug nanocarriers due to their structural instability. For these reasons this part of macromolecular prodrugs ended here without further investigations.

4.4. RESULTS AND DISCUSSION ON PTEROSTILBENE-PMOXA COPOLYMERS

I started the design and synthesis of this second system with a copolymer made by polymethyloxazoline and pterostilbene (PTS), a natural bioactive polyphenol. I synthesized and tested a series of $PMOXA_n$-PSP_m-PIP (PMP) copolymers with different n/m ratios (m represents the number of PTS units) able to assemble in water giving stable polymeric micelles with relatively narrow PDI and size. This is only the first attempt to prove the usefulness and feasibility of these kinds of self-assembling system, but hopefully in the near future, PTS could be replaced directly with an anticancer agent (i.e. mitomycin C, doxorubicin, taxodone, etc.).

Polyoxazolines are a class of very modular polymers with interesting characteristics. Many studies have shown that they can be considered, from many points of view, a valid alternative to PEG. They not only possess the key beneficial properties of PEG, but have characteristics that are novel and unique for drug delivery applications. They are nonionic, peptidomimetic, stable, and highly soluble in water and in organic solvents. Finally, they can be made with high quality, different scaffold structures, and different functional groups. The synthesis of these systems was performed by living cationic ring opening

polymerization (LCROP) that can be conducted in batch solution or by using microwave irradiation under almost neat conditions. In both cases, the synthesis is also safer if compared with that of PEG.

4.4.1. PMP COPOLYMERS PREPARATION AND CHARACTERIZATION

In this chapter, I describe the synthesis and characterization of polymethyloxazoline copolymers obtained by using different proportions of the monomers 2-methyl-2oxazoline and 2-methylsuccynate-2-oxazoline (SucOxa). This second monomer was synthesized according to a previously described procedure[22] which was slightly modified (see Materials and Methods). The polymerization was started with four different amounts of methyl triflate and terminated with an excess of piperidine (Figure 44).

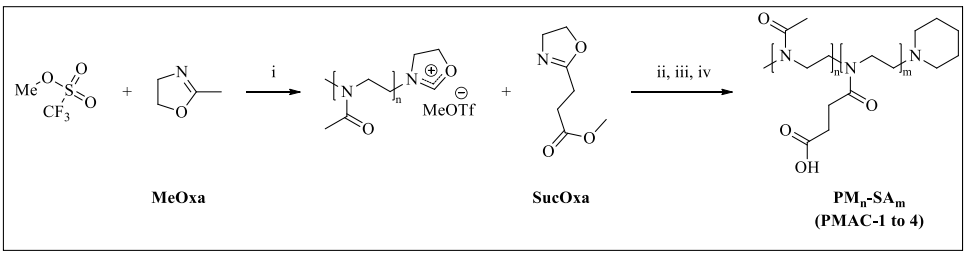

Figure 44. Synthesis of PMACs (1 to 4): i) ACN, 80°, 24h; ii) SucOxa in ACN, 80°, overnight; iii) piperidine, 80°,12h; iv) 10 % KOH in water, 24h, rt.

Using this approach I was able to obtain a series of copolymers with different polymethyloxazoline chain length and an almost constant succinic ester chain length part that was modified later with PTS pendant moieties (Figure 45).

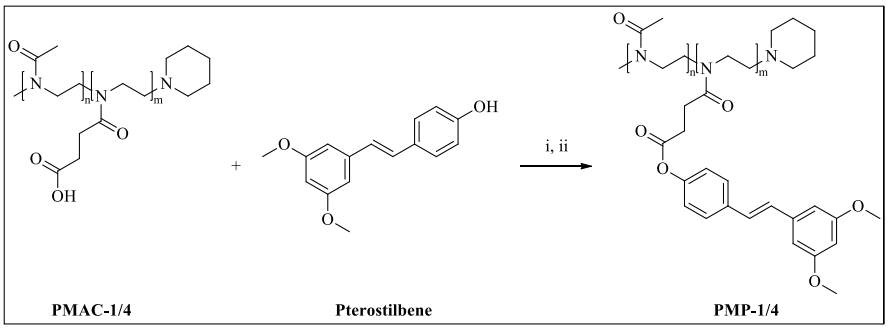

Figure 45. Synthesis of amphiphilic copolymer PMP: i) pentafluorophenol, DCC, DMF, 12h, 0° to rt; ii) PTS, DMAP, DMF, 24h, rt.

After this modification, the copolymers acquire the ability to assemble in water giving stable polymeric micelles. All the new macromolecular systems were characterized using ^{1}H-NMR; finally, the critic micellar concentrations (CMC) were determined by UV-Vis method (Table 4).

Copolymer	n/m ratio[a]	$M_n^{NMR,a}$	CMC (μg/mL)
PMP-1	25/2	2.5	14
PMP-2	40/4	3.7	16
PMP-3	77/6	9.8	110
PMP-4	113/6	11.8	130

Table 4. Analytical data of studied copolymers: a. determined by ^{1}H-NMR.

The determination of the average molecular weight was done using NMR spectroscopy. The CMC values were determined using a UV probe instead of fluorescent probes such as pyrene, because of interference by pterostilbene in fluorescence measurements. PTS has very broad excitation (290–340 nm) and emission (380–420 nm) ranges. These broad ranges overlap with those of fluorescent probes such as pyrene. To overcome this problem, I performed the measurements using dimethyl yellow (DMY) as solvatochromic probe[23]. I studied the UV absorption of DMY at 441 nm and monitored the solvatochromic change in wavelength of the maximum absorption as a function of surfactant or amphiphilic polymer concentration[24]. The obtained CMC values are summarized in Table 4. It is clear that the general CMC trend strongly depends on the hydrophilic chain length: the longer it is, the higher is the CMC value.

Concluding the synthetic part, I also synthesized a fluorescein labelled PMP-4 derivative (Figure 46) in order to have a probe for performing fluorescence microscopy measurements.

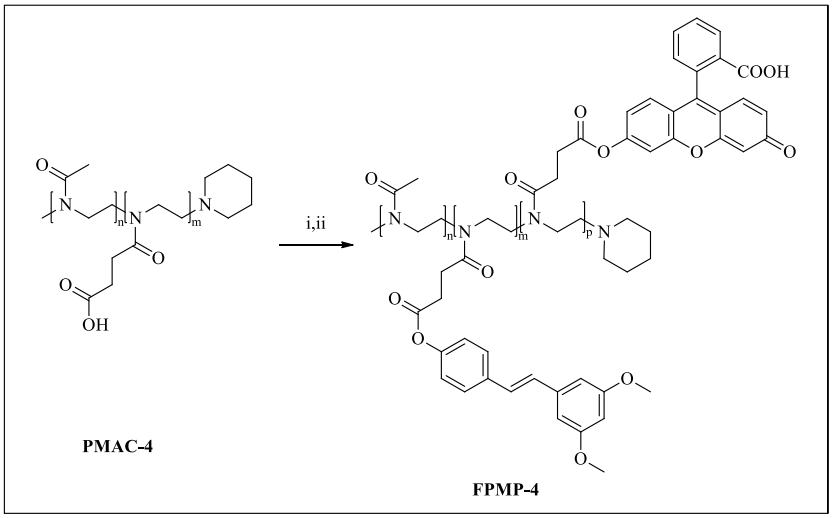

Figure 46. Synthesis of fluorescein labelled amphiphilic copolymer FPMP-4: i) pentafluorophenol, DCC, DMF, 12h, 0° to rt; ii) PTS (95% mol) and fluorescein (5% mol), DMAP, DMF, 24h, rt.

In order to conduct internalization experiments, I needed a fluorescent modified PMP system. I chose to modify the PMP-4 copolymer systems with less than 5% (mol) of

fluorescein. Following this approach I created FPMP-4 that had the same self-assembly properties as PMP-4 and that could be used for fluorescence microscopy assays.

4.4.2. COPOLYMER SYSTEM pH STABILITY

All the PMP micellar systems were also tested in order to study their chemical stability under different pH conditions. The chosen buffers mimic the average blood pH (7.4) and the average lysosomal pH (4.5). The results of these stability assays are summarized in Figure 47.

Only in the first case (Figure 47, A), the system undergoes quantitative hydrolysis already after 2 days. After all, PMP-1 is the smallest copolymer, with the shortest hydrophilic part, which is probably too short to effectively protect the hydrophobic core of the polymeric micelle from hydrolytic degradation. In all cases, the hydrolysis rate is faster under acidic pH conditions and this is in good agreement with what we expect for an aromatic ester. The hydrolysis behavior of PMPs is interesting, because they are able to resist for days at pH values as found in blood and, on the other hand, they show an moderate hydrolysis at lysosomal pH that represents the final target of polymeric micelles.

It is important to remember that these kinds of assays are a simplified situation with respect to what really happens at the systemic level. The enzymatic and the immune system activity are fundamental and not negligible for the effectiveness of these types of polymer-based nanocarriers.

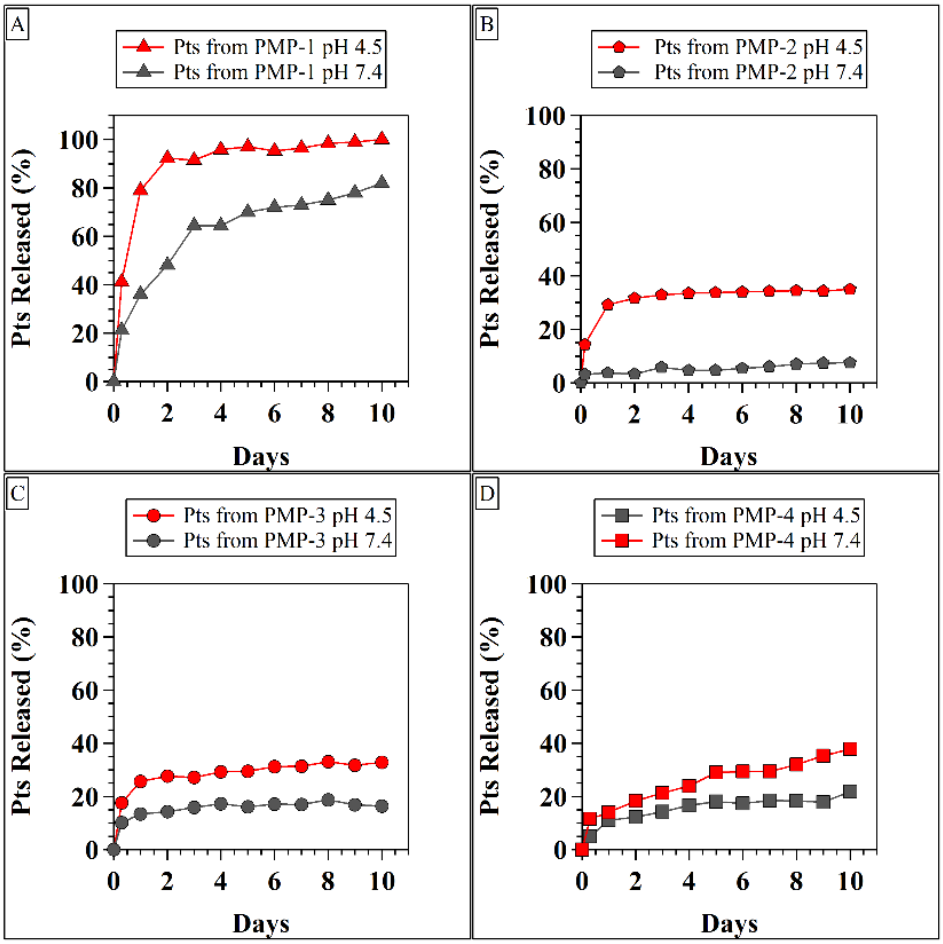

Figure 47. Stability tests on empty PMP copolymers micelles at pH 7.4 (grey line) and 4.5 (red line).

For our purposes, these hydrolysis profiles represented, above all, a good result to prove the stability and endurance of our polymeric scaffold under physiological pH conditions. Subsequently we also tested the cytotoxicity of these micellar systems to clearly demonstrate their (*in vitro*) biocompatibility and safe biodegradability.

4.4.3. PREPARATION OF DRUG LOADED POLYMERIC MICELLES

As for the AnRG copolymer, also in this case PMP micelles were prepared using the nanoprecipitation method[20,21]. The copolymer (PMP) was dissolved in ethanol at a concentration of 20 mg/mL and, in the same solution, CFZ was dissolved at a concentration of 0.1 mg/mL to form the diffusing phase. This phase was then added to 20 mL of distilled water (the dispersing phase) by means of a syringe positioned with the needle directly in the medium under high magnetic stirring for 24 hours at room temperature. The freshly formed nanoparticles were then centrifuged 2 times for 10-min cycles at 4300 × g to precipitate all aggregates and unloaded CFZ. The precipitate was analyzed using UV-Vis in order to quantify the drug loading percentage.

4.4.4. SIZE DISTRIBUTION AND STABILITY OF CFZ-LOADED PMP MICELLES

The water PMP nanosuspension was used for DLS size distribution quantification and stability assays; all these data are summarized in Table 5.

NPs	Average diameter (nm)	PDI	LC (%)	LE (%)	DL (%)
PMP-1	132 ± 2	0.13	-	-	-
Loaded PMP-1	190 ± 1	0.25	0.55	98	0.55
PMP-2	105 ± 1	0.21	-	-	-
Loaded PMP-2	102 ± 1	0.17	0.52	95	0.55
PMP-3	130 ± 5	0.23	-	-	-
Loaded PMP-3	200 ± 4	0.08	0.50	90	0.55
PMP-4	58 ± 1	0.32	-	-	-
Loaded PMP-4	79 ± 2	0.29	0.55	98	0.55

Table 5. PMP NPs characterization by DLS measurements on water diluted solutions. For LC, LE and DL equations see Materials and Methods.

The intensity-mean z-averaged particle size and the PDI obtained from DLS analysis were given to reflect hydrodynamic diameters of drug loaded PMP micelles. The general trend is observed as in all other cases, i.e. when the polymeric micelles were loaded with CFZ their diameter increased. The loading efficiency (LE) was practically quantitative in all cases, even if LC was very small. However, this was not a problem in our case, because CFZ was deliberately used in small amounts since its function was to stabilize the core by hydrophobic interaction and to inhibit MDR pumps (see Chapter 3)[9] when the system reach the tumor cells.

4.4.5. MORPHOLOGY OF CFZ-LOADED PMP MICELLES

The morphology of CFZ-loaded micelles was investigated by AFM (Figure 48). In all cases the observed surface-deposited nanoparticles were round-shaped. All the observed samples show an almost uniform size distribution. As is commonly observed, the size data determined by AFM were smaller when compared to those from DLS results. This can be attributed to the fact that AFM analyses were performed under dry conditions while DLS determined the hydrodynamic diameter, i.e. with swollen and hydrated particles in an aqueous environment[25].

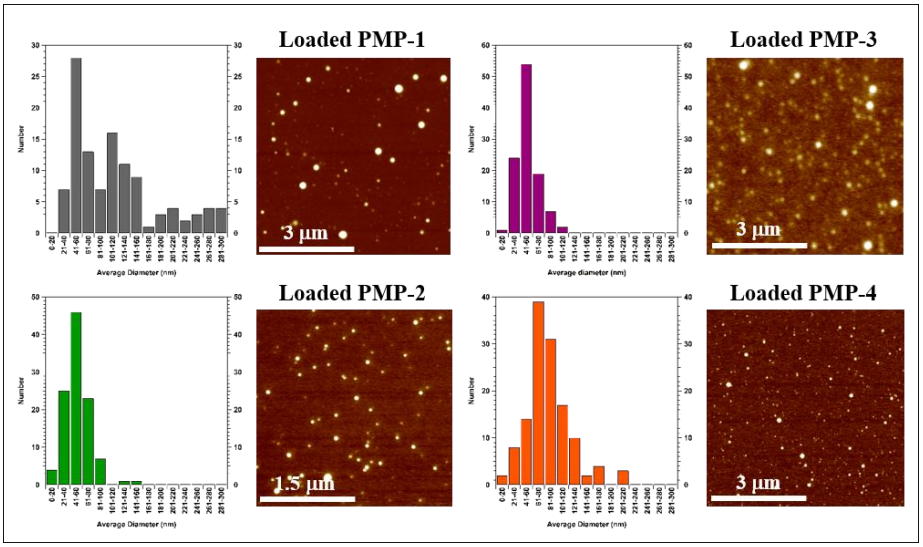

Figure 48. AFM analysis and size distribution of all CFZ-loaded PMPs nanoparticles. The size distribution was obtained using a graphic elaborator (imageJ).

TEM results remark some characteristics already observed with AFM, and in particular, the circular and very well defined shape of these nanoparticles. This analysis also shows (Figure 49) a reasonable correspondence with DLS analysis – on loaded PMP-3 in this case – in which an average size distribution in the range 70 - 200 nm was observed.

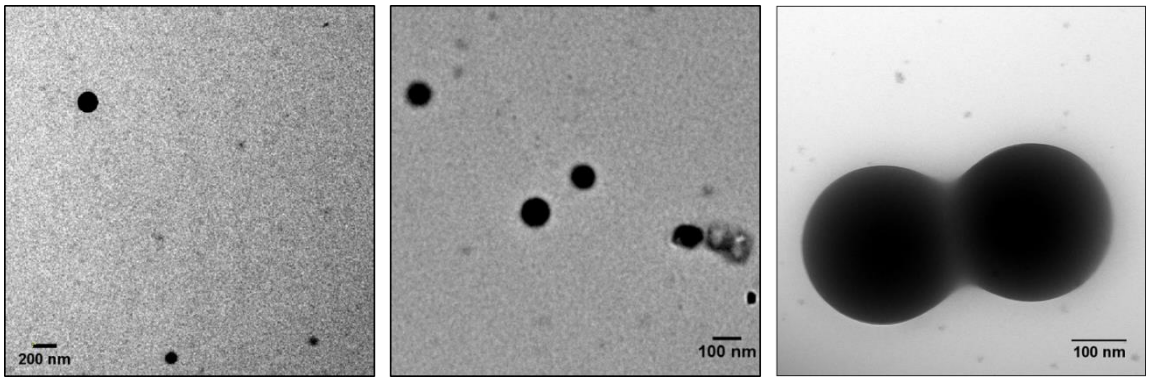

Figure 49. TEM analysis of PMP-3 CFZ-loaded nanoparticles stained with ammonium molybdate.

4.4.6. PRELIMINARY *IN VITRO* CYTOTOXICITY STUDIES

The toxicity of PMP block copolymers were tested in RAW 264.7 cells using MTS assay (Figure 50). The tests were conducted on macrophages because they are the first cells of the immune system that usually recognize nanocarrier systems after iv administration. Phagocytosis in classical sense is the engulfment of the endogenous and exogenous particulate materials, such as bacteria, erythrocytes, latex beads and colloidal particles. Multiple attachments of particle associated ligands with membrane receptors is an essential stimulus for phagocytic capture of particles. Extent of particle sequestration and clearance

by macrophages is determined primarily by the physicochemical nature of the surface, however, other factors, such as nature of the particle matrix and particle stability can be important[26].

Obviously, avoiding the macrophages recognition and their endocytosis process is fundamental for our systems in order to increase their circulating time. Furthermore, nanocarriers must not show high toxicity against macrophages to avoid possible immunodeficiency effects.

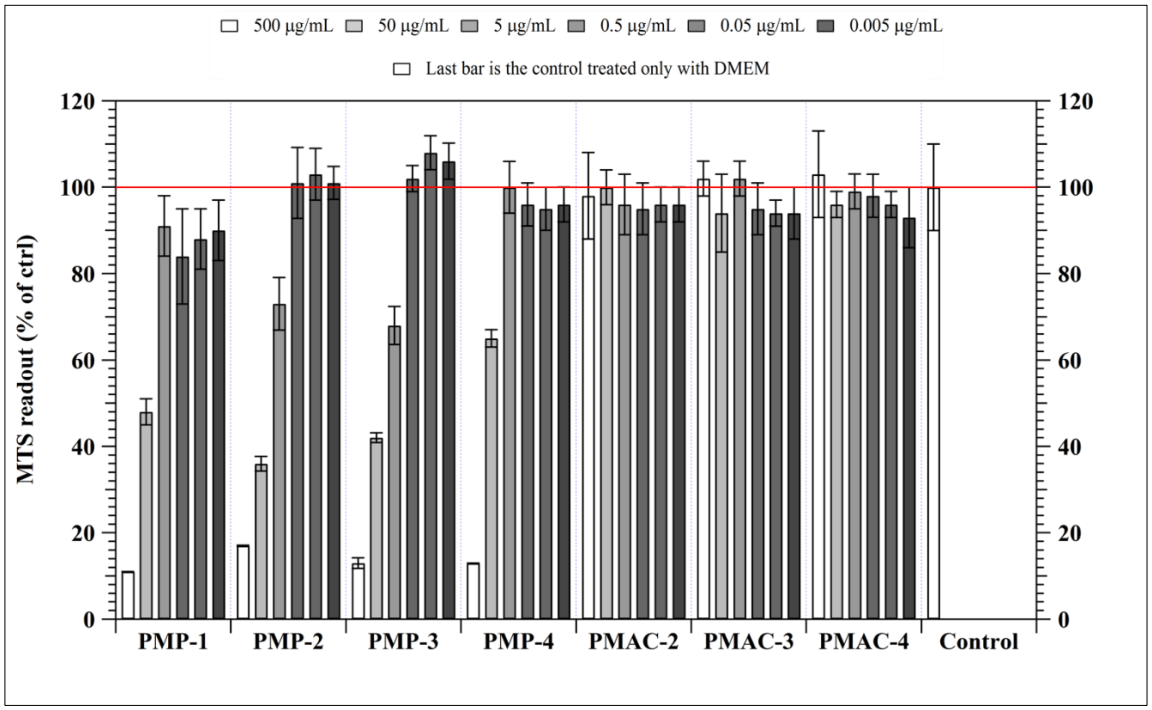

Figure 50. MTS cytotoxicity results on RAW 264.7 cells treated with PMP-1 to PMP-4 and their precursors with free acidic functions PMACs.

Based on the results on PMPs cytotoxicity shown in Figure 50, IC-50 values were estimated. What is clear from the tests is that in almost all cases the IC-50 of PMPs is between 20 and 70 µg/mL.

Finally, in order to prove that our polymeric scaffolds (PMACs, without PTS on side chains) are non-toxic and fully biocompatible, we also tested the naked copolymers (PMAC-1 to 4). The results clearly indicate that they are not toxic for these cells. One explanation for this phenomenon is that the PMACs are completely water-soluble and they don't assemble in water to form macromolecular aggregates: since they are completely solubilized, they can not easily cross the plasma membrane.

4.4.7. CELLULAR INTERNALIZATION OF CFZ-LOADED PMP MICELLES

The fluorescein-labeled PMP-4 copolymer (FPMP-4) was used to evaluate drug and block copolymer internalization in RAW 264.7 cells by fluorescence microscopy. Before starting the experiments, the fluorescence intensity of different empty and CFZ-loaded NPs solutions were evaluated (Figure 51).

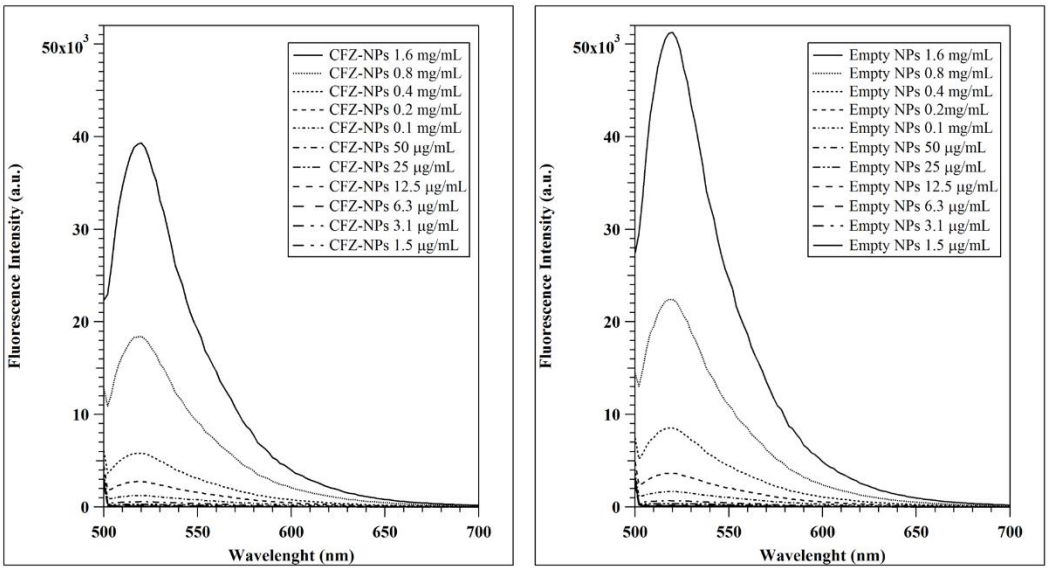

Figure 51. Fluorescence spectra of CFZ-loaded (left) and empty (right) PMP nanoparticles at different concentrations.

It is evident that after the loading with CFZ of the polymeric micelles, the systems lost almost 10% of fluorescence intensity: a possible explanation is due to the moderate quenching interaction between CFZ and fluorescein inside the hydrophobic core. We then decided to evaluate the internalization efficiency of CFZ-loaded (Figure 52) and empty (Figure 53) micelles by macrophages RAW 264.7 after 4 hours of incubation and at a concentration of 0.5 mg/mL of PMP-4.

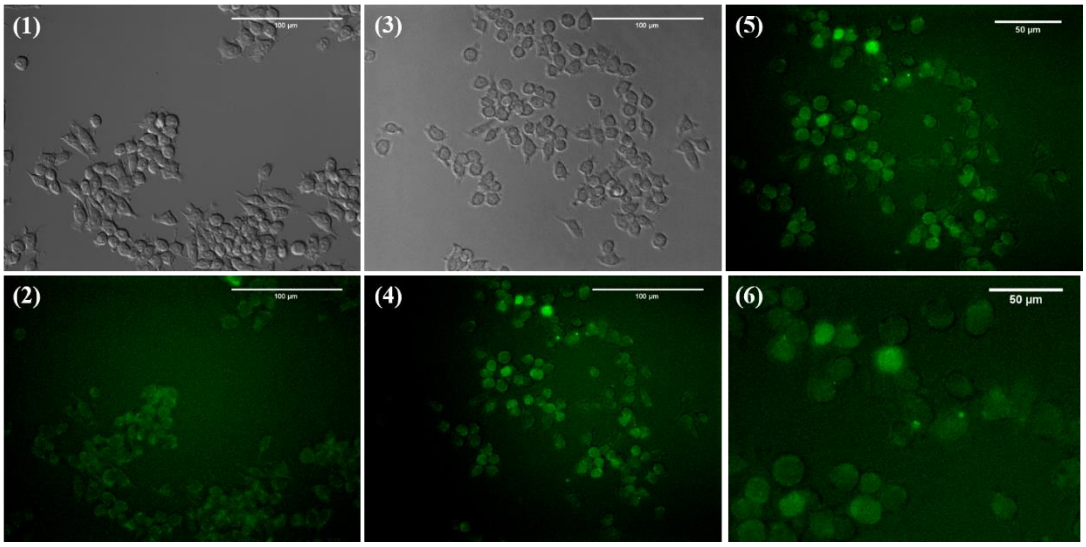

Figure 52. Internalization of fluorescein labelled empty FPMP-4 polymeric micelles on RAW 264.7 cells after 4 hours of incubation: 1 and 2 are the controls; 5 and 6 are different region magnifications of the same image represented in 3 and 4.

After 4 hours of incubation, the empty FPMP-4 polymeric micelles were not found inside the cells, but in some parts of the image the fluorescent background seems to be more intense (Figure 52, 4-6). A possible explanation is that nanoparticles entered into macrophages and were disrupted. Thus, the disassembled copolymers are still present, but in a random coil configuration and are possibly entrapped on the inner plasma membrane by hydrophobic interaction between pterostilbene, fluorescein moieties and the phospholipidic bilayer. This phenomenon explains the absence of discrete fluorescent spots that, on the contrary, are present in the case of CFZ-loaded nanoparticles (Figure 53).

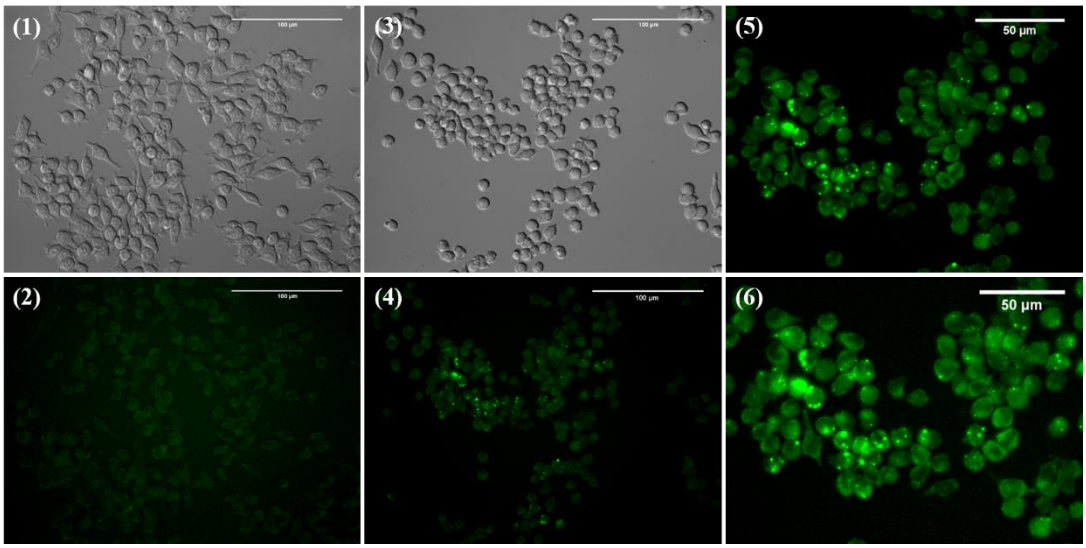

Figure 53. Internalization of fluorescein labelled CFZ-loaded FPMP-4 polymeric micelles on RAW 264.7 cells after 4 hours of incubation: 1 and 2 are the controls; 5 and 6 are different region magnifications of the same image represented in 3 and 4.

The same copolymer system shown in Figure 52, but loaded with CFZ gave different results. After 4 hours of incubation, the CFZ-loaded polymeric micelles are clearly present inside cells in the form of small fluorescent agglomerates (Figure 53, 4-6). It is possible that the presence of CFZ inside the micelles stabilizes them thus favoring their plasma membrane crossing and their stay inside the cells until the release of their content over time. What is clear at the moment, based on these preliminary experiments, is that the loaded polymeric micelles are able to accumulate inside the cells more efficiently than their empty analogues.

In the near future we plan to clarify the internalization mechanism by means of confocal microscopy analysis and to perform some FACS measurements to quantify the internalization efficiency and nanoparticles cellular localization.

4.5. CONCLUSIONS ON PMP COPOLYMERS PROJECT

I designed and synthesized four new amphiphilic polymethyloxazoline-co-pterostilbene based polymers able to assemble in water giving polymeric micelles by nanoprecipitation technique. These structures were successfully loaded with clofazimine that apparently stabilized the nanoparticle core by hydrophobic interactions. The obtained micelles showed a spherical shape when observed by AFM microscopy, with a size distribution between 50 and 200 nm and relatively low PDI values. These structures were stable in water for at least a few months and their size did not vary during this time. These systems represent the first attempt to make bioactive polyoxazolines copolymers capable of self-assemblying in water giving new promising drug delivery nanocarriers. The first four PMP derivatives were modified by decorating the hydrophobic portion of the copolymer with pterostilbene that could form the hydrophobic core by interaction with CFZ. I observed also that in buffer solutions at pH 7.4 (which is the blood average pH) the systems did not release appreciable amounts of clofazimine and pterostilbene. This is an important feature, because it means that during the blood circulation time the nanocarrier releases only a negligible fraction of CFZ and structural PTS. Therefore the system could achieve the solid tumor site by exploiting the EPR effect and then it could be internalized by cancer cells where it will be destroyed, releasing its cargo (CFZ and PTS). The internalization ability of these new nanocarriers was tested on macrophages and it was observed that the CFZ-loaded ones (FPMP-4) are better able to cross the plasma membrane and accumulate into cytosol micro-aggregates than the empty ones (FPMP-4).

In the near future, the same platform could be modified by replacing pterostilbene with other anticancer drugs (i.e. etoposide, doxorubicin, etc.) while maintaining CFZ as MDR pump inhibitor and core-stabilizer. It is reasonably expected that the self-assemblying behavior of the system should not change much provided that the selected anticancer drug has, like pterostilbene, marked aromatic and hydrophobic characteristics.

4.6. EXPERIMENTAL SECTION

4.6.1. MATERIALS AND METHODS

Pterostilbene was purchased from Wonda Science (Changzhou, Jiang, People's Republic of China, batch n. WF12062501). Clofazimine and 2-Chloroethylamine hydrochloride were purchased from Sigma-Aldrich and used without further purification. Methyl succinyl chloride was purchased from Acros Organics and used without further purification. 2-Methyl-2-oxazoline (MeOx), methyl triflate (MeOTf), piperidine (PIP) and triethylamine (TEA) were purchased from Sigma-Aldrich and distilled under N_2 atmosphere before use. The solvents were analytical or synthetic grade and were used without further purification.

Cell culture and MTS/fluorescence microscopy experiments materials

Cells were cultured in DMEM medium (Gibco 11965-092) supplemented with 10% of FBS and 1% penicillin-streptomycin. For cytotoxicity studies: two Dulbecco's Modified Eagle media were obtained from Invitrogen: a) the DMEM, High Glucose, GlutaMAX™, Pyruvate (Catalog No. 31966021), herein named as "DMEM with phenol red" b) the DMEM, High Glucose, no Glutamine, no Phenol Red (Catalog No. 31053028), herein named as "DMEM without phenol red". Also Penicillin-Streptomycin Solution, liquid (Catalog No.15140122), herein named as "PenStrep", Sodium Pyruvate 100 mM Solution (Catalog No. 11360039), herein named as "Sodium Pyruvate", GlutaMAX^{TM} Supplement (Catalog No. 35050038), herein named as "GlutaMAX", Foetal Bovine Serum (FBS, Catalog No. 10270106) and Phosphate Buffered Saline (PBS) (1x) (Catalog No. 10010015) were obtained from Invitrogen.

The DMEM with phenol red was supplemented with 1 vol% PenStrep and 10 vol% FBS and used for normal cell growth. The DMEM without phenol red was used as "complete" and as "serum-free" medium. The "complete" medium contained 1 vol% PenStrep, 1 vol% Sodium Pyruvate, 2 vol% GlutaMAX and 10 vol% FBS. The "serum-free" medium had similar composition with the complete medium but with 0 vol% FBS.

Synthesis of A3RG and A6RG

Rem-3GME: resveratrol (3.5 g, 15.4 mmol, 1 eq), 3GME-OTs (4.9 g, 15.4 mmol, 1 eq) and Cs_2CO_3 (7.5 g, 23.04 mmol, 1.5 eq) were stirred in anhydrous DMF (100 mL) at 50°C for 5 hours under inert atmosphere. Then, 150 mL of EtOAc were added to the solution. The organic phase was washed 3 times with HCl 0.5 M (3 x 100 mL) and dried over $MgSO_4$.

After filtration and evaporation of the solvent, the oily residue was purified using flash silica gel column chromatography (65:35, DCM/EtOAc, R_f = 0.3) affording **Rem-3GME** as yellow oil (2.4 g, 6.4 mmol, 42%).^{1}H NMR (300 MHz, DMSO) δ = 9.21 (s, 2H), 7.45 (dd, *J* = 26.0, 8.6 Hz, 2H), 7.09 – 6.73 (m, 4H), 6.58 (d, *J* = 16.3 Hz, 1H), 6.44 (d, *J* = 1.6 Hz, 2H), 6.21 (d, *J* = 22.6 Hz, 1H), 4.13 – 3.99 (m, 2H), 3.78 – 3.64 (m, 2H), 3.62 – 3.35 (m, 9H), 3.23 (s, 3H) ppm. ^{13}C NMR (75 MHz, $CDCl_3$) δ = 159.86, 158.63, 158.58, 158.16, 157.37, 139.51, 139.13, 129.77, 128.49, 128.06, 127.90, 127.77, 127.48, 126.76, 125.39, 115.57, 114.67, 106.04, 104.48, 103.06, 102.02, 100.93, 71.31, 69.99, 69.85, 69.83, 69.64, 69.03, 68.98, 67.20, 67.01, 58.03, 30.61 ppm.

A3RG: Rem-3GME (500 mg, 1.34 mmol, 1 eq) and triethylamine hydrochloride (18 mg, 0.13 mmol, 0.1 eq) were vigorously stirred in dry 1,2-dichlorobenzene at room temperature. The solution was heated until reflux and then adipoyl chloride (245 mg, 1.34 mmol, 1 eq) in 1,2-dichlorobenzene (5 mL) was slowly added to the solution. After 48 h, the reaction was let to raise room temperature and then the slutty solution was precipitated in cold MeOH. The MeOH was removed and the brown sticky residue was dissolved in acetone (20 mL) and the product was purified by dialysis against acetone using 1.0kkk kDa cut-off tubes. Finally the solvent was evaporated under vacuum yield **A3RG** (600 mg). ^{1}H NMR (500 MHz, DMSO) δ = 9.71 (s, 0.16H), 7.69 (dd, *J* = 57.7, 7.7 Hz, 2H), 7.48 – 6.65 (m, 6H), 6.62 (s, 1H), 4.10 (s, 2H), 3.93 – 3.45 (m, 9H), 3.2 (s, 3H), 2.56 (s, 2H), 1.7 (s, 2H) ppm.

Rem-6GME: resveratrol (3.0 g, 13.3 mmol, 2 eq), 6GME-OTs (3.0 g, 6.7 mmol, 1 eq) and Cs_2CO_3 (3.25 g, 9.9 mmol, 1.5 eq) were stirred in anhydrous DMF (150 mL) at 50°C for 5 hours and under inert atmosphere. Then, 150 mL of EtOAc were added to the solution. The organic phase was washed 3 times with HCl 0.5 M (3 x 100 mL) and dried over $MgSO_4$. After filtration and evaporation of the solvent, the oily residue was purified using flash silica gel column chromatography (80:30:10, DCM/Acetone/Hexane, R_f = 0.25) affording **Rem-6GME** as yellow oil (1.25 g, 2.5 mmol, 40%).^{1}H NMR (300 MHz, DMSO) δ = 9.15 (s, 2H), 7.41 (dd, *J* = 26.0, 8.6 Hz, 2H), 7.10 – 6.72 (m, 4H), 6.6 (d, *J* = 16.3 Hz, 1H), 6.44 (d, *J* = 1.6 Hz, 2H), 6.21 (d, *J* = 22.6 Hz, 1H), 4.03 – 3.9 (m, 2H), 3.8 – 3.6 (m, 2H), 3.55 – 3.43 (m, 20H), 3.25 (s, 3H). ^{13}C NMR (75 MHz, $CDCl_3$) δ = 159.86, 158.63, 158.58, 158.16, 157.37, 139.51, 139.13, 129.77, 128.49, 128.06, 127.90, 127.77, 127.48, 126.76,

125.9, 115.57, 114.6, 106.04, 104.48, 103.06, 102.0, 100.93, 71.31, 70.99, 69.85, 69.75, 69.64, 69.03, 68.98, 68.20, 67.01, 59.03, 30.6 ppm.

A6RG: Rem-6GME (500 mg, 0.99 mmol, 1 eq) and triethylamine hydrochloride (14 mg, 0.09 mmol, 0.1 eq) were vigorously stirred in dry 1,2-dichlorobenzene at room temperature. The solution was heated until reflux and then adipoyl chloride (181 mg, 0.99 mmol, 1 eq) in 1,2-dichlorobenzene (5 mL) was slowly added to the solution. After 48 h, the reaction was let to raise room temperature and then the slutty solution was precipitated in cold MeOH. The MeOH was removed and the brown sticky residue was dissolved in acetone (20 mL) and the product was purified by dialysis against acetone using 3.5 kDa cut-off tubes. Finally the solvent was evaporated under vacuum yield **A6RG** (450 mg). ^{1}H NMR (500 MHz, DMSO) δ = 12.05 (s, 0.16H), 9.73 (s, 0.16H), 7.55 (dd, *J* = 57.7, 7.7 Hz, 2H), 7.33 – 6.73 (m, 6H), 6.66 (s, 1H), 4.08 (s, 2H), 3.83 – 3.33 (m, 30H), 3.21 (s, 3H), 2.66 (s, 2H), 1.75 (s, 2H) ppm.

MetSucOx synthesis[22]

Methyl-7-chloro-4-oxo-5-azaheptanoate: Methyl succinyl chloride (25.0 g, 0.17 mol, 1 eq) and 2-chloroethylammonium chloride (19.3 g, 0.17 mol, 1 eq) were suspended in dry dichloromethane (190 mL). At 0 °C triethylamine (53 mL, 0.38 mol, 2.2 eq) was added dropwise over a period of 1 h. The reaction mixture was allowed to warm up to room temperature and was stirred overnight before water (40 mL) was added. The organic phase was washed twice with water and once with brine and dried over anhydrous sodium sulfate. After filtration and solvent removal, the residue was purified on neutral Alumina gel using chloroform. The product appear as a light yellow oil. Yield: 26.4 g (83 %) of a yellow oil. ^{1}H NMR (300 MHz, $CDCl_3$) δ = 6.33 (s, 1H), 3.65 (s, 3H), 3.61 – 3.49 (m, 4H), 2.64 (t, *J* = 6.8 Hz, 2H), 2.49 (t, *J* = 6.7 Hz, 2H). ^{13}C NMR (76 MHz, $CDCl_3$) δ = 173.45, 171.78, 51.94, 43.91, 41.36, 30.89, 29.30 ppm.

Methyl 3(oxazol-2-yl)propionate (SucOxa): Methyl-7-chloro-4-oxo-5-azaheptanoate (10.0 g, 0.052 mol) and anhydrous sodium carbonate (4.2 g, 0.040 mol) were reacted (neat) under stirring at a pressure of less than 0.1 mbar and at 130°C. A clear colorless liquid was obtained after distillation Yield: 5.7 g (69 %) of a colorless liquid; ^{1}H NMR ($CDCl_3$): δ = 2.58 (t, J = 7.44 Hz, 2 H), 2.68 (t, J = 7.44 Hz, 2 H), 3.70 (s, 3 H), 3.82 (t, J = 9.16 Hz, 2 H), 4.24 ppm (t, J = 9.73 Hz, 2 H); ^{13}C NMR ($CDCl_3$): δ = 23.1, 30.1, 51.8, 54.4, 67.5, 167.0, 172.8 ppm;

PMAC synthesis

PMAC-1 to **PMAC-4** were synthesized according to a literature protocol[27].

PMAC-1: 2-Methyl-2-oxazoline (15 g, 0.18 mol, 25 eq, distilled from KOH) was dissolved in dry acetonitrile (75 mL) under N_2 atmosphere. Methyl triflate (800 µL, 7.05 mmol, 1 eq) was added at 0 °C under N_2. The mixture was heated to 80 °C for 24 h always keeping the inert atmosphere. After this time, SucOxa (5.5 g, 0.035 mmol, 5 eq) was added at 80°C and the reaction proceeded for other 12 h. The polymerization was terminated by adding 1.8 g of piperidine when the mixture reached room temperature and it was let stirring for other 48 h. The solvent was removed under reduced pressure, the oily residue was dissolved in the minimum amount of ACN and precipitated twice in Et_2O. The white solid residue obtained (**PMEC-1**) was then dried overnight under high vacuum. The methyl ester hydrolysis reaction was performed under alkaline conditions. PMEC-1 (8 g) was dissolved in 50 mL of 5 % KOH aqueous solution and stirred for 24 h. After this time, glacial acetic acid was added dropwise until pH 6 was reached. After addition of Milli-Q water the product was purified by dialysis against water using 1 kDa cut-off tubes, and it was finally freeze-dried to yield **PMAC-1** (7.5 g) as white hygroscopic powder. ^{1}H NMR (500 MHz, D_2O) δ = 3.65-3.5 (m, 100 H, N-$\underline{CH_2}\underline{CH_2}$), 3.10-2.95 (m, 3H, N-$\underline{CH_3}$), 2.01 - 1.95 (m, 72 H, C=O-$\underline{CH_3}$) ppm.

PMAC-2: 2-Methyl-2-oxazoline (10 g, 0.12 mol, 50 eq, distilled from KOH) was dissolved in dry acetonitrile (60 mL) under N_2 atmosphere. Methyl triflate (281 µL, 2.4 mmol) was added at 0 °C under N_2. The mixture was heated to 80 °C for 24 h always keeping the inert atmosphere. After this time, SucOxa (1.88 g, 12 mmol, 5 eq) was added at 80°C and the reaction proceeded for other 12 h. The polymerization was terminated by adding 1.8 g of piperidine when the mixture reached room temperature and it was let stirring for other 48 h. The solvent was removed under reduced pressure, the oily residue was dissolved in the minimum amount of ACN and precipitated twice in Et_2O. The white solid residue obtained (**PMEC-2**) was then dried overnight under high vacuum. The methyl ester hydrolysis reaction was performed under alkaline conditions. PMECs (7.3 g) were dissolved in 50 mL of 5 % KOH aqueous solution and stirred for 24 h. After this time, glacial acetic acid was added until pH 6 was reached. After addition of Milli-Q water the products were purified by dialysis against water using 1 kDa cut-off tubes, and they were finally freeze-dried to yield **PMAC-2** (6.1 g) as white hygroscopic powder. ^{1}H NMR (500 MHz, D_2O) δ = 3.67-

3.51 (m, 206H, N-$\underline{CH_2}\underline{CH_2}$), 3.08-2.91 (m, 3H, N-$\underline{CH_3}$), 2.11-2.04 (m, 125H, C=O-$\underline{CH_3}$) ppm.

PMAC-3: 2-Methyl-2-oxazoline (5 g, 0.059 mol, 75 eq, distilled from KOH) was dissolved in dry acetonitrile (50 mL) under N_2 atmosphere. Methyl triflate (128 μL, 0.78 mmol, 1 eq) was added at 0 °C under N_2. The mixture was heated to 80 °C for 24 h always keeping the inert atmosphere. After this time, SucOxa (0.615 g, 3.51 mmol, 5 eq) was added at 80°C and the reaction proceeded for other 12 h. The polymerization was terminated by adding 1.8 g of piperidine when the mixture reached room temperature and it was let stirring for other 48 h. The solvent was removed under reduced pressure, the oily residue was dissolved in the minimum amount of ACN and precipitated twice in Et_2O. The white solid residue obtained (**PMEC-3**) was then dried overnight under high vacuum. The methyl ester hydrolysis reaction was performed under alkaline conditions. PMEC-3 (4.5 g) were dissolved in 50 mL of 5 % KOH aqueous solution and stirred for 24 h. After this time, glacial acetic acid was added until pH 6 was reached. After addition of Milli-Q water the products were purified by dialysis against water using 1 kDa cut-off tubes, and they were finally freeze-dried to yield **PMAC-3** (4 g) as white hygroscopic powder. ^{1}H NMR (500 MHz, D_2O) δ = 3.69-3.55 (m, 346H, N-$\underline{CH_2}\underline{CH_2}$), 3.14-2.96 (m, 3H, N-$\underline{CH_3}$), 2.09-2.01 (m, 257H, C=O-$\underline{CH_3}$) ppm.

PMAC-4: 2-Methyl-2-oxazoline (10 g, 0.12 mol, 100 eq, distilled from KOH) was dissolved in dry acetonitrile (50 mL) under N_2 atmosphere. Methyl triflate (136 μL, 1.17 mmol) was added at 0 °C under N_2. The mixture was heated to 80 °C for 24 h always keeping the inert atmosphere. After this time, SucOxa (1.1 g, 7.05 mmol, 5 eq) was added at 80°C and the reaction proceeded for other 24 h. The polymerization was terminated by adding 1.8 g of piperidine when the mixture reached room temperature and it was let stirring for other 48 h. The solvent was removed under reduced pressure, the oily residue was dissolved in the minimum amount of ACN and precipitated twice in Et_2O. The white solid residue obtained (**PMEC-4**) was then dried overnight under high vacuum. The methyl ester hydrolysis reaction was performed under alkaline conditions. PMEC-4 (8.5 g) were dissolved in 50 mL of 5 % KOH aqueous solution and stirred for 24 h. After this time, glacial acetic acid was added until pH 6 was reached. After addition of Milli-Q water the products were purified by dialysis against water using 3.5 kDa cut-off tubes, and they were finally freeze-dried to yield **PMAC-4** (7.2 g) as white hygroscopic powder. ^{1}H NMR (500

MHz, D_2O) δ = 3.66-3.53 (m, 503H, N-$\underline{CH_2}\underline{CH_2}$), 3.10-2.93 (m, 3H, N-$\underline{CH_3}$), 2.13-2.06 (m, 383H, C=O-$\underline{CH_3}$) ppm.

PMPs synthesis

PMP-1: under inert atmosphere, to a stirring solution of PMAC-1 (6.08 g) and DCC (2.3 g, 11.04 mmol, 4 eq) in dry DMF (100 mL) at 0°C, pentafluorophenol (2.03 g, 11 mmol, 4 eq) in 5 mL of DMF was added and the reaction was then let at room temperature overnight. Successively, PTS (2.8 g, 11.4 mmol, 4 eq) and DMAP (cat. 10 mg) dissolved in 5 mL of dry DMF were added and let at room temperature for 24 h. The solvent was evaporated under reduced pressure. The solid residue was suspended in Milli-Q water, filtered and purified by dialysis against water using 1 kDa cut-off tubes, and they were finally freeze-dried to yield **PMP-1** (5.5 g). ^{1}H NMR (300 MHz, DMSO) δ = 7.62-6.37 (m, 18H, Ar), 3.77 (d, 12H, -O$\underline{CH_3}$), 3.45-3.34 (m, 99H, N-$\underline{CH_2}\underline{CH_2}$), 2.01-1.97 (m, 4H, C=O-$\underline{CH_3}$) ppm.

PMP-2: under inert atmosphere, to a stirring solution of PMAC-2 (1 g) and DCC (200 mg, 1 mmol, 5 eq) in dry DMF (20 mL) at 0°C, PTS (450 mg, 1.76 mmol, 7 eq) and DMAP (cat. 15 mg) dissolved in 5 mL of dry DMF were added and let at room temperature for 24 h. The solvent was evaporated under reduced pressure. The solid residue was suspended in Milli-Q water, filtered and purified by dialysis against water using 1 kDa cut-off tubes, and they were finally freeze-dried to yield **PMP-2** (753 mg). ^{1}H NMR (300 MHz, MeOD) δ = 7.59-6.35 (m, 18H, Ar), 3.81 (s, 12H, -O$\underline{CH_3}$), 3.61-3.48 (m, 205H, N-$\underline{CH_2}\underline{CH_2}$), 3.10-2.96 (m, 3H, N-$\underline{CH_3}$) 2.16-2.09 (m, 158H, C=O-$\underline{CH_3}$) ppm.

PMP-3: under inert atmosphere, to a stirring solution of PMAC-3 (1 g) and DCC (150 mg, 0.73 mmol) in dry DMF (15 mL) at 0°C, pentafluorophenol (140 mg, 0.73 mmol) in 5 mL of DMF was added and the reaction was then let at room temperature overnight. Successively, PTS (190 mg, 0.73 mmol) and DMAP (cat. 10 mg) dissolved in 5 mL of dry DMF were added and let at room temperature for 24 h. The solvent was evaporated under reduced pressure. The solid residue was suspended in Milli-Q water, filtered and purified by dialysis against water using 1 kDa cut-off tubes, and they were finally freeze-dried to yield **PMP-3** (625 mg). ^{1}H NMR (300 MHz, DMSO) δ =7.59-6.36 (m, 63H, Ar), 3.77-3.76 (d, 42H, -O$\underline{CH_3}$), 3.50-3.34 (m, 340H, N-$\underline{CH_2}\underline{CH_2}$), 2.01-1.97 (m, 261H, C=O-$\underline{CH_3}$) ppm.

PMP-4: under inert atmosphere, to a stirring solution of PMAC-4 (800 mg) and DCC (90 mg, 0.43 mmol) in dry DMF (10 mL) at 0°C, pentafluorophenol (80 mg, 0.43 mmol) in 5 mL of DMF was added and the reaction was then let at room temperature overnight. Successively, PTS (110 mg, 0.43 mmol) and DMAP (cat. 10 mg) dissolved in 5 mL of dry DMF were added and let at room temperature for 24 h. The solvent was evaporated under reduced pressure. The solid residue was suspended in Milli-Q water, filtered and purified by dialysis against water using 3.5 kDa cut-off tubes, and they were finally freeze-dried to yield **PMP-4** (527 mg). ^{1}H NMR (300 MHz, DMSO) δ = 7.42-6.36 (m, 54H, Ar), 3.77-3.76 (d, 36H, -O$\underline{CH_3}$), 3.45-3.34 (m, 503H, N-$\underline{CH_2CH_2}$), 2.01-1.97 (m, 380H, C=O-$\underline{CH_3}$) ppm.

FPMP-4 synthesis

FPMP-4: under inert atmosphere, to a stirring solution of PMAC-4 (700 mg) and DCC (130 mg, 0.63 mmol) in dry DMF (25 mL) at 0°C, pentafluorophenol (90 mg, 0.5 mmol) in 5 mL of DMF was added and the reaction was then let at room temperature overnight. Successively, PTS (130 mg, 0.5 mmol), fluorescein (10 mg, 0.025 mmol) and DMAP (cat. 5 mg) dissolved in 5 mL of dry DMF were added and let at room temperature for 24 h. The solvent was evaporated under reduced pressure. The solid residue was suspended in EtOH, filtered and purified by dialysis against EtOH using 3.5 kDa cut-off tubes, and they were finally dried to yield **FPMP-4** (415 mg). ^{1}H NMR (300 MHz, DMSO) δ = 7.95-6.13 (m, 64H, Ar), 3.78-3.75 (d, 36H, -O$\underline{CH_3}$), 3.49-3.33 (m, 503H, N-$\underline{CH_2CH_2}$), 2.05-1.96 (m, 380H, C=O-$\underline{CH_3}$) ppm.

Drug loading calculations

The following equations were used to determine drug loading capacity (LC), loading efficiency (LE) and drug loading (DL):

$$LC = \frac{m_{drug}}{m_{drug} + m_{excipient}} \times 100\%$$

$$LE = \frac{m_{drug}}{m_{drug\ added}} \times 100\%$$

$$DL = \frac{m_{drug}}{m_{excipient}} \times 100\%$$

Where m_{drug} and $m_{excipient}$ are the weight amounts of the solubilized drug and polymer excipient in the dispersion, while $m_{drug\ added}$ is the weight amount of the drug added to the dispersion.

Dynamic light scattering (DLS)

The size distribution of polymeric micelles was investigated with DLS using a Nano-ZS (Malvern Instruments Inc., U.K.). Each sample was diluted 20 times with Milli-Q water yield 1 mg/mL final polymer concentration. The intensity-mean z-averaged particle size (effective diameter) and the polydispersity index (PDI) obtained from cumulant analysis were given to reflect hydrodynamic diameters of drug loaded AnRG and PMP micelles. Measurements were repeated over prolonged time periods in order to evaluate stability of empty and CFZ-loaded micelles.

MTS cytotoxicity/fluorescence microscopy studies protocol

In 96-well plates I use 12500 cells per well (i.e. $12.5*10^4$ cells/mL in DMEM+10%FBS without phenol red and seed 100 μfor 24 h prior to experiment. During the experiment I am using as negative control a mixture of sterilized Milli-Q with serum-free DMEM (without phenol red) in volume ratio 1:3 and incubate for 6 h (100 uL per well). After this time, I added 20 μL MTS solution. After 3 hours, the absorbance was read using a multi-plate reader set at 490 nm.

Atomic Force Microscopy (AFM)

Three drops of the diluted polymeric micelle solution (2 mg/mL) were deposited on freshly cleaved silica surface. Then the sample was spin for 1 minute and then the system was let to water evaporation overnight before start the analysis. A Bruker Dimension Icon atomic force microscope was used in tapping mode employing a SiN cantilever with a resonance frequency of 300 kHz.

pH stability studies

The PTS release from PMP micelles was studied using membrane dialysis method against phosphate buffered saline (PBS, pH 7.4) and acetate buffer (pH 4.7) at 37 °C. Briefly, the PMP micelle formulations were diluted with buffer solution to yield solutions of approximately 1 mg/mL of each PMP polymer. Then the resulting solutions were placed into a dialysis tube with a MWCO of 3.5 kDa and suspended in 200 mL of each buffer. At each time point, 1 mL of sample was withdrawn from the external buffer solution and PTS amount was quantified by UV-Vis.

4.7. REFERENCES

(1) Seo, Y.; Schulz, A.; Han, Y.; He, Z.; Bludau, H.; Wan, X.; Tong, J.; Bronich, T. K.; Sokolsky, M.; Luxenhofer, R.; Jordan, R.; Kabanov, A. V. Polym. Adv. Technol. 2015, 26, 837–850.

(2) Zalipsky, S.; Hansen, C. B.; Oaks, J. M.; Allen, T. M. J. Pharm. Sci. 1996, 85, 133–137.

(3) Kataoka, K.; Harada, A.; Nagasaki, Y. Adv. Drug Deliv. Rev. 2001, 47, 113–131.

(4) Gref, R.; Minamitake, Y.; Peracchia, M. T.; Trubetskoy, V.; Torchilin, V.; Langer, R. Science 1994, 263, 1600–1603.

(5) Kataoka, K.; Ishihara, A.; Harada, A.; Miyazaki, H. Macromolecules 1998, 31, 6071–6076.

(6) Kazunori, K.; Glenn S., K.; Masayuki, Y.; Teruo, O.; Yasuhisa, S. J. Control. Release 1993, 24, 119–132.

(7) Garay, R. P.; El-Gewely, R.; Armstrong, J. K.; Garratty, G.; Richette, P. Expert Opin. drug Deliv. 2012, 9, 1319–1323.

(8) Yang, Q.; Lai, S. K. Wiley Interdiscip. Rev. Nanomedicine Nanobiotechnology 2015, 7, 655–677.

(9) Leanza, L.; Henry, B.; Sassi, N.; Zoratti, M.; Chandy, K. G.; Gulbins, E.; Szabò, I. EMBO Mol Med 2012, 4, 577–593.

(10) Van Rensburg, C. E. J.; Van Staden, A. M.; Anderson, R. The Riminophenazine Agents Clofazimine and B669 Inhibit the Proliferation of Cancer Cell Lines in Vitro by Phospholipase A2-mediated Oxidative and Nonoxidative Mechanisms. Cancer Research, 1993, 53, 318–323.

(11) Yasuhiro, M.; Hiroshi, M. Cancer Res. 1986, 46, 6387–6392.

(12) Boucher, Y.; Jain, R. K. Cancer Res. 1992, 52, 5110–5114.

(13) Brown, E.; McKee, T.; diTomaso, E.; Pluen, A.; Seed, B.; Boucher, Y.; Jain, R. K. Nat. Med. 2003, 9, 796–800.

(14) Diop-Frimpong, B.; Chauhan, V. P.; Krane, S.; Boucher, Y.; Jain, R. K. Proc. Natl. Acad. Sci. United States Am. 2011, 108, 2909–2914.

(15) Yuan, F.; Leunig, M.; Huang, S. K.; Berk, D. A.; Papahadjopoulos, D.; Jain, R. K. Cancer Res. 1994, 54, 3352–3356.

(16) McCormack, D.; McFadden, D. J. Surg. Res. 2012, 173, 53.

(17) Mena, S.; Rodríguez, M. L.; Ponsoda, X.; Estrela, J. M.; Jäättela, M.; Ortega, A. L. PLoS ONE 2012, 7.

(18) Kapetanovic, I.; Muzzio, M.; Huang, Z.; Thompson, T.; McCormick, D. Cancer Chemother. Pharmacol. 2010, 68, 593–601.

(19) Quideau, S.; Deffieux, D.; Douat-Casassus, C.; Pouységu, L. Angew. Chem. Int. Ed. 2011, 50, 586–621.

(20) Fessi, H.; Puisieux, F.; Devissaguet, J. P.; Ammoury, N.; Benita, S. Int. J. Pharm. 1989, 55, R1–R4.

(21) Bilati, U.; Allémann, E.; Doelker, E. Eur. J. Pharm. Sci. 2005, 24, 67–75.

(22) Zarka, M. T.; Nuyken, O.; Weberskirch, R. Chem. – Eur. J. 2003, 9, 3228–3234.

(23) Mallakpour, S.; Asadi, P. Colloid Polym. Sci. 2010, 288, 1341–1349.

(24) Siddalingappa, B.; Benson, H. A. E.; Brown, D. H.; Batty, K. T.; Chen, Y. PLOS ONE 23AD, 10.

(25) Han, Y.; He, Z.; Schulz, A.; Bronich, T. K.; Jordan, R.; Luxenhofer, R.; Kabanov, A. V. Mol. Pharm. 2012, 9, 2302–2313.

(26) Dube, D.; Gupta, M.; Vyas, S. Proc. Natl. Acad. Sci. India Sect. B - Biol. Sci. 2012, 82, 151–165.

(27) Konradi, R.; Pidhatika, B.; Mühlebach, A.; Textor, M. Langmuir 2008, 24, 613–616.

ACKNOWLEDGMENTS

Tranquilli. Solo il titolo di questo paragrafo è in inglese, ciò che seguirà sarà interamente nella lingua più bella del mondo: la nostra.

Per cominciare, e volendo ovviamente ricollegarmi alla dedica iniziale, ci tengo a ringraziare la mia famiglia: mamma, papà, Marzia, Andrea (con mariti/mogli e figlie tutte al seguito, chiaramente) e lo zio Alfonso che però ora più non c'è. Senza il vostro continuo supporto, stimolo ed esempio nella vita questo dottorato forse non sarebbe neppure mai iniziato. Grazie.

A tutti gli amici e le amiche che nei week end provano da anni a farmi staccare il cervello dalle reazioni chimiche (rimanete degli illusi). Vi devo molto: mi siete sempre vicini anche quando ci sono stati momenti un po' bui, anzi soprattutto in quelli. Grazie Erika. Grazie Sizzy, George, Tino, Zubi, Fede, Refo, Michele e Robi. Grazie Sara, Vale (quella comunista), Franci, Giorgia, Valentina (la farmacista omeopata – asemo perdare), Miha e Mary. Ed ovviamente grazie ai miei coinquilini: Gabri, la Rizzi, Lucia, Albe, Davide, la Ci, Ilaria, Alessandra ed Annalisa.

Ora ci si prepari, poiché arriva tutto il treno di persone che hanno percorso con me la strada di questo dottorato, spero arricchendoci a vicenda.

In primis, un grazie col cuore al mio supervisore Cristina "la prof" Paradisi, mi ha insegnato la calma e la determinazione in ciò che si fa e l'importanza dell'essere pragmatici. Grazie al mio "supervisore nell'ombra" Mario Zoratti, forse tra le persone che più ammiro: onesto, sapiente e (anche se non sempre lo sembra) paziente. Se non è abbastanza chiaro sei il mio punto di riferimento su quello che vorrei scientificamente divenire.

Grazie ad Andrea Mattarei, il mio mentore e maestro (nel senso antico del termine); grazie per avermi insegnato tutto quello che so fare sotto una cappa. Anche se a volte ci siamo scontrati, poi una birretta ha sempre risolto le cose. Grazie Massimo, Lucia, Michele e Martina Esmeralda Eustachia etc., Ildiko, Gigi e Antonella per avermi sempre assistito, insegnato e regalato momenti indimenticabili. Grazie anche alle altre persone con cui ho collaborato in questi anni: Ennio, Giorgia e Monica, i miei cari studenti.

Grazie Eddy. Uomo incredibile, buono, infaticabile e scienziato pazzesco. La stima che provo non può certo essere riassunta in queste poche righe. Grazie di tutto quello che tu, la Giulia e Stefano avete fatto e continuate a fare da Zurigo. Se Mario è uno dei miei punti di riferimento, indubbiamente tu sei l'altro, grazie ancora. Ti ammiro.

Grazie Pez. Genio maledetto, ribelle bevitore e grande amico. Sei una delle persone più belle che ho conosciuto in questi anni. Uno che come me sogna di poter scoprire sempre qualcosa di stupendo col proprio lavoro.
Grazie a tutti i colleghi del Dipartimento di Chimica Organica (e me ne frego di chi vuole chiamarlo in altro modo). Grazie per tutte le bevute, le notti di festa, i caffè e le partite di calcetto. Grazie Agata, Viviana, Alvaro, Elisa, Valerio, Maiti, Jack, Silvia, Sara, Squirtina, Luca, Giovanni, Carlo, Claudia, Sergio & la Simo, Tommy, Antonio, Andrea, Enrico, Emanuele, Andrea, Valentina, Nicola, l'Arcifone, Michele, Stefano, Nicolino e Marta e grazie a tutti quelli che mi sono scordato di ringraziare.

Grazie.